

1-1-2012

On-Site Total Phosphorus Removal From Wastewater

Amanda L. Alaica
Ryerson University

Follow this and additional works at: <http://digitalcommons.ryerson.ca/dissertations>



Part of the [Civil Engineering Commons](#)

Recommended Citation

Alaica, Amanda L., "On-Site Total Phosphorus Removal From Wastewater" (2012). *Theses and dissertations*. Paper 1231.

This Thesis is brought to you for free and open access by Digital Commons @ Ryerson. It has been accepted for inclusion in Theses and dissertations by an authorized administrator of Digital Commons @ Ryerson. For more information, please contact bcameron@ryerson.ca.

ON-SITE TOTAL PHOSPHORUS REMOVAL FROM WASTEWATER

by

Amanda Lidia Alaica, B.Eng.

Ryerson University

Toronto, Ontario, Canada 2010

A Thesis Presented to Ryerson University

In Partial Fulfillment of the Requirements for the Degree of

Master of Applied Science

In the Program of Civil Engineering

Toronto, Ontario, Canada 2012

© Amanda Lidia Alaica 2012

DECLARATION

AUTHOR'S DECLARATION FOR ELECTRONIC SUBMISSION OF A THESIS

I hereby declare that I am the sole author of this thesis. This is a true copy of the thesis, including any required final revisions, as accepted by my examiners.

I authorize Ryerson University to lend this thesis to other institutions or individuals for the purpose of scholarly research.

I further authorize Ryerson University to reproduce this thesis by photocopying or by other means, in total or in part, at the request of other institutions or individuals for the purpose of scholarly research.

I understand that my thesis may be made electronically available to the public.

ON-SITE TOTAL PHOSPHORUS REMOVAL FROM WASTEWATER

Amanda Lidia Alaica

Master of Applied Science, Civil Engineering

Ryerson University, Toronto, Ontario, Canada 2012

ABSTRACT

Eutrophication is attributed to high phosphorus concentrations in our ecosystem, modifying water and habitat quality. As an industry-academia collaboration program, this thesis assists the development of Virtual Engineers' (VE) technology of a cost-effective, efficient, and affordable on-site Total Phosphorus (TP) removal unit. By investigating the chemical adsorption of a clay-zeolite media, the objective was to demonstrate TP removal capacity; primarily focusing on pellet media composition and formation, influent concentration, contact time to overall removal efficiency. All stages of optimization analyses were conducted in a scaled-down testing unit based on a $\frac{3}{4}$ inch pellet diameter construction, for a modest 45 minute detention time, and achieved an optimized removal of approximately 45%. The final pellet selected was the non-conditioned VE design, at maximum furnace exposure, scaled up to a 1 inch diameter. Results showed that an equilibrium removal of 72% is achieved after a 3 hour contact time; supporting the research of Sun (2010) on the Freundlich Adsorption Isotherm linearization of solute adsorption to equilibrium solvent concentration.

ACKNOWLEDGEMENTS

The collaborative efforts and financial provision of both Virtual Engineers (VE) and the Ontario Centres of Excellence (OCE) are forever valued, as this project is a direct result of their contributions. This thesis is based on the continuation of VE research, which began in 2009, from September 2010 to June 2012; conducted in the Environmental Engineering, Hydraulics Engineering, and Structural Labs of the Civil Engineering Department at Ryerson University.

I give my sincerest gratitude to everyone who assisted me to reach this project's successful completion within the Ryerson community. I wish to acknowledge my supervisor, whom I owe the greatest appreciation towards, Dr. Grace K. Luk. I am thankful that she has provided me with this opportunity to embark into industry-academia collaborative research. This thesis would not have been possible without her continuous direction and encouragement. I would also like to thank Mr. Robin Luong for all of his aid in materials and equipment selection, test setup, and apparatus construction, as well as Mr. Nidal Jaalouk for his assistance in equipment calibration.

I would like to recognize the members of the industry who have provided their assistance. From the Ontario Centres of Excellence, I would like to thank Ms. Balinder Rai for her administration of this project. From Virtual Engineers, I would like to thank Mr. R. Anthony Warner and Ms. Michele Warner, working together as a team to bring their vision into reality. For experimental materials, Bear River Zeolite, Tucker's Pottery Suppliers, and Ontario Sawdust Suppliers should all be credited for their involvement in this project.

I wish to express my deepest thank you to Tomasz Ciosek for his continuous support and love, and for his assistance throughout this project in its entirety; including all OCE Discovery materials and the student video competition. Finally, I wish to thank my family; Mama, Tata, Aleksa, Alivia, and Adam. I am eternally grateful for their patience, support, and love.

DEDICATION

Tom

Je t'aime – Ja te волим – Ja cię kocham

TABLE OF CONTENTS

DECLARATION	ii
ABSTRACT.....	iii
ACKNOWLEDGEMENTS.....	iv
DEDICATION	v
LIST OF TABLES.....	viii
LIST OF FIGURES.....	x
LIST OF APPENDICES	xii
1 INTRODUCTION.....	1
1.1 PROBLEM STATEMENT.....	1
1.1.1 EUTROPHICATION SYNDROMES	2
1.1.2 TERRESTRIAL PLANT PROGRESSION.....	3
1.1.3 ECOLOGICAL CONCERNS.....	4
1.1.4 IMPROVEMENT	5
1.2 RESEARCH OBJECTIVES	6
1.3 INDUSTRY-ACADEMIA COLLABORATION PROGRAM	7
1.4 THESIS OVERVIEW.....	8
2 BACKGROUND AND LITERATURE REVIEW	9
2.1 PHOSPHORUS.....	9
2.1.1 SOLUBLE REACTIVE PHOSPHORUS (SRP)	10
2.1.2 SOLUBLE UNREACTIVE PHOSPHORUS (SUP).....	10
2.1.3 SOLUBLE PHOSPHORUS (SP)	10
2.1.4 PARTICULATE PHOSPHORUS (PP)	11
2.1.5 TOTAL PHOSPHORUS	11
2.2 PHOSPHORUS COLLECTION AND ANALYSIS.....	11
2.2.1 LIMITS OF DETECTION.....	11
2.2.2 DIGESTION METHODS.....	12
2.2.3 INTERFERENCES.....	12
2.2.4 RECOMMENDATIONS.....	12
2.3 EXISTING PHOSPHORUS REMOVAL TECHNOLOGIES	13
2.3.1 BIOLOGICAL.....	18
2.3.2 CHEMICAL	20
2.3.3 PHYSICAL	23
2.4 PHOSPHORUS REMOVAL ABSORBENTS.....	25
2.4.1 PHOSPHORUS RETENTION CAPACITY INFLUENCING FACTORS	27
2.4.2 ADSORBENT LIFECYCLE	30
2.5 INDUSTRY REMOVAL TECHNOLOGIES	31
2.5.1 SORBTIVE™ MEDIA.....	31
2.5.2 PHOSLOCK®	34
3 ZEOLITE	37
3.1 MINERALOGY	38
3.1.1 CHEMICAL COMPOSITION.....	38
3.1.2 CRYSTAL STRUCTURE	39
3.1.3 CLINOPTILOLITE.....	45
3.2 COMMERCIAL PROPERTIES	47
3.2.1 ADSORPTION CAPACITY	47
3.2.2 ION-EXCHANGE CAPACITY	53

3.3	UTILIZATION	55
3.4	CONDITIONING	56
3.4.1	ACID/BASE TREATMENT	56
3.4.2	SURFACTANT MODIFICATION	57
4	EXPERIMENTAL DEVELOPMENT FROM RECENT LITERATURE.....	58
4.1	EQUILIBRIUM ADSORPTION CAPACITY AND ISOTHERMS.....	58
4.2	ADSORPTION ISOTHERMS AND KINETICS	60
4.3	ZEOLITE MODIFICATION AND REGENERATION	62
4.4	PELLET COMPOSITION	65
4.5	DEVELOPMENT SUMMARY	66
5	EXPERIMENTAL DESIGN	69
5.1	PARAMETERS	69
5.2	MATERIALS AND METHODS	69
5.2.1	OPTIMIZATION TESTING UNIT	69
5.2.2	PELLET COMPOSITION AND FORMATION	71
5.2.3	PELLET SACK DEVELOPMENT	79
5.2.4	APPARATUS PROTOTYPE.....	80
5.2.5	DEIONIZED DISTILLED WATER (DDW)	81
5.2.6	CLEANING PROCEDURE	83
5.3	DESIGN STAGES.....	85
5.3.1	PRE-OPTIMIZATION.....	90
5.3.2	OPTIMIZATION	92
5.3.3	FINAL APPARATUS.....	96
6	RESULTS.....	103
6.1	PRE-OPTIMIZATION RESULTS.....	103
6.2	OPTIMIZATION RESULTS	105
6.3	FINAL APPARATUS RESULTS.....	107
7	ANALYSIS.....	110
7.1	PRE-OPTIMIZATION ANALYSIS	110
7.2	OPTIMIZATION ANALYSIS.....	111
7.2.1	CONTACT TIME.....	111
7.2.2	INFLUENT CONCENTRATION	113
7.2.3	FURNACE EXPOSURE	115
7.2.4	SURFACE AREA	116
7.2.5	OPTIMIZATION ANALYSIS SUMMARY	117
7.3	FINAL APPARATUS ANALYSIS	118
7.3.1	ANALYSIS BREAKDOWN	118
7.3.2	EXPERIMENT-LITERATURE ASSESSMENT	122
7.4	LIMITATIONS	125
8	CONCLUSIONS AND RECOMMENDATIONS.....	126
	REFERENCES.....	143
	BIBLIOGRAPHY	144

LIST OF TABLES

TABLE 1.1 – TECHNICAL PROBLEM SOLVING AGREEMENT	7
TABLE 2.1 – P REMOVAL TECHNOLOGY EVOLUTION (MORSE, 1998)	15
TABLE 2.2 – P REMOVAL TECHNOLOGY PROCESS (MORSE, 1998)	16
TABLE 2.3 – P REMOVAL TECHNOLOGY PROCESS (MORSE, 1998)	17
TABLE 2.4 – WASTEWATER TREATMENT (MORSE, 1998)	21
TABLE 2.5 – PHOSPHORUS REMOVAL CRYSTALACTOR TECHNOLOGIES (MORSE, 1998)	24
TABLE 2.6 – FILTER MEDIA (VOHLA, 2011)	26
TABLE 3.1 – TYPICAL FORMULAE AND SELECTED PHYSICAL PROPERTIES OF IMPORTANT ZEOLITES (MUMPTON, 1977)	40
TABLE 3.2 – BUILDING UNITS IN ZEOLITE STRUCTURES (MUMPTON, 1977)	43
TABLE 3.3 – ZEOLITE GROUP – SBU – CLASSIFICATION (MUMPTON, 1977)	44
TABLE 3.4 – IMPORTANT PROPERTIES OF NATURAL ZEOLITES (WANG, 2010)	45
TABLE 3.5 – PHYSICAL CHARACTERISTICS OF CLINOPTILOLITE (AMETHYST GALLERIES, 2011)	46
TABLE 3.6 – COMPARISON OF ADSORPTION ISOTHERMS (MASEL, 1996)	50
TABLE 3.7 – SELECTED CHEMICAL CHARACTERISTICS OF NATURAL ZEOLITE (WANG, 2010)	54
TABLE 3.8 – ZEOLITE APPLICATIONS IN PRACTICE (BEKKKUM, 1991)	55
TABLE 4.1 – ZEOLITE REGENERATION (LI, 2011)	64
TABLE 4.2 – ZEOLITE MODIFICATION MATERIALS OVERVIEW	66
TABLE 4.3 – ZEOLITE MODIFICATION PROCEDURES	67
TABLE 4.4 – TECHNOLOGY ANALYSIS COMPARISON	68
TABLE 5.1 – EXPERIMENTAL PARAMETERS	69
TABLE 5.2 – PELLET OPTIMIZATION MATERIALS	74
TABLE 5.3 – TESTING UNIT PROPERTIES	86
TABLE 5.4 – RANDOMLY SELECTED ORIGINAL VE PELLETS	86
TABLE 5.5 – MEASURING SPOON ANALYSIS	87
TABLE 5.6 – PRE-OPTIMIZATION STOCK-SUMP DETERMINATION	90
TABLE 5.7 – PHASE I PELLET DETERMINATION	93
TABLE 5.8 – PHASE II PELLET DETERMINATION	93
TABLE 5.9 – HEATING-COOLING RATE	95
TABLE 5.10 – CONDITIONING DETERMINATION	96
TABLE 5.11 – CONDITIONING BRINE CALCULATIONS	96
TABLE 5.12 – BURLAP SACK PROPERTIES	97
TABLE 5.13 – FURNACE/KILN CALIBRATION	99
TABLE 5.14 – APPARATUS ELEMENTS	100
TABLE 5.15 – CONTACT TIME TO FLOW DETERMINATION	101
TABLE 5.16 – APPARATUS STOCK-SUMP DETERMINATION	101
TABLE 6.1 – INFLUENT DILUTION	104
TABLE 6.2 – EFFLUENT DILUTION	104
TABLE 6.3 – PRE-OPTIMIZATION PELLET RESULTS SUMMARY	104
TABLE 6.4 – PHASE BLANK SUMMARY	106
TABLE 6.5 – LEAKAGE RATE TEST	109
TABLE 7.1 – OPTIMIZATION 45 MINUTE PERCENT REMOVAL ANALYSIS	117
TABLE 7.2 – APPARATUS LAYERS' R ² VALUES	118
TABLE 7.3 – INFLUENT TIME APPLIED APPARATUS LAYERS' R ² VALUES	119
TABLE 7.4 – LINEARIZATION OF ADSORPTION ISOTHERM VALUES	123

TABLE A.1 – TYPE 1 PELLETT TEST	129
TABLE A.2 – TYPE 2 PELLETT TEST	129
TABLE A.3 – TYPE 3 PELLETT TEST	129
TABLE A.4 – TYPE 4 PELLETT TEST	129
TABLE A.5 – TYPE 5 PELLETT TEST	129
TABLE A.6 – TYPE 6 PELLETT TEST	130
TABLE A.7 – PELLETT TEST COMPOSITION AND FORMATION SUMMARY.....	130
TABLE B.1 – TYPE 1 PELLETT PRE-OPTIMIZATION	131
TABLE B.2 – TYPE 2 PELLETT PRE-OPTIMIZATION	131
TABLE B.3 – TYPE 3 PELLETT PRE-OPTIMIZATION	131
TABLE B.4 – TYPE 4 PELLETT PRE-OPTIMIZATION	132
TABLE B.5 – TYPE 5 PELLETT PRE-OPTIMIZATION	132
TABLE B.6 – TYPE 6 PELLETT PRE-OPTIMIZATION	132
TABLE B.7 – PELLETT PRE-OPTIMIZATION COMPOSITION AND FORMATION SUMMARY.....	132
TABLE C.1 – PRE-OPTIMIZATION - TYPE 7 PELLETT TEST	133
TABLE C.2 – INFLUENT ANALYSIS	133
TABLE C.3 – PRE-OPTIMIZATION - TYPE 6 PELLETT	133
TABLE C.4 – PRE-OPTIMIZATION NON-CONDITIONED PELLETT ANALYSIS	133
TABLE C.5 – PRE-OPTIMIZATION CONDITIONED PELLETT ANALYSIS	133
TABLE D.1 – TYPE 6I PELLETT PRE-OPTIMIZATION.....	134
TABLE D.2 – TYPE 6II PELLETT PRE-OPTIMIZATION.....	134
TABLE E.1 – OPTIMIZATION NON-CONDITIONED TYPE 6I PELLETT ANALYSIS.....	135
TABLE E.2 – OPTIMIZATION CONDITIONED 1&2 A TYPE 6I PELLETT ANALYSIS.....	135
TABLE E.3 – OPTIMIZATION CONDITIONED 1&2 B TYPE 6I PELLETT ANALYSIS	136
TABLE E.4 – OPTIMIZATION NON-CONDITIONED TYPE 6II PELLETT ANALYSIS.....	136
TABLE E.5 – OPTIMIZATION CONDITIONED 1&2 A TYPE 6II PELLETT ANALYSIS.....	137
TABLE E.6 – OPTIMIZATION CONDITIONED 1&2 B TYPE 6II PELLETT ANALYSIS	137
TABLE E.7 – OPTIMIZATION NON-CONDITIONED TYPE 7I PELLETT ANALYSIS.....	138
TABLE E.8 – OPTIMIZATION CONDITIONED 1&2 A TYPE 7I PELLETT ANALYSIS	138
TABLE E.9 – OPTIMIZATION CONDITIONED 1&2 B TYPE 7I PELLETT ANALYSIS	139
TABLE E.10 – OPTIMIZATION NON-CONDITIONED TYPE 7II PELLETT ANALYSIS.....	139
TABLE E.11 – OPTIMIZATION CONDITIONED 1&2 A TYPE 7II PELLETT ANALYSIS	139
TABLE E.12 – OPTIMIZATION CONDITIONED 1&2 B TYPE 7II PELLETT ANALYSIS	140
TABLE E.13 – NON-CONDITIONED TYPE 7II – SURFACE AREA ANALYSIS	140
TABLE E.14 – NON-CONDITIONED BR1&2 TYPE 7II – SURFACE AREA ANALYSIS	140
TABLE E.15 – FINAL APPARATUS TEST	141

LIST OF FIGURES

FIGURE 1.1 – PHOSPHORUS CYCLE (ENCYCLOPÆDIA BRITANNICA, 2011)	1
FIGURE 1.2 – ALGAL BLOOM IN ORIELTON LAGOON, AUSTRALIA (1994) (CLOERN ET AL, 2010)	2
FIGURE 1.3 – AQUATIC ENVIRONMENT EUTROPHICATION-CONTAMINANTS’ INTERACTION PROCESSES AND MECHANISMS (SKEI, 2011)	3
FIGURE 1.4 – ENVIRONMENTAL IMPACTS OF EUTROPHICATION (ENCYCLOPÆDIA BRITANNICA, 2011)	4
FIGURE 1.5 – EUTROPHICATION INDUCED FISH KILL IN THE SALTON SEA (CLOERN ET AL, 2010)	5
FIGURE 2.1 – PHOSPHORUS COMPONENTS (CARLSON, 1996).....	9
FIGURE 2.2 – BIOLOGICAL PHOSPHORUS REMOVAL (MORSE, 1998).....	18
FIGURE 2.3 – COMMERCIAL BIOLOGICAL PHOSPHORUS REMOVAL PROCESSES (MORSE, 1998).....	19
FIGURE 2.4 – CHEMICAL PRECIPITATION (MORSE, 1998).....	21
FIGURE 2.5 – THE HYDRO CONCEPT (MORSE, 1998)	22
FIGURE 2.6 – DHV CRYSTALACTOR (MORSE, 1998)	24
FIGURE 2.7 – RELATIONSHIP OF P RETENTION CAPACITY, (A) CA and (B) CAO CONTENT, AND PH LEVEL OF VARIOUS ADSORBENTS (VOHLA, 2011)	28
FIGURE 2.8 – P RETENTION CAPACITY AND HYDRAULIC RETENTION TIME RELATIONSHIP	29
FIGURE 2.9 – ADSORPTION 1-POINT ISOTHERM EQUILIBRIUM CAPACITY (MG/G) OF DP (IMBRIUM SYSTEMS, 2012).....	32
FIGURE 2.10 – NUMBER OF BED VOLUMES (BV) AT BREAKTHROUGH OF 50% DISSOLVED PHOSPHORUS (DP) REMOVAL (IMBRIUM SYSTEMS, 2012).....	33
FIGURE 2.11 – PHOSLOCK PRODUCTION (PHOSLOCK, 2010)	34
FIGURE 2.12 – PHOSLOCK WATER BODY REMOVAL (PHOSLOCK, 2010)	35
FIGURE 3.1 – THE ANNUAL NUMBER OF PAPERS AND PATENTS ON THE PREPARATION OF ZEOLITE SINCE FIRST PUBLICATION IN 1972 (MUMPTON, 1977)	37
FIGURE 3.2 – THREE-DIMENSIONAL ARRANGEMENT OF SILICATE TETRAHEDRA IN TEKOSILICATES (MUMPTON, 1977)	38
FIGURE 3.3 – SIMPLE POLYHEDRON OF SILICATE (SiO ₄) AND ALUMINATE (AlO ₄) TETRAHEDRA – TRUNCATED CUBO-OCTAHEDRA; A) GEOMETRICAL FORM – BALL AND PEG MODEL; B) LINE DRAWING (LINES CONNECT MIDPOINTS OF EACH TETRAHEDRON) (MUMPTON, 1977).....	41
FIGURE 3.4 – ARRANGEMENT OF SIMPLE POLYHEDRA TO ENCLOSE LARGE CENTRAL CAVITIES - TRUNCATED CUBO-OCTAHEDRA CONNECTED BY DOUBLE 4-RINGS OF OXYGEN IN STRUCTURE OF SYNTHETIC ZEOLITE A (INDIVIDUAL POLYHEDRAL CONNECTIONS – FRAMEWORK STRUCTURES) (MUMPTON, 1977)	41
FIGURE 3.5 – SOLID-SPHERE MODEL OF CRYSTAL STRUCTURE OF SYNTHETIC ZEOLITE A (INDIVIDUAL POLYHEDRAL CONNECTIONS – SOLID-SPHERE STRUCTURES) (MUMPTON, 1977)	41
FIGURE 3.6 – ZEOLITE STRUCTURES’ SECONDARY BUILDING UNITS (SBU) (MUMPTON, 1977)	43
FIGURE 3.7 – GROUP 7 ZEOLITES - CONFIGURATION OF T ₁₀ O ₂₀ UNITS OF TETRAHEDRA IN THE FRAMEWORK STRUCTURES (MUMPTON, 1977).....	44
FIGURE 3.8 – ADSORPTION ISOTHERMS (MASEL, 1996)	48
FIGURE 3.9 – LANGMUIR’S MODEL OF ADSORBED LAYER STRUCTURE (MASEL, 1996)	49
FIGURE 3.10 – SCHEMATIC ILLUSTRATION – ENTRY OF STRAIGHT-CHAIN HYDROCARBONS AND THE BLOCKAGE OF BRANCH-CHAIN HYDROCARBONS AT CHANNEL OPENINGS (MUMPTON, 1977)	51
FIGURE 3.11 – PORE SIZE DISTRIBUTION IN MICRO-POROUS ADSORBENTS; A) DEHYDRATED CRYSTALLINE ZEOLITE; B) TYPICAL SILICA GEL; C) ACTIVATED CARBON (MUMPTON, 1977)	52

FIGURE 3.12 – LANGMUIR-TYPE ISOTHERM FOR ADSORPTION ON CRYSTALLINE ZEOLITES – NEAR SATURATION COMPLETION AT LOW PARTIAL PRESSURES OF ADSORBENT (X – AMOUNT ADSORBED AND P – PRESSURE) (MUMPTON, 1977).....	52
FIGURE 3.13 – POSITION OF ZEOLITE CHARACTERIZATION (BEKKUM, 1991)	56
FIGURE 3.14 – HEMIMICELLE FORMATION.....	57
FIGURE 3.15 – ADMICELLE FORMATION.....	57
FIGURE 4.1 – ADSORPTION ANALYSIS EXPERIMENTAL DESIGN (LI, 2011).....	63
FIGURE 4.2 – ADSORPTION CAPACITY-ZEOLITE REGENERATION METHODS COMPARISON (LI, 2011)	64
FIGURE 5.1 – OPTIMIZATION TESTING UNIT SEGMENTATION OF APPARATUS	69
FIGURE 5.2 – OPTIMIZATION TESTING UNIT.....	70
FIGURE 5.3 – ORIGINAL VE PROCEDURE TEMPERATURE EFFECTS	71
FIGURE 5.4 – MODIFIED VE PROCEDURE	73
FIGURE 5.5 – OPTIMIZATION PELLET PROCEDURE	75
FIGURE 5.6 – PELLET COMPOSITION, FORMATION AND TEMPERATURE MONITORING	78
FIGURE 5.7 – APPARATUS SACK CONFIGURATION	79
FIGURE 5.8 – PELLET SACK DEVELOPMENT	79
FIGURE 5.9 – APPARATUS DEVELOPMENT	80
FIGURE 5.10 – SCHEMATIC DRAWING	81
FIGURE 5.11 – DDW LOADING AND TRANSPORTATION.....	82
FIGURE 5.12 – CIVIL ENGINEERING LAB SCALE DDW MACHINE	83
FIGURE 5.13 – GLASSWARE AND SAMPLE BOTTLE PREPARATION	84
FIGURE 5.14 – STEPS OF THE LABORATORY BENCH SCALE TESTING	88
FIGURE 5.15 – PRE-OPTIMIZATION PROCESS	90
FIGURE 5.16 – PRE-OPTIMIZATION PELLET CONDITIONING PROCEDURE.....	91
FIGURE 5.17 – OPTIMIZATION PROCESS.....	92
FIGURE 5.18 – OPTIMIZATION PHASE PROCEDURES.....	94
FIGURE 5.19 – MUFFLE FURNACE TEMPERATURE VERIFICATION - OMEGA HH12A.....	95
FIGURE 5.20 – PELLET FORMATION SCALE-UP	97
Figure 5.21 – Final Apparatus Process	98
FIGURE 5.22 – APPARATUS PELLET HEAT TREATMENT	99
FIGURE 5.23 – APPARATUS CONFIGURATION	102
FIGURE 6.1 – CONCENTRATED PHOSPHORUS SOLUTION.....	103
FIGURE 6.2 – PELLET TYPE 7 PHASE I CA – EXPANSION OBSERVATION.....	105
FIGURE 6.3 – PELLET SURFACE AREA DEVELOPMENT (10% LEFT AND 40% RIGHT).....	107
FIGURE 6.4 – EFFLENT SAMPLING ARRANGEMENT.....	109
FIGURE 7.1 – PRE-OPTIMIZATION PELLET ANALYSIS	110
FIGURE 7.2 – PHASE I – 6 MGP/L INFLUENT	111
FIGURE 7.3 – PHASE I – 18 MGP/L INFLUENT	112
FIGURE 7.4 – PHASE II – 6 MGP/L INFLUENT	112
FIGURE 7.5 – PHASE II – 18 MGP/L INFLUENT	113
FIGURE 7.6 – PHASE I INFLUENT ANALYSIS.....	114
FIGURE 7.7 – PHASE II INFLUENT ANALYSIS.....	114
FIGURE 7.8 – FURNACE EXPOSURE – 6 MGP/L INFLUENT	115
FIGURE 7.9 – FURNACE EXPOSURE – 18 MGP/L INFLUENT	115
FIGURE 7.10 – PELLET TYPE NC7II – CONTACT TIME ANALYSIS.....	116
FIGURE 7.11 – PELLET TYPE NC7II – INFLUENT ANALYSIS.....	116
FIGURE 7.12 – FINAL APPARATUS ANALYSIS – LOGARITHMIC	118
FIGURE 7.13 – FINAL APPARATUS ANALYSIS – INFLUENT TIME APPLIED.....	119

FIGURE 7.14 – FINAL APPARATUS ANALYSIS – OVERALL CORRELATION	120
FIGURE 7.15 – FINAL APPARATUS ANALYSIS – OVERALL CORRELATION <i>CORRECTED</i>	120
FIGURE 7.16 – FINAL APPARATUS ANALYSIS – EXTRAPOLATION	121
FIGURE 7.17 – LINEARIZATION OF ADSORPTION ISOTHERM BY LANGMUIR ISOTHERM	124
FIGURE 7.18 – LINEARIZATION OF ADSORPTION ISOTHERM BY FREUNDLICH ISOTHERM	124

LIST OF APPENDICES

APPENDIX A – PELLET TEST COMPOSITION AND FORMATION	129
APPENDIX B – PRE-OPTIMIZATION PELLET COMPOSITION AND FORMATION	131
APPENDIX C – PRE-OPTIMIZATION PELLET DETERMINATION	133
APPENDIX D – OPTMIZATION PELLET COMPOSITION AND FORMATION	134
APPENDIX E – OPTMIZATION PELLET DETERMINATION	135
APPENDIX F – ORBECO MC500 COLORIMETER PROCEDURE.....	142

1 INTRODUCTION

This chapter of the report provides a general overview of the research, including the problem statement, objectives, and the features of the industry-academia collaboration program that was involved.

1.1 PROBLEM STATEMENT

The world water crisis is growing as clean drinking water availability diminishes. Wastewater pollutants include cationic and anionic ions, oil and organics; poisonous and toxic effects on ecosystems from untreated sewage discharges and treatment plants or fertilizer from agricultural or urban land runoff. Consequently, a global issue has grown – *eutrophication*. Eutrophication is how the ecosystem retorts to human, animal and industrial activities that infect water bodies with nitrogen (N) and phosphorus (P). Eutrophication modifies animal and plant populations, as well as their water and habitat quality. As displayed in Figure 1.1, these nutrients play a critical role in our lifecycle; both N and P are essential components of our water bodies that employ light and chemical energy to support life through structural proteins, enzymes, cell membranes, nucleic acids, and molecules (Cloern et al, 2010).

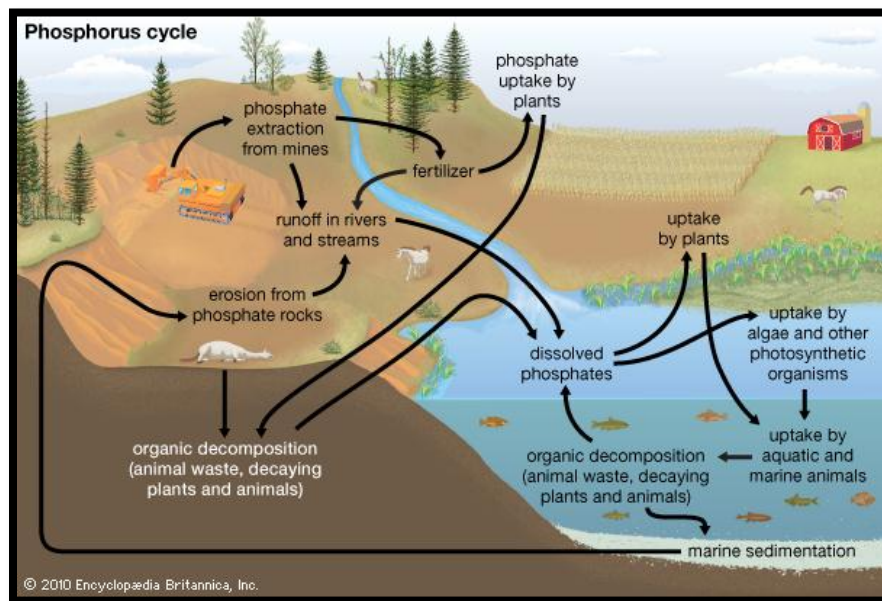


FIGURE 1.1 – PHOSPHORUS CYCLE (ENCYCLOPÆDIA BRITANNICA, 2011)

Both nutrients are biologically present in lakes, rivers, estuaries, and in vast regions of the upper ocean. These aquatic ecosystems are pristine when the nutrients' concentrations are low. Nitrogen and phosphorus are exposed to the system as microbial and animal metabolism, where a relatively steady state is achieved with primary production of new plant biomass.

Once the water bodies are artificially enriched with excess N and P, high rates of plant production and accumulation of organic matter occur. (Cloern et al, 2010).

1.1.1 EUTROPHICATION SYNDROMES

The research of eutrophication followed after the initial 1960 discovery of choking lakes and rivers with excessive rooted plants and floating algal scums. This involved investigating the prohibition of phosphate detergents and development of sewage treatment to reduce N and P wastewater discharges into inshore waters. In the 1980s, human activities encouraged nutrient transport, doubling N and tripling P transfer from land to oceans. As a result, eutrophication is now considered a major contributor to the stress imposed upon the global coastal ecosystems (Cloern et al, 2010).

Excessive nutrients encourage algae growth, as either multicellular forms (i.e. sea lettuce) or as suspended microscopic phytoplankton. Minimal surge in algal abundance or biomass have subtle ecological effects; increase production in food webs sustaining fish and shellfish, producing higher fish yields. Conversely, extreme algal growth causes complex, interconnected biological and chemical responses. These may severely destroy water quality, as well as endanger human health and coastal zone sustainability (Cloern et al, 2010).

The bloom of algal biomass encourages bacterial growth in bottom waters and sediments, as shown in Figure 1.2. If the water aeration rate is slower than bacterial metabolism (which ingests oxygen), then bottom waters become hypoxic (low in oxygen) or anoxic (devoid of oxygen), which generates a dangerous condition for aquatic life. This may include the reduction of seagrass, as well as the production of phytoplankton mucilage and toxic chemicals (i.e. domoic acid which encourages metabolic risks to fish and marine mammals) (Cloern et al, 2010).



FIGURE 1.2 – ALGAL BLOOM IN ORIELTON LAGOON, AUSTRALIA (1994) (CLOERN ET AL, 2010)

1.1.2 TERRESTRIAL PLANT PROGRESSION

As pond and lake eutrophication proceed, detritus layers form to create consecutively shallower surface water depths. Eventually, the water body becomes a marsh or bog, such that the aquatic environment transforms into a terrestrial ecosystem. As displayed in Figure 1.3, a very intense interaction occurs among the eutrophication process and the contributing pollutants. The entire ecosystem fanatically changes; once an aquatic habitat, and then inhabited by plants and water oriented wildlife (Cloern et al, 2010).

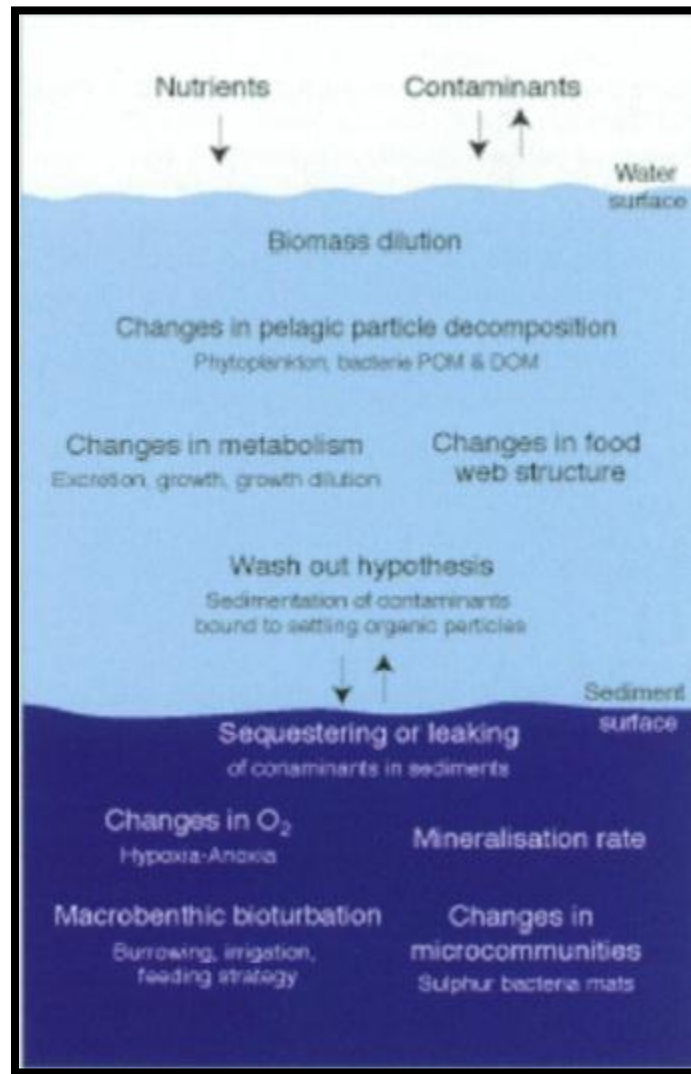


FIGURE 1.3 – AQUATIC ENVIRONMENT EUTROPHICATION-CONTAMINANTS’ INTERACTION PROCESSES AND MECHANISMS (SKEI, 2011)

1.1.3 ECOLOGICAL CONCERNS

Eutrophication greatly affects the biota, which is characteristic of a specific habitat. Impacts include (Cloern et al, 2010):

1. decline in biodiversity
2. die-off of organisms
3. reduction in visibility and mobility caused by biotic overgrowth; plant metabolism and aquatic animal transport hindrance
4. decrease in dissolved oxygen and animal fitness

An extreme case may occur when lakes transform into bogs and meadows; the original ecosystem is replaced. Human generated additions of N and P accelerate this progression, rather than natural landscape evolution, where organisms do not have time to migrate or adapt to the new milieu (Cloern et al, 2010). The environmental impacts of extreme eutrophication are demonstrated in Figure 1.4 and Figure 1.5.

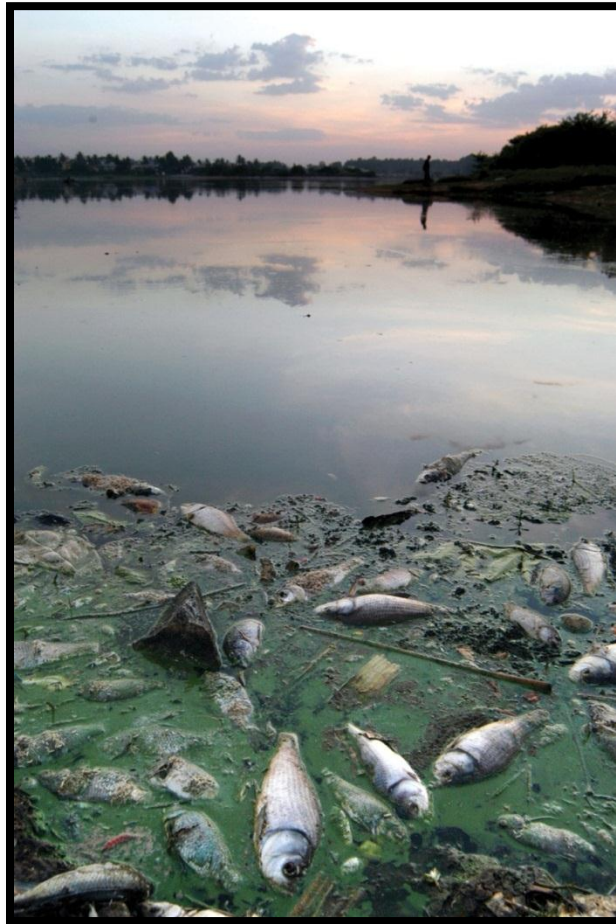


FIGURE 1.4 – ENVIRONMENTAL IMPACTS OF EUTROPHICATION (ENCYCLOPÆDIA BRITANNICA, 2011)



FIGURE 1.5 – EUTROPHICATION INDUCED FISH KILL IN THE SALTON SEA (CLOERN ET AL, 2010)

1.1.4 IMPROVEMENT

The pathway of the nutrients' source and delivery are diverse, making it problematic to protect water bodies from enrichment. In addition, the global population is growing disproportionately in the coastal zone, making it challenging to control N and P nutrient inputs from municipal waste, septic systems, and fertilizer runoff. The eutrophication problem conveys how human activities degrade the coastal water quality and damage habitats, with both economic and ecological costs. Solutions must be applied to the activities within the watersheds and air sheds. This is a multidimensional response, which consists of the (Cloern et al, 2010):

- restoration of wetlands and riparian buffer zones
- reduction livestock densities
- improvement of fertilizer applications' efficiencies
- treatment of streets and storm drains' urban runoff
- reduction of vehicles and power plants' N emissions
- increase in municipal wastewater's N and P removal efficiency

1.2 RESEARCH OBJECTIVES

As expressed in Section 1.1, sensitive areas prone to phosphorus contamination from domestic sewage must meet stringent effluent limits, following surface and subsurface disposal in order to address the eutrophication process.

In addition, the Ontario Ministry of Environment standards, outlined in The Lake Simcoe – Phosphorus Reduction Strategy must be taken greatly into consideration; to meet the current baseline compliance limit of 0.30 mgP/L (MOE, 2010). This strategy involves adaptive management, watershed approach, stewardship and community action, source-specific actions, monitoring compliance, and research, modelling and innovation (MOE, 2010). The issue of eutrophication is addressed in this research by applying the strategic direction of a source-specific action through the development of an on-site phosphorus removal and pH stabilization unit.

The overall objective of this research project was to develop a cost-effective, efficient, and affordable on-site Total Phosphorus (TP) removal unit, transferrable across the target market to individual facility owners. By primarily focusing on residential/domestic wastewater, of on-site aerobic treatment (septic tank) or urban storm water runoff discharge characteristics, analysis to overall removal efficiency was based on:

- pellet composition as well as channel and pore size
- media conditioning and manufacturing
- influent concentration
- contact time

Employing a chemical adsorption technology of a clay-zeolite media (natural adsorptive, ionic chargeable material), is unique to the industry as follows:

- small foot print (installed in ground or underground)
- controlled effluent pH
- naturally available raw materials employed (no synthetic resins or reagents)
- spent TP removal material after life cycle completion used as soil conditioner
- modular design

The project outcome was intended to create and test a bench scale apparatus with engineered adsorption clay-zeolite media, and prepared for further field analysis, such as pH stabilization, life-cycle, environmental impacts, as well as disposal and/or regeneration.

1.3 INDUSTRY-ACADEMIA COLLABORATION PROGRAM

Under the guidance of Dr. G. Luk as the Principal Investigator (PI), the MASc graduate student of the Department of Civil Engineering at Ryerson University was responsible for conducting all experiments; collecting samples and correlating those with various literature reviews. Scheduled updates were established between the PI and the industry sponsor, Virtual Engineers.

This program provided the graduate student with the essential skills for the project specifics on both a practical as well as theoretical basis for the team to address and solve the problem; a valued platform for applied knowledge.

A set of five (5) milestones were established for this collaboration program, and was approved by OCE as follows:

TABLE 1.1 – TECHNICAL PROBLEM SOLVING AGREEMENT

	Milestone	Anticipated Outcome
1	<i>Review of existing phosphorus removal technologies</i>	Evaluation of methodology, strengths and limitations of phosphorus removal units on the market
2	<i>Study the chemical process for zeolite conditioning</i>	Experimental results demonstrating the significance and overall effectiveness of various chemicals for zeolite conditioning
3	<i>Phosphorus removal performance for various operating conditions and waste characteristics</i>	Experimental results of phosphorus removal under different environmental and operating conditions for a range of wastewater characteristics
4	<i>Design the process configuration for optimizing the unit performance</i>	Comparison of the merits of various design configurations and the recommendation of the most optimal design
5	<i>Prepare design drawings for unit fabrication</i>	AutoCAD drawings for the complete design of the phosphorus removal unit

All milestones have been completed, in addition to the attendance and representation in the Ontario Centres of Excellence Discovery Conferences of 2011 and 2012. The project overview was compiled in participation of the OCE Discovery 2012 Video Competition, with a YouTube link titled ‘OCE Discovery 2012 Video Contest -- TP Removal -- Ryerson University’ at <http://www.youtube.com/watch?v=9w4iemolcIA>. This provided the opportunity for industry, academia and public alike to become aware of the problem, objective, outcome and impact of this research venture.

1.4 THESIS OVERVIEW

This thesis is composed of 8 chapters. Chapter 1 presents an overview of the research. Chapter 2 provides an understanding of the background knowledge behind phosphorus as well as the various removal technologies that have evolved. Chapter 3 initiates the experimental element of this research, providing an in-depth look into the unique material – *zeolite*; including mineralogy and material modification techniques. Chapter 4 presents key research findings, which were employed to develop the experimental design parameters, outlined in chapter 5. Materials and methods are also described in chapter 5. Chapters 6 and 7 provide the results and analysis, respectively based on the various stages of the investigation. Finally, chapter 8 provides the study limitations, conclusions, and recommendations for future research.

2 BACKGROUND AND LITERATURE REVIEW

This report chapter provides key literature findings that pertain to the many aspects that embody phosphorus, including its collection and analysis process as well as existing removal technologies.

2.1 PHOSPHORUS

Phosphorus within natural waters is divided into the following three constituents, as illustrated in Figure 2.1 (Carlson, 1996):

1. Soluble Reactive Phosphorus (SRP)
2. Soluble Unreactive or Soluble Organic Phosphorus (SUP)
3. Particulate Phosphorus (PP)

$$\text{Soluble Phosphorus (SP)} = \text{SRP} + \text{SUP} \quad [2.1]$$

$$\text{Total Phosphorus (TP)} = \text{SRP} + \text{SUP} + \text{PP} \quad [2.2]$$

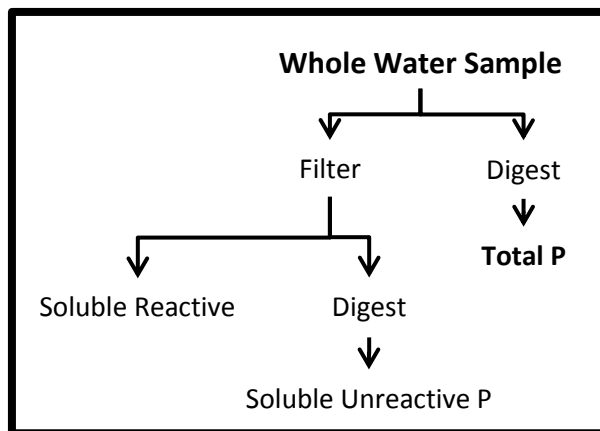


FIGURE 2.1 - PHOSPHORUS COMPONENTS (CARLSON, 1996)

The following subsections outline the chemical characteristics of the various components of phosphorus.

2.1.1 SOLUBLE REACTIVE PHOSPHORUS (SRP)

This fraction consists mainly of the inorganic orthophosphate form of phosphorus. Orthophosphate (PO_4) is directly consumed by algae, and its concentration establishes an index of the amount of phosphorus directly accessible for algal growth (Carlson, 1996).

Orthophosphate must be very low to undetectable when phosphorus limited situations are a requirement. As its concentrations increase, it is implied that phosphorus is either not relied upon by algae or that the rate of increase is greater than what the biota is able to consume. Consequently, SRP measurements relatively indicate the degree of phosphorus limitation of algae (Carlson, 1996).

2.1.2 SOLUBLE UNREACTIVE PHOSPHORUS (SUP)

Filterable phosphorus forms exist in this division, which do not react with testing reagents. It is composed of organic phosphorus forms and chains of inorganic phosphorus molecules (polyphosphates). The relative fraction size is reliant on the type of filter used to isolate the soluble from particulate fractions (Carlson, 1996).

Two key organic phosphorus molecules' categories prevail in natural waters. Firstly, algal and bacterial metabolically derived small molecular weight compounds; they release orthophosphate upon alkaline phosphatase treatment and must be digested to react with phosphorus testing reagents. Next, coloured, large molecular weight compounds that release orthophosphate in ultraviolet light environments. These compounds' reactivity varies with respect to digestion, and maybe detected as SRP. These organic forms encourage algal and bacterial growth, but must first be converted to orthophosphate through enzymes or ultraviolet light in order for the biota to consume it (Carlson, 1996).

2.1.3 SOLUBLE PHOSPHORUS (SP)

This phosphorus constituent is determined after filtrate digestion and should contain both the organic and inorganic forms converted to orthophosphate by digestion. The amount of phosphorus present depends on the filter implemented; large effective filter pore size allows more particulate material to pass through, be digested, and be deemed soluble. The further the filtering becomes from the standard of a 0.45 micron membrane, the greater the effect on SP concentration as well as the soluble organic phosphorus (difference between SP and SRP) (Carlson, 1996).

2.1.4 PARTICULATE PHOSPHORUS (PP)

Particulate phosphorus is the filter's retained materials; inorganic and organic, particulate and colloidal. This contains bacteria, algae, detritus, and inorganic particulates (clays, zooplankton, zooplankton, sediments, and large plant material).

It is measured by filtering a known volume of water through a membrane filter, followed by digesting the filter. This approach concentrates samples from low particulate waters, increasing the test sensitivity but also increases the likelihood of capturing large particles. A size-fractionated phosphorus would be best, such that phosphorus is sampled fitting for each size fraction. Given experimental circumstances, this would not be possible, such that PP is optimally determined by the subtraction from TP; particulate value is affected by filter pore size (Carlson, 1996).

2.1.5 TOTAL PHOSPHORUS

Total Phosphorus (TP) is a compilation of all filterable and particulate forms. It is applied to various freshwater empirical models, connecting loading and content estimates within lakes; for example, the algal variable such as chlorophyll. Consequently, TP is the most analyzed phosphorus fraction (Carlson, 1996).

TP is characterized based on how much phosphorus is present in its various forms, to be oxidized into orthophosphate. Analytical tests for digestion and analysis vary, which introduce error, data limitations, and subsequent empirical relationship modifications; all of which must be noticed and applied accordingly (Carlson, 1996).

2.2 PHOSPHORUS COLLECTION AND ANALYSIS

2.2.1 LIMITS OF DETECTION

The Ascorbic Acid Method is most frequently used of all tests. The molybdate reagent reacts with orthophosphate (synonymous with phosphate), creating phosphomolybdic acid, and forms the coloured molybdenum blue once reduced with ascorbic acid. Once the blue appearance is exposed, the peak absorbance at 885 nm is in the infrared region. According to Beers Law, absorbance is linearly correlated to concentrations; phosphate concentrations are detected at 5 to 1,300 µg/L with a pathlength of 1 cm (Carlson,1996).

Appropriately defined phosphorus limits are critical. Common practice suggests that detection limits of 10 or 5 µg/L (or lower) is necessary for adequate resolution in monitoring. As a rule of thumb, the detection level is approximately double the standard deviation of replicate blanks, and the lowest level of quantification is approximately five times this standard deviation. Therefore, the level of quantification better defines the lower levels of identifiable concentrations of TP, which occur with lower detection levels. Results should be reported as phosphorus concentrations, not phosphate, present in the water. As orthophosphate is the form measured in the test, the results may be presented as PO₄P (Carlson, 1996).

It is to be noted that for all bench scale testing, the Orbeco MC500 Colorimeter was employed (with reference to Appendix F). It involves the Total Phosphorus Analysis (326); a tube test reagent, with a narrow detection range of 0.02-1.1 mgP/L and absorbance of 660 nm. This meter employs the Acid Persulfate Digestion (4500-P.B.5) and Ascorbic Acid Method (4500-P.E), as per the Standard Methods for the Examination of Water and Wastewater (Greenberg, 1992).

2.2.2 DIGESTION METHODS

TP and total soluble phosphorus must be exposed to digestion, in order to measure the orthophosphate form. The Acid Persulfate Test extracts most but not all phosphorus, and it is the safest and most common technique (Carlson, 1996).

2.2.3 INTERFERENCES

Phosphorus analysis is affected by various substances; such as arsenate (algae and aquatic macrophytes control) and high concentrations of silica. Also, physical appearance of samples, such as substantial humic colour or clay turbidity, interferes. Overall, phosphorus tests are very sensitive to small contaminations, as it is detected in tap water, on fingers, in soap and detergents, and buffers. As a result, cleanliness must be optimized in both the field and laboratory (Carlson, 1996).

It is to be noted that prior to inserting the vials into the Colorimeter, they were thoroughly wiped down with a lint-free, Kim Tech delicate task wipers to avoid further interference.

2.2.4 RECOMMENDATIONS

It is recommended that Total Phosphorus be the major form of phosphorus measured. In addition, total sample preservation is recommended, along with strong acid handling safety. Pre-cleaned, acid washed sample containers should be provided, in order to minimize sample and container manipulations (Carlson, 1996).

2.3 EXISTING PHOSPHORUS REMOVAL TECHNOLOGIES

There are various technologies that remove phosphorus, biological, chemical and physical. In order to make essential engineering decisions, a stringent screening methodology must be considered towards a step-by-step selection process. However, the effectiveness of this process depends on the quantity and detail of the treatment information provided (Bowker, 1990).

The selection procedure must consider all aspects of the phosphorus removal process, including its influence on the performance, operation and maintenance of the treatment plant. There are many significant factors, comprised of the following (Bowker, 1990):

- degree of phosphorus removal
- plant size
- impact on sludge handling
- total cost
- impact on operation and maintenance
- permanent or temporary nature of phosphorus removal required

The development of a phosphorus removal system relies on data collection, which depends on both the effluent discharge requirements and wastewater characteristics. With regards to the former, daily, weekly, monthly, and seasonal limits must be recorded. These restrictions may be set as minimum percent removal, specific effluent concentration, or mass per day basis. Permit limits for BOD₅, TSS, pH, NH₄-N and Total N must be identified. Data collection of influent wastewater quality includes the following (Bowker, 1990):

- flow (average, maximum m³/d; peak/average ratio)
- total P (average mg/L)
- soluble P (average mg/L)
- BOD₅ (average mg/L)
- BOD (average mg/L)
- TSS (average mg/L)
- NH₄-N (average mg/L²)
- total N (average mg/L²)
- pH
- temperature
- alkalinity (average mg/L)
- TBOD:Total P ratio

When selecting the proper removal approach, there are other influences to consider, such as the sludge disposal alternatives, service area characteristics, plant size and location, facility design lifetime, and local availability and cost of chemicals. Consequently, pilot testing is highly recommended, assessing performances of all TP removal processes (Bowker, 1990).

The development of phosphorus removal technologies commenced during the 1950s in Switzerland. This was initiated to address eutrophication concerns caused by phosphorus invasion of surface waters. Chemical precipitation was initially the leading global technology; this has evolved into various biological and physical processes. Tables 2.1 to 2.3 provide an overview of the evolution, processes, and wastewater treatment framework of the various technologies. With greater detail, the various phosphorus removal technologies are summarized in Table 2.1. The application of phosphorus adsorbents, indicated in Table 2.2, is of primary importance in this report; the zeolite substrate will be researched further. As indicated in Table 2.3, the adsorption technology must be further investigated (Morse, 1998).

TABLE 2.1 – P REMOVAL TECHNOLOGY EVOLUTION (MORSE, 1998)

Phosphorus Removal/ Recovery Technology	Development Status	Development Timescale	Country of Origin
<i>Chemical Precipitation</i>	Commercial	~ 1950 to date	Global
<i>Biological P (and N) Removal</i>	Commercial	~ 1960 to date	Global
Phostrip	Commercial	~ 1965	USA
Modified Bardenpho	Commercial	~ 1974 to date	South Africa
Phoredox	Commercial	~ 1976 to date	South Africa
A/O	Commercial	~ 1980 to date	USA
University of Cape Town (UCT)	Commercial	~ 1983 to date	South Africa
Modified UCT	Commercial	~ 1990	South Africa
Retanox	Commercial	~ 1982	UK
Biodenipho	Commercial	~ 1980	USA
<i>Crystallisation</i>			
DHV Crystalactor™	Full-scale	~ 1979 to date	Netherlands
CSIR	Laboratory	~ 1992 to date	South Africa
Kurita	Laboratory	~ 1984 to date	Japan
Phosnix	Laboratory	~ 1994 to date	Japan
Sydney Water Board	Laboratory	~ 1993 to date	Australia
OFMSW	Laboratory	~ 1994 to date	Italy, Spain
<i>Novel Nutrient Removal</i>			
HYDRO concept	Full-scale	~ 1991 to date	Scandinavia
AFBP	Pilot	~ 1994 to date	Japan
Maezawa FBPS	Pilot	~ 1993 to date	Japan
<i>Other Wastewater</i>			
RIM-NUT (ion exchange)	Demonstration	~ 1986 to date	Italy
Smit-Nymegen (magnetic)	Pilot/FS	~ 1991 to date	Netherlands
Sirofloc (magnetic)	Demonstration	~ 1979 to date	Australia
Phosphorus adsorbents	Laboratory	~ 1970 to date	Global
<i>Tertiary Filtration</i>			
Slow sand filters	Commercial		
Shallow bed filters	Commercial		
Rapid gravity filters	Commercial		
Rapid deep-bed filters	Commercial		
Moving bed filters	Commercial		
Pressure filters	Commercial		
<i>Sludge Treatment</i>			
Simon-N-Viro	Full-scale	~ 1990 to date	USA
Swiss Combi	Full-scale	~ 1980 to date	Switzerland
Recovery from sludge ash	Laboratory	~ 1995 to date	Japan

TABLE 2.2 – P REMOVAL TECHNOLOGY PROCESS (MORSE, 1998)

Technology	Objective	Process Summary	Main Input	Auxiliary Inputs	Main Output	P Form/ Content
<i>Chemical precipitation</i>	Phosphorus removal	Addition of metal salt to precipitate metal phosphate removed in sludge	Wastewater (primary, secondary, tertiary or sidestream)	Fe, Al, Ca; may require anionic polymer	Chemical sludge	Mainly chemically bound as metal phosphate
<i>Biological phosphorus removal</i>	Phosphorus removal (also nitrogen removal)	Luxury uptake of P by bacteria in aerobic stage following anaerobic stage	Wastewater (primary effluent)	May require external carbon source (e.g. methanol)	Biological sludge	Phosphorus Biologically bound
<i>Crystallisation (DHV Crystalactor™)</i>	Phosphorus removal recovery	Crystallisation of calcium phosphate using sand as a seed material	Wastewater (secondary effluent or sidestream)	Caustic soda/milk of lime, sand; may need sulphuric acid	Calcium phosphate, sand	Calcium Phosphate (40-50%)
<i>Advanced chemical precipitation (HYDRO)</i>	Phosphorus and nitrogen removal	Crystallisation of phosphorus/organic matter and hydrolysis to give carbon source for N removal	Wastewater (primary influent)	Polyaluminum chloride PAC)	Chemical sludge	Chemical sludge
<i>Ion exchange (RIM-NUT)</i>	Fertiliser (struvite) production	Ion exchange removes ammonium and phosphate which are precipitated	Wastewater (secondary effluent)	H ₂ PO ₄ , MgCl, NaCl, NaCO ₃ , NaOH	Struvite (MgNH ₄ PO ₄)	Phosphate slurry
<i>Magnetic (Smit-Nymegen)</i>	Phosphorus removal	Precipitation, magnetite attachment, separation and recovery	Wastewater (secondary effluent)	Lime, magnetite	Primarily calcium phosphate	Calcium phosphate
<i>Phosphorus adsorbents</i>	Phosphorus removal	Adsorption and separation	Wastewater	NA	No information	Calcium phosphate
<i>Tertiary filtration</i>	Effluent polishing	Filtration	Secondary effluent	Media	Tertiary sludge	Insoluble phosphate
<i>Sludge treatment</i>	Sludge disposal	e.g. sludge drying, reaction with cement dust	Sludge	Depends on process	Soil conditioner	Dry granule, low in P
<i>Recovery from sludge ash</i>	Phosphorus recovery	Extraction from sludge ash	Sludge ash from biological removal	NA	NA	NA

TABLE 2.3 – P REMOVAL TECHNOLOGY PROCESS (MORSE, 1998)

Technology	Works Application	Retrofit Option	Recovery Value		Technology Advantages	Technology Disadvantages
			Industrial	Agriculture		
<i>Chemical precipitation</i>	Primary, secondary or tertiary treatment, or activated sludge recycle	Can be flexibly applied, depending on circumstances	Low: metal-bound P makes recycling difficult	Moderate: P availability variable	Established low technology; Easy to install and operate; P removal can be high	Requires chemicals; Sludge production increases; P recyclability variable
<i>Biological phosphorus removal</i>	Secondary treatment or activated sludge recycle	Difficult, unless existing capacity is available or reallocated	Moderate: biologically-bound P more recyclable	Moderate: biologically-bound P more available	Establishing technology; No need for chemicals: N and P removal possible; P more recyclable	More complex technology to install and operate; Sludge handling may be more difficult
<i>Crystallisation (DHV Crystalactor™)</i>	Tertiary treatment or recycle stream	Can be retrofitted to most types of works	Very high: easily recycled by industry	Moderate: P availability variable	Demonstrated technology; Can be retrofitted; Product recyclable	Requires chemicals and operation skills
<i>Advanced chemical precipitation (HYDRO)</i>	Primary (precipitation), secondary nitrogen removal	Retrofit possible, but extensive modifications usually required	Low: metal-bound P makes recycling difficult	Moderate: P availability variable	Proven (pilot) technology; Enhanced P and N removal; Part of a complete recycling concept	Requires chemical; Complex technology; P may not be in a convenient form for recycling
<i>Ion exchange (RIM-NUT)</i>	Tertiary treatment only	Retrofit possible, depending on situation	Moderate: would require modifications	High: struvite is a good slow-release fertiliser	High P removal; Struvite produced has high recycling potential for agriculture	Requires chemical; Complex technology; Waste elate
<i>Magnetic (Smit-Nymegen)</i>	Tertiary treatment only	Retrofit possible, depending on situation	Moderate: would require modifications	Low: agricultural suitability unknown	High P removal	Unnecessarily complex technology; Requires chemicals
<i>Phosphorus adsorbents</i>	Not sufficiently developed	Not sufficiently developed	Low: unknown	Low: unknown	Potential for P recovery with few chemicals	Unproven technology
<i>Tertiary filtration</i>	Tertiary treatment only	Easy to retrofit to most works	None: no potential	None: no potential	Established technology; Easy to retrofit and use	Not a recovery technology (no useful product)
<i>Sludge treatment</i>	Sludge stream	Typically requires modification	Low: difficult to recycle	High: P re-use high	Increases sludge value	More complex technology; Chemicals required
<i>Recovery from sludge ash</i>	After sludge incineration	Easy to append to treatment stream	High: p readily leached	Moderate: P re-use possible	Potential for recovery P at high concentration	Undeveloped technology; Only possible if incineration is the usual disposal route

2.3.1 BIOLOGICAL

This phosphorus removal technology evolved from research conducted in the 1950s. It follows the concept called luxury uptake; within specific circumstances, activated sludge consumes substantial phosphorus amounts in excess to encourage normal biomass growth. This technology's application and process is established for new or redeveloped works of large operations. Advantages include the avoidance of chemicals and excess sludge production however, plant configurations and operations are more complex (Morse, 1998).

As observed in Figure 2.2, an anaerobic and/or anoxic zone positioned prior to the aerobic stage encourages P removal in the activated sludge process. Note that degradable Chemical Oxygen Demand (COD) must be available from volatile fatty acids generated from pre-fermenting sludge using storage or thickeners, as well as acetic acid or sodium acetate addition (Morse, 1998).

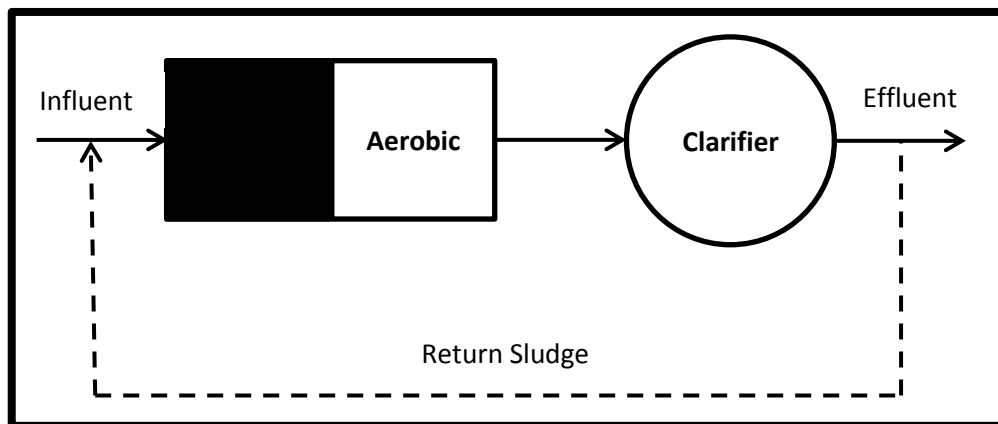


FIGURE 2.2 - BIOLOGICAL PHOSPHORUS REMOVAL (MORSE, 1998)

The lack of oxygen or nitrates causes bacteria to consume acids and release P into solution. During the aerobic stage luxury uptake, P removal rate increases to 80-90%. Given that biological removal is inconsistent, chemical secondary precipitation balance is required to meet effluent standards. Recovered P is biologically bound and may be released into solution under anaerobic conditions (Morse, 1998).

There are various biological phosphorus removal alternatives, as indicated below. Figure 2.3 displays the removal sequence of options 1, 2 and 4 (Bowker, 1990).

1. Phostrip Process
2. Modified Bardenpho Process
3. UCT (University of Captown) Process
4. A/O process
5. Sequencing Batch Reactor (SBR) Process

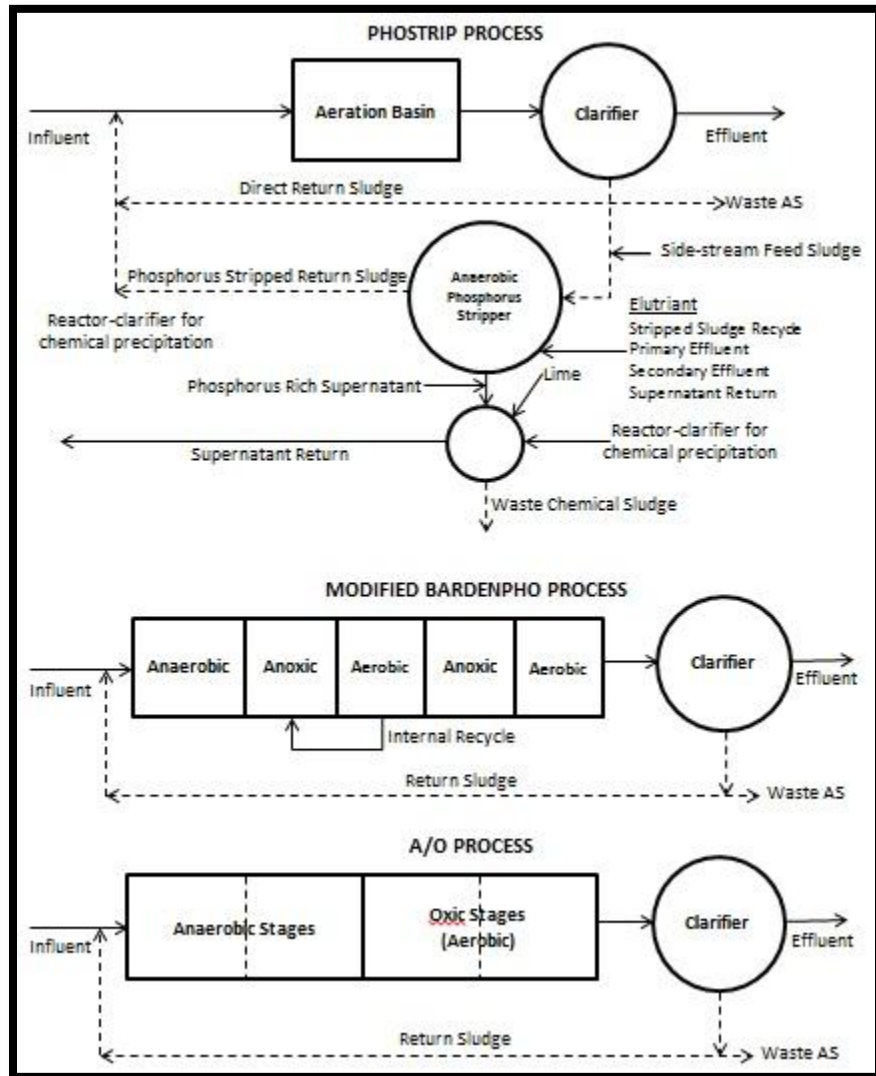


FIGURE 2.3 – COMMERCIAL BIOLOGICAL PHOSPHORUS REMOVAL PROCESSES (MORSE, 1998)

The Phostrip Process incorporates an anaerobic zone in the sludge recycle system. It retrieves side-stream from return activated sludge and imposes anaerobic conditions in a separate tank prior to returning the sludge to aeration basin. Activated sludge exposed to an anaerobic condition requires maintenance, causing the release of phosphorus. Once sludge is returned or re-aerated, excess phosphorus is consumed by the activated sludge biota. Lime added to precipitate the phosphorus is released in the anaerobic tank (Bowker, 1990).

The Modified Bardenpho and UCT Processes are both designed to remove nitrogen and phosphorus from wastewaters. The A/O Process is predominantly intended for phosphorus removal, but also nitrification is accomplishable. The SBR Process involves limited full-scale tests, modifying sequencing periods and aeration schedules in order to fulfill phases of anaerobic/aerobic mixing (Bowker, 1990).

The aforementioned processes' degree of phosphorus removal (excluding Phostrip) depends on the ratio of influent BOD to Phosphorus of wastewater; final effluent levels range from 1.0-2.0 mg/L TP. The ratio of TBOD: TP of at least 20:1 (SBOD:soluble P of 12:1 to 15:1) is required (Bowker, 1990).

2.3.2 CHEMICAL

2.3.2.1 CHEMICAL PRECIPITATION

This removal technology is a physico-chemical process, using di- or tri- valent metal salt that is added to wastewater. Consequently, insoluble metal phosphate precipitation is settled out by sedimentation. This is followed by the addition of iron or aluminum suitable metal, added as chlorides or sulphates, including lime to precipitate calcium phosphate (Morse, 1998).

Through the metal salt addition process, metal salts of aluminum and iron are added to the wastewater to react with phosphorus to form insoluble aluminum or iron phosphate precipitates; compounds include aluminum sulfate (alum), sodium aluminate, ferric chloride, and ferrous sulfate. It is commonly added upstream of a primary or secondary clarifier, or in all processes (including tertiary). The addition quantity depends on the phosphorus species' concentration within the influent and permit requirements. Metal salt addition may achieve 80-95% Total Phosphorus (TP) removal, for effluent of TP at 1.0 mg/L limitations such that TSS is maintained to less than 15 mg/L, along with the conventional treatment process (Bowker, 1990).

The lime addition process involves adding lime to the primary clarifier or to effluent from the secondary clarifier. It is a water softening process, such that lime quantity depends on the wastewater's alkalinity rather than phosphorus content. The single-stage method is low-lime at a pH below 10.0 and 1.0 mg/L effluent TP levels. The high-lime method is a two-stage process, at a pH of 11.0-11.5 and <1.0 mg/L (very low) effluent TP levels. The latter process is more time consuming, requiring re-carbonation to reduce the wastewater's pH prior to discharge. Overall, the lime addition procedure produces substantial sludge quantities, compared to the metal salt addition process. This system is pH controlled, relying on lime storage, and mixing units (Bowker, 1990).

As observed by Table 2.4 and Figure 2.4 below, chemical precipitation is a flexible approach that is applied to several wastewater treatment stages (Morse, 1998).

TABLE 2.4 – WASTEWATER TREATMENT (MORSE, 1998)

Wastewater Treatment Stage	Chemical Dosage	P Removal
<i>Primary Precipitation</i>	Prior to primary sedimentation	In primary sludge
<i>Secondary/Simultaneous Precipitation</i>	Directly to aeration tank of activated sludge process	In secondary sludge
<i>Tertiary Treatment</i>	Follows secondary treatment	

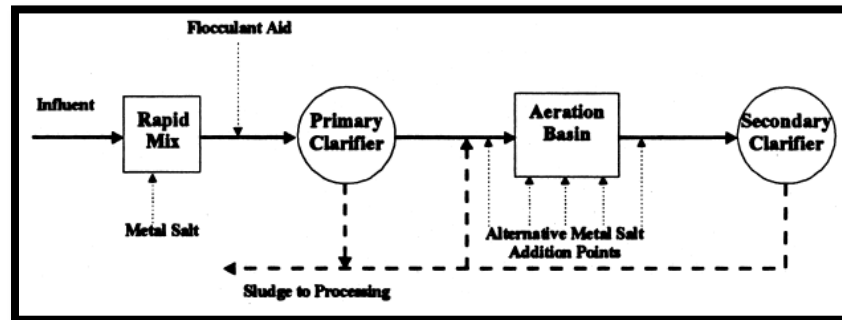


FIGURE 2.4 – CHEMICAL PRECIPITATION (MORSE, 1998)

2.3.2.2 ADVANCED CHEMICAL PRECIPITATION AND NUTRIENT REMOVAL

The nutrient entitled nitrate is a growing issue in both surface and coastal waters. Its removal commonly occurs in conjunction with that of phosphorus. The biological nitrification-denitrification process requires both carbon and energy sources. Figure 2.5 shows the process configuration of the HYDRO Concept, which is a highly-effective and very popular method of phosphorus removal for large-scale treatment (Morse, 1998).

The HYDRO Concept employs chemical precipitation to develop carbon and energy availability. It is a combination of pre-precipitation, sludge hydrolysis and biological denitrification. Pre-precipitation involves ferric/aluminium chloride (polyaluminum chloride, PAC) assisted by coagulants. It removes 75% of organic matter from wastewater influent, as well as incoming phosphorus. The removed sludge is then hydrolyzed, breaking organic material into soluble, biodegradable substances. A standardized nitrification-denitrification stage follows. The excess sludge is treated by employing standard anaerobic digesters. The recovered phosphorus is contained in the primary sludge. All in all, phosphorus removal achieved through chemical precipitation and/or biological removal is to satisfy effluent quality standards (Morse, 1998).

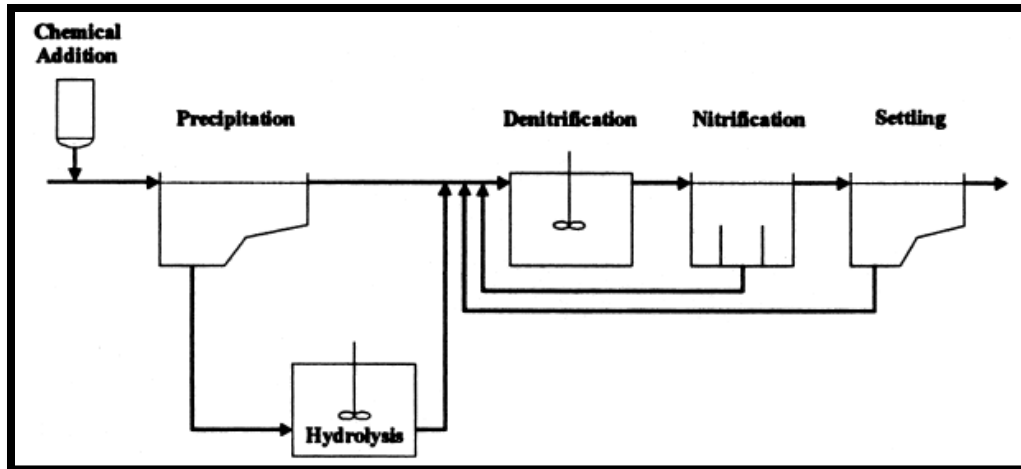


FIGURE 2.5 - THE HYPRO CONCEPT (MORSE, 1998)

The HYPRO Concept has generated various modifications, including the Anaerobic Fluidized Bed Bioreactor (AFPB) and the Maezawa Fluidized Bed Pellet Separator Reactor.

The AFPB is the synchronized removal of suspended solids, organic matter, phosphorus and nitrogen. It involves a two-stage pilot-scale treatment system; the first stage involves dosing influent wastewater with PAC, then the AFPB replaces the primary clarifier in the HYPRO concept. The second stage involves conventional nitrification treatment; recycled denitrified in the anaerobic AFPB. The phosphorus is precipitated by PAC and removed in the chemical sludge. The Maezawa Fluidized Bed Pellet Separator Reactor is similar to AFPB Bioreactor, with addition of a tertiary micro-membrane filter and no denitrification occurrence. The phosphorus is removed as chemically precipitated sludge from the AFPB (Morse, 1998).

2.3.2.3 MAGNETIC ATTRACTION

The magnetic attraction water treatment system follows the Smit-Nymegen Process. This is a tertiary treatment procedure, such that lime is used to precipitate calcium phosphate, attached to magnetite and separated using a prompted magnetic field. After isolation, magnetite is disengaged from the phosphate in a separator unit by shear forces and a drum separator. Depending on the final intensions of the by-product, separated suspension of calcium phosphate or carbonate in water is processed accordingly (Morse, 1998).

2.3.2.4 PHOSPHORUS ABSORBENTS

The adsorbent technique is currently facing extensive laboratory scale research. It is most advantageous given that no additional sludge is produced, reagents are not required to overcome high alkalinity and the pH of the wastewater is not affected. Various filter materials (absorbents or molecular sieves) have been investigated, including activated alumina, half-burned dolomite, and red mud (Morse, 1998). The material entitled zeolite will be of primary analysis. Section 3.2 (Commercial Properties), Subsection 3.2.1 (Absorption Capacity) will provide a greater insight of this removal technology, specifically pertaining to the adsorbent material under analysis (Morse,1998).

2.3.3 PHYSICAL

2.3.3.1 CRYSTALLIZATION

This physical removal technology began in the 1970s, in order to address more rigorous removal requirements. The DHV Consulting Engineers are the leaders in this technology; DHV Crystalactor W Process. It involves calcium phosphate crystallization on seeding grain (sand) within a fluidized reactor (Figure 2.6). It is a fully automated operation that may be retrofitted for various treatment facilities, where favourable conditions involve caustic soda or lime milk. Pellets must be replaced occasionally by smaller diameter seed grains in order to ensure continuous operation and optimal fluidization. Ultimately, it is of high rate – short retention time – small reactor. Crystallization may require pre-degasification and post-filtration. Degasification is administered with the addition of sulphuric acid, which reduces carbonate that causes calcium carbonate formation and recycling complications. Filtration of the effluent through dual-media anthracite sand reduces the phosphorus concentrations further (Morse, 1998).

An advantage of this technology is that it does not produce any additional sludge, and only a quantity of water-free pellets consisting almost entirely of calcium phosphate (40-50%) and seed material (30-40%) are present in minimal quantity. Also, pellet production occurs approximately 7-14 kg/PE/year and is recyclable by the phosphate industry (Morse, 1998).

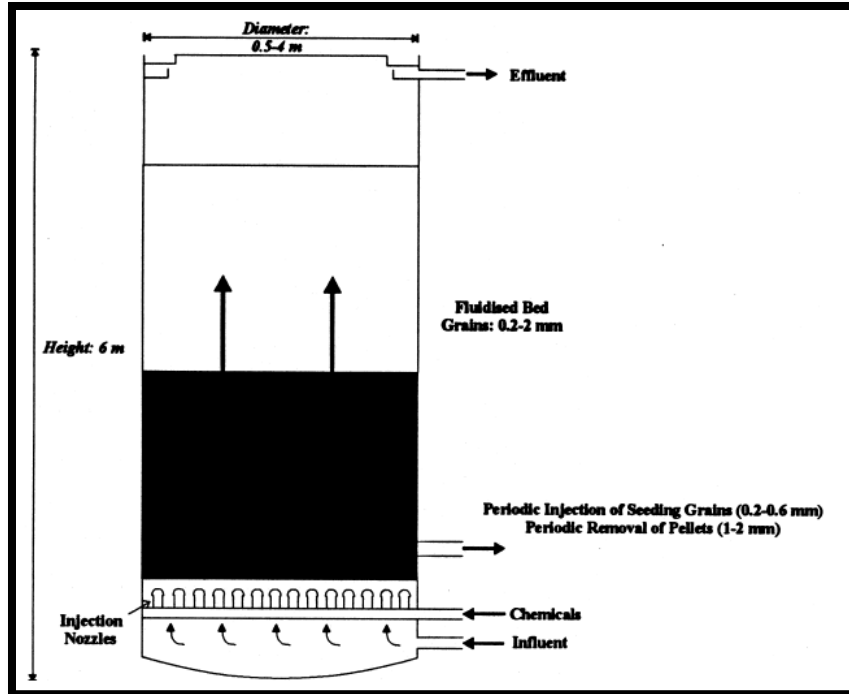


FIGURE 2.6 – DHV CRYSTALACTOR (MORSE, 1998)

Various crystallization-based phosphorus removal technologies have yet to proceed past the demonstrative stage. However, many modifications to this technology have been developed, as observed in Table 2.5 (Morse, 1998).

TABLE 2.5 – PHOSPHORUS REMOVAL CRYSTALACTOR TECHNOLOGIES (MORSE, 1998)

Technology Variations	Description
<i>CSIR Fluidized Bed Crystallization Column</i>	<ul style="list-style-type: none"> Different seeding materials to produce granular hydroxyapatite or struvite (magnesium ammonium phosphate) To re-use these products as fertilizer; such that struvite has slow release potential
<i>Kurita Fixed Bed Crystallization Column</i>	<ul style="list-style-type: none"> Phosphate rock as seed material to produce hydroxyapatite Proper reaction conditions with the addition of calcium chloride and caustic soda
<i>Unitika Phosnix Process</i>	<ul style="list-style-type: none"> Magnesium chloride and alkali are mixed with wastewater to promote nucleation and growth of struvite crystals
<i>Sydney Water Board Process</i>	<ul style="list-style-type: none"> Gypsum provides a calcium ions source and magnesia is implemented as a contact bed for amorphous precipitation of calcium phosphate
<i>Anaerobic Fermentation Biological Nutrient Removal – Struvite Crystallization Process</i>	<ul style="list-style-type: none"> Involves a crystallization stage within a innovative approach to wastewater and waste management Struvite is produced from an enriched phosphorus stream following anaerobic digestion

2.3.3.2 ION-EXCHANGE MEMBRANE

This removal technology is formally entitled as the RIM-NUT Ion-Exchange-Precipitation Process. It involves the removal of ammonia and phosphate ions from tertiary wastewater to produce struvite. Cationic resin removes ammonium ions and a basic resin removes phosphate ions. Regeneration releases ammonium and phosphate, precipitated as struvite. With the addition of phosphate and magnesium salts, proper stoichiometry is established (Morse, 1998). Section 3.2 (Commercial Properties), Subsection 3.2.2 (Ion-Exchange Capacity) will provide a greater insight of this removal technology (Morse, 1998).

2.3.3.3 TERTIARY FILTRATION

Tertiary filtration is primarily conducted to with the intention to polish the effluent; the phosphorus removal is an accompaniment. In addition, the recovered sludge from backwashing is not recyclable (Morse, 1998).

2.4 PHOSPHORUS REMOVAL ABSORBENTS

With the generation of excess phosphorus content in lakes and rivers, eutrophication has become a major issue. Governmental regulatory pressure, such as the Ontario Ministry of the Environment standards indicated in The Lake Simcoe – Phosphorus Reduction Strategy (MOE, 2010), has increased in order to lower phosphorus concentrations through enhanced removal from wastewater and subsequent environmental quality improvement (Vohla, 2011).

Phosphorus removal through the adsorption technology is associated with physical-chemical and hydrological properties of filter material, such that phosphorus is adsorbed by or precipitated in substrate. A medium with high binding capacity is susceptible to clogging, affecting its life expectancy. As a result, the filter media selection is critical, based on hydraulic conductivity, chemical composition, and Ca:Fe:Al content. Table 2.6 displays three material categories; 1) natural materials, 2) industrial by-products, and 3) man-made products (Vohla, 2011).

TABLE 2.6 – FILTER MEDIA (VOHLA, 2011)

Natural Materials	Industrial By-Products	Man-Made Products
1. Apatite	1. Bauxsol™	1. Alumite
2. Bauxite	2. Burnt Oil Shale (BOS)	2. Filtra P
3. Dolomite	3. Coal Fly Ashes	3. Filtralite P™
4. Gravels	4. Ochre	4. Lightweight Aggregates (LWA)
5. Laterite	5. Red Mud	5. Norlite
6. Limestone	6. Oil Shale Ash Sediment	6. Oyster Shell
7. Maerl	7. Slag	7. Polonite
8. Marble		
9. Sands		
10. Opoka		
11. Peat		
12. Shale		
13. Sellsand		
14. Soils		
15. Wollastonite		
16. Zeolite*		

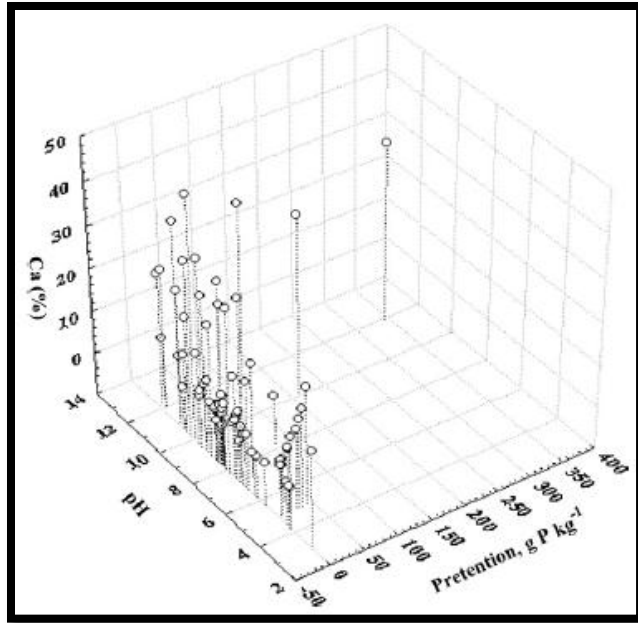
Research conducted by Vohla, C. et al. (2011) based their adsorbent selection on local availability and high phosphorus retention (removal efficiency). In addition, calcium-rich media was exposed to high temperatures to augment the CaO content and thereby modifying it for performance improvements. Applying a 95% confidence level of analysis, the phosphorus-retention – pH level – Ca/(CaO) content – hydraulic parameter relationship was generated (Vohla, 2011).

As the primary research focus to Vohla's report, it was decided that zeolite analysis was to be conducted through batch testing. This adsorbent at 3 g was added to 30 mL of phosphorous solution, such that 500-10,000 mg P L⁻¹ was exposed for 48 hours. The retention calculation was computed by the Langmuir Equation, where 2.15 g P kg⁻¹ was adsorbed. Zeolite is hydrated aluminum-silicate mineral, such that Al and Si polyhedral are linked by sharing O atoms. Maximum adsorption ranges variability from 0.01-0.05 g P kg⁻¹ to 0.462 g P kg⁻¹ (Vohla, 2011).

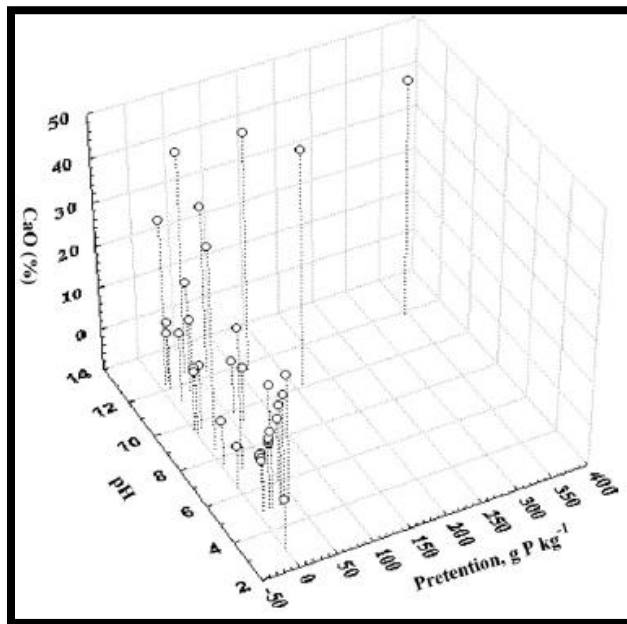
2.4.1 PHOSPHORUS RETENTION CAPACITY INFLUENCING FACTORS

2.4.1.1 ADSORBENT PH LEVEL AND Ca AND/OR CaO CONTENT

Calcium ions form stable and insoluble products with phosphate. Consequently, calcium-based materials are considered as potential adsorbents for phosphorus removal. Vohla, C. et al. determined that pH did not affect the phosphorus retention capacity. With a calcium content greater than 15%, a slight increase in retention capacity occurred. Although high Ca content correlated with high pH, this did not impose high retention capacity. The determination coefficient (R^2) of P-retention – pH level – Ca/(CaO) content relationships were also determined; the strongest correlation occurred between CaO and phosphorus retention at 0.51, relative to the visual representation of Figure 2.7 below (Vohla, 2011). The Langmuir Equation was used to determine maximum retention capacity, such that the highest phosphorous retention was observed during batch analysis (Vohla, 2011).



(A)



(B)

FIGURE 2.7 - RELATIONSHIP OF P RETENTION CAPACITY, (A) CA and (B) CAO CONTENT, AND PH LEVEL OF VARIOUS ADSORBENTS (VOHLA, 2011)

2.4.1.2 ADSORBENT SIZE AND COMPOSITION

Clogging becomes an issue when using reactive media in filtration. The size, biofilm development, carbon dioxide capture/precipitation, and flow rate are all contributing factors. Phosphorus adsorption on reactive material is mainly based on CaO dissolution, as well as phosphorus precipitation and crystallization. With a smaller adsorbent size, greater surface area is available for CaO dissolution. This encourages an increase in pH and probability of CaCO₃ precipitation and crystallization to form the system. Consequently, high pH at the outlet of the system becomes a major issue with respect to phosphorus removal efficiency (Vohla, 2011).

2.4.1.3 HYDRAULIC LOADING RATE AND RETENTION TIME

The relationship of Hydraulic Loading Rate (HLR) and Hydrological Retention Time (HRT; contact time) towards phosphorus removal is limited. Nevertheless, full- and pilot-scale treatment filter system analyses and column experiments demonstrate HLR at an optimal level contributes to phosphorus removal maximization. Furthermore, too long of a HRT encourages chemical clogging of hydrated oil shale ash and reduces the phosphorus removal capacity. As observed in Figure 2.8 (where the diamonds represent full-/pilot-scale constructed wetlands, and the triangles represent column experiments), filter media is selected at a medium HLR level to optimize P removal (Vohla, 2011).

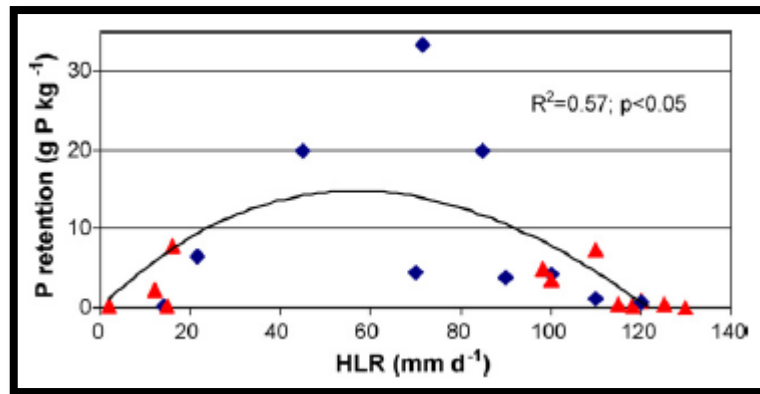


FIGURE 2.8 – P RETENTION CAPACITY AND HYDRAULIC RETENTION TIME RELATIONSHIP (VOHLA, 2011)

2.4.2 ADSORBENT LIFECYCLE

The phosphorus retention capacity is influenced by the following factors (Vohla, 2011):

- study duration
- water/material ration
- temperature
- initial P concentration range
- chemicals
- rotation speed
- regeneration effects of resting periods

Presently, performance analysis of long-term saturation time of adsorbents is limited. However, data experiments suggest filter materials' phosphorus retention capacity diminishes after 5 years (Vohla, 2011).

Zeolites are variable towards ion selectivity and competitive adsorption for multi-component systems. In addition, they are not suitable adsorbents for adsorption of anionic ions and organics, and must therefore be modified. Zeolite-contaminant-surfactant interactions require further investigations (Wang, 2010). A large number of filter media have been reviewed for phosphorus removal substrates for wastewater. There is an essential difference among the experimental conditions, which vastly affect the normalization of results. Previous tests conducted on batch mode, with emphasis on natural zeolites' applicability and selectivity. Future research must test industry feasibility through field-pilot-plant scale tests once batch conditions, adsorptive capacity, and uptake mechanisms are verified with real rather than artificial wastewater (Johansson Westholm, 2006; Wang, 2010).

2.5 INDUSTRY REMOVAL TECHNOLOGIES

2.5.1 SORBTIVE™ MEDIA

“SorbtiveMEDIA is an oxide-coated, high surface area reactive engineered media that performs absorption, surface complexation and filtration of storm water for total phosphorus removal.” It captures dissolved phosphorus by sorption, which enables high TP removal. It provides 100 to 1,000 times more pollutant removal, as it does not desorb or leach other pollutants.”

(Corporation’s Claim by Imbrium Systems, 2012)

2.5.1.1 WHAT IS SORBTIVEMEDIA?

SorbtiveMedia is a combination of Storm water Best Management Practices (BMPs) to capture Total Phosphorus as well as Total Suspended Solids. It is unique with its fast-reactive kinetics and long-lasting Bed Volume capacity for capturing dissolved phosphorus (Imbrium Systems, 2012).

Its high surface area and oxide coating characteristics sorb dissolved phosphorus and filters particulate-bound phosphorus by seizing fine sediment. High TP removal is achieved through the following mechanisms (Imbrium Systems, 2012):

1. Physical Filtration –particulate-bound phosphorus and sediment removal
2. Sorption – physio-chemical removal of dissolved phosphorus

SorbtiveMEDIA is considered a cost-effective solution due to its high and fast abilities, with excellent treatment life-cycle (Imbrium Systems, 2012).

2.5.1.2 PERFORMANCE

SorbtiveMEDIA is applicable to storm water treatment systems to inertly obtain very high TP removal rates, with a high sorption capacity, fast reaction kinetics and optimal treatment life-cycle compared to conventional media. Performance indicators include (Imbrium Systems, 2012):

- Percent (%) TP or DP (Dissolved Phosphorus) removal
- TP or DP effluent mg/L discharge maximum limit (low TP effluent concentrations at < 0.1 mg/L)
- TP or DP annual load reduction pounds/acre/year
- Maintenance frequency (media replacement).

2.5.1.3 SPECIFICATIONS

SorbtiveMEDIA specifications are obtainable in a variety of granular sizes. An 800 to 5,000 micron media gradation is common for thorough storm water filtration cartridges and infiltration (0.74 g/cm³ bulk density, 75-100 m²/g specific surface area, and 1.5 cm/s hydraulic conductivity). For sand filters and bioretention, 150 to 4,750 microns would be applied (Imbrium Systems, 2012).

2.5.1.4 ANALYSIS

Various experimental analyses were conducted by the corporation. *Adsorption Equilibrium Isotherm* testing was performed on various media (including a Zeolite, Perlite and Carbon mix); under simulated storm water conditions, through a range of dissolved phosphorus concentrations to determine the sorption capacity for dissolved phosphorus obtainable for each media (Imbrium Systems, 2012).

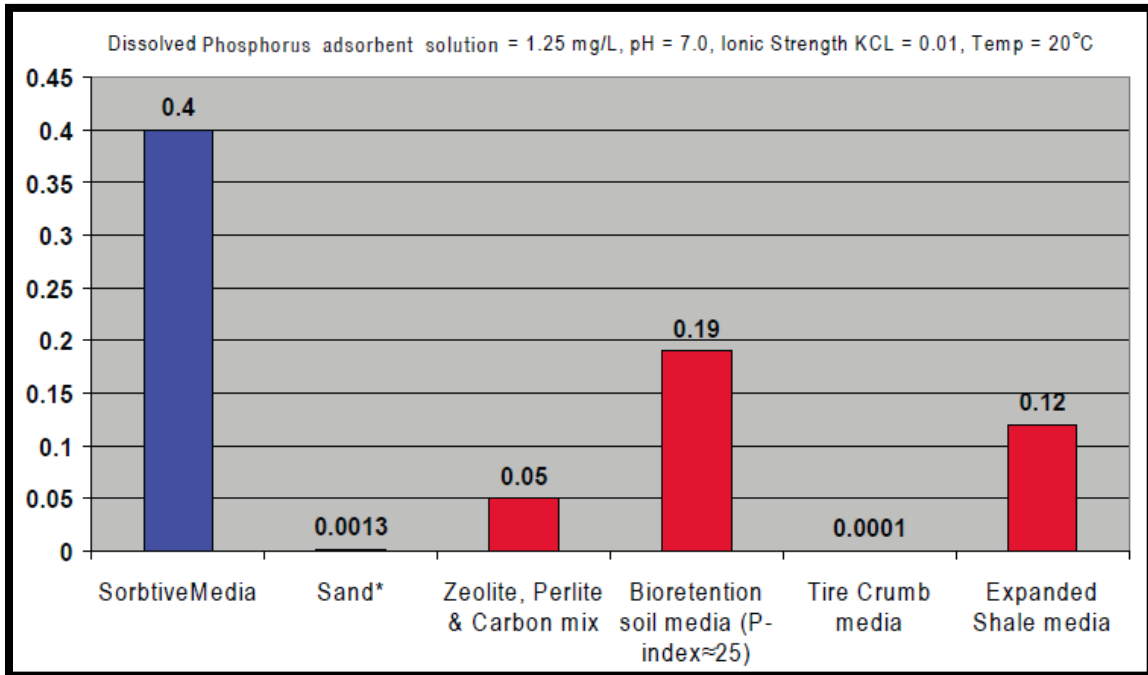


FIGURE 2.9 – ADSORPTION 1-POINT ISOTHERM EQUILIBRIUM CAPACITY (MG/G) OF DP (IMBRIUM SYSTEMS, 2012)

Applying the Freundlich Isotherm Model to determine sorption capacity, a point from the isotherms was selected, indicated above by milligrams of dissolved phosphorus sorbed per gram of media. Media quantities and dissolved phosphate solution of 0.5 g and 40 mL, respectively, were mixed in a 50 mL polyethylene centrifuge tube, on a bench shaker at 100 rpm for 24 hours and 20°C. This was followed by filtering the contents through 0.45 µm syringe filter. The total dissolved phosphate concentration in the filtrate was measured. The Adsorption Capacity (mg/g) was determined as the amount of dissolved phosphorus adsorbed by the media (i.e. difference between the initial and final equilibrium concentrations) (Imbrium Systems, 2012).

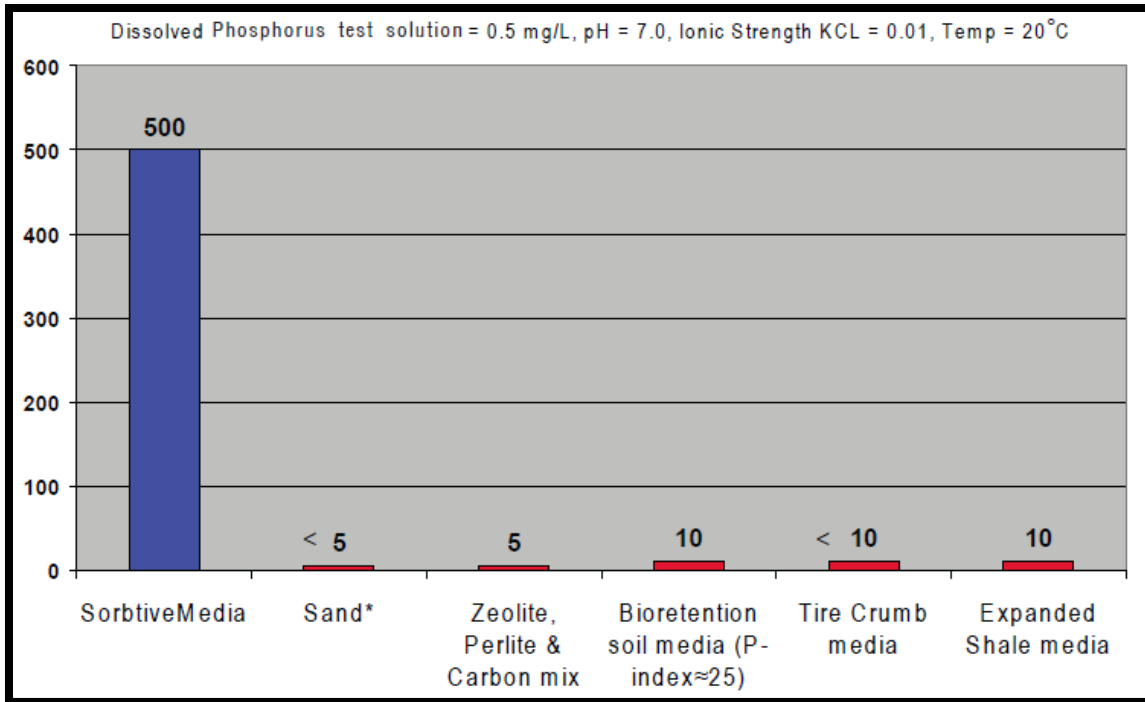


FIGURE 2.10 – NUMBER OF BED VOLUMES (BV) AT BREAKTHROUGH OF 50% DISSOLVED PHOSPHORUS (DP) REMOVAL (IMBRIUM SYSTEMS, 2012)

A *Column Breakthrough Study* was performed to assess phosphorus adsorption under continuous loading, thereby establishing removal capabilities. A predetermined mass of media was packed into a Teflon PEA column, where a 0.5 mg/L dissolved phosphorus influent solution flowed through. Dissolved phosphorus effluent concentrations were measured at timed points, determining removal capability and the number of bed volumes loaded prior to breakthrough. Notably, breakthrough reveals the volume of media tested that can be introduced prior to a certain level of performance is no longer attainable. As indicated above, 50% dissolved phosphorus removal indicated breakthrough, measured by the number of bed volumes (Imbrium Systems, 2012).

It is to be noted that phosphorus was measured by HACH DR/5000 Spectrophotometer using PhosVer 3 Ascorbic Acid Method (Standard Method 1998). The Ascorbic Acid Method was used to detect orthophosphate, and a Persulfate Digestion was employed to convert any other forms of phosphorus to orthophosphate (Imbrium Systems, 2012).

2.5.1.5 ADVANTAGES

SorbitiveMEDIA upholds five key advantages, as follows (Imbrium Systems, 2012):

1. *Hydraulic Conductivity* - Fast reaction kinetics, enabling substantial performance.
2. *Flexibly Sized and Long Lasting* - Significantly high sorption capacity and longevity, with optimal footprint impact and removal efficiency
3. *Simple* - Straightforward installation and replacement procedure as a storm water filtration system
4. *Robust* - Un-friable, maintaining its composition with transit, installation and long-term use.
5. *Safe* - Non-hazardous solid granular material; before, during and after use.

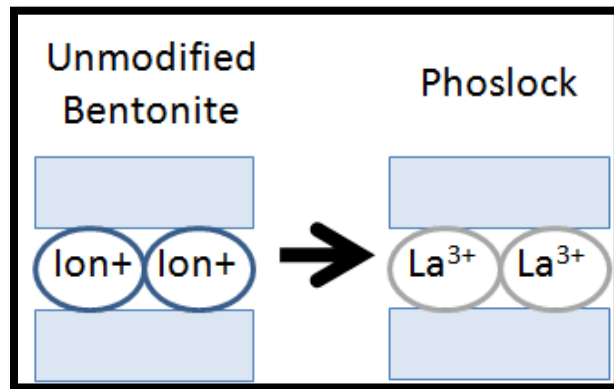
2.5.2 PHOSLOCK®

2.5.2.1 WHAT IS PHOSLOCK?

Phoslock is bentonite clay that has been altered with lanthanum (a rare earth element) into its structure (as indicated in Figure 2.11) (PHOSLOCK, 2010).



(a) Phoslock Particles



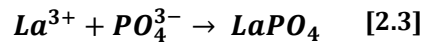
(b) Lanthanum Alteration

FIGURE 2.11 – PHOSLOCK PRODUCTION (PHOSLOCK, 2010)

Phoslock production involves the exchanging of lanthanum cations onto the charged surface of the bentonite clay; the electrostatically bounded lanthanum ions encourage separation. The ions then react with phosphate anions that they are exposed to. This production process creates a dry granule material that is applied to a water body surface in slurry form. As the slurry traverses down the water column, a 95% removal occurs as the clay surface adsorbs the phosphate (PHOSLOCK, 2010).

2.5.2.2 HOW DOES PHOSLOCK WORK?

Phoslock employs the molar ratio of 1:1 of lanthanum to phosphate, making the reaction and removal very efficient.



When Phoslock is applied to a water body, the lanthanum adsorbed onto the charged clay surface reacts with phosphate ions in the water column or sediment pore water. If phosphate is not present, the lanthanum remains 'locked' within the bentonite structure (Figure 2.12). The product of this reaction creates lanthanum phosphate; a highly insoluble, naturally occurring mineral – rhabdophane.

Phoslock particles are mixed with on-site water and introduced to a water body in slurry form. As slurry settlement occurs, phosphate anions present in the water column are bound to the bentonite clay's lanthanum cations. Once Phoslock has settled on the water interface, it forms a thin layer (approximately 1 mm). As long as adequate binding sites are present on the clay, this layer removes phosphorus that would generally be released from the sediment into the water column when anoxic conditions develop (PHOSLOCK, 2010).

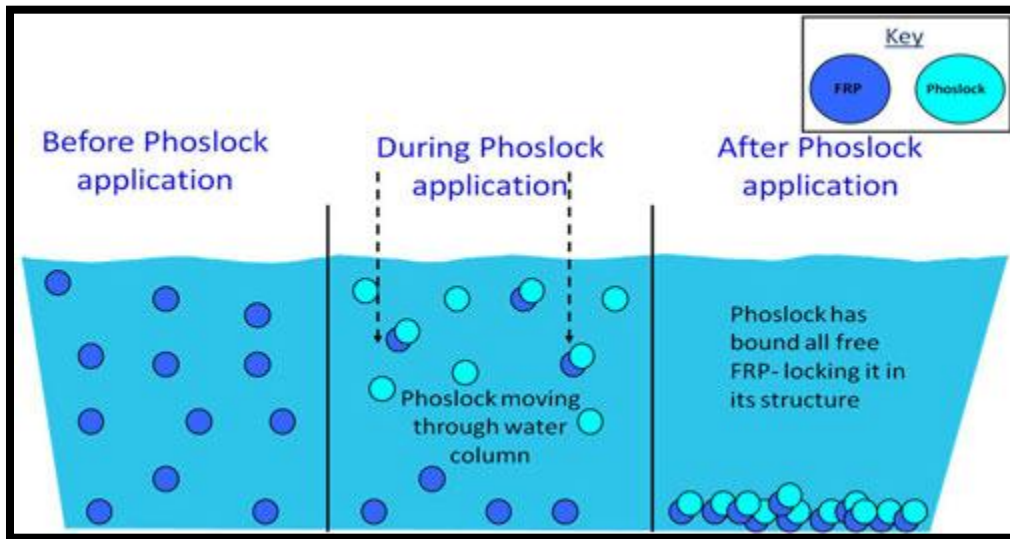


FIGURE 2.12 - PHOSLOCK WATER BODY REMOVAL (PHOSLOCK, 2010)

Phoslock-bounded phosphorus is not bioavailable for use by blue-green algae due to the lack of nutrients, inhibiting it to incorporate and grow, and flourish within the water body (PHOSLOCK, 2010).

The pH operative circumstances of Phoslock are within a wide range (4-11), with the ability to bind phosphate in anoxic conditions. One tonne of Phoslock is able to remove 34 kg of phosphate (PO₄) or 11 kg of phosphorus (P) (PHOSLOCK, 2010).

It is to be noted that a pilot project is being conducted in the Lake Simcoe watershed. Field testing is underway in order to investigate the impact of Phoslock as a reduction strategy (MOE, 2010).

2.5.2.3 ADVANTAGES

Phoslock offers the following key benefits to reduce phosphorus concentrations in lakes and reservoirs, as a solution to eutrophication control (PHOSLOCK, 2010).

1. *Phosphate Reduction* - Able to reduce phosphate levels to or below standard detection limits (<10µL), as well as to desired, controllable phosphorus concentrations to prevent algae growth and simultaneous system productivity.
2. *Rapid Phosphate Uptake* - Water chemistry dependent, generally 90% of phosphate bounded within 3 hours of application.
3. *Eco-toxicological Safety* - Based on 10 years of academic and government research, it has been confirmed that Phoslock has a low toxicity level, and safe to operate in all natural conditions within recommended dosages. It will not affect pH or the water body conductivity.
4. *Stability* - Unresponsive to lakes and reservoirs' range of redox, temperature and pH conditions; buffering is not required.
5. *Re-suspension Resistance* - Research confirms Phoslock suitability with greater density than flocculants, having significantly higher re-suspension resistance than other phosphorus immobilizing salts.
6. *Long-term Effects* - Phosphate reacted with the lanthanum is permanently constrained, and un-reacted lanthanum sites remain active and able to bind phosphate.

3 ZEOLITE

Many cost-effective and efficient adsorbents for phosphorus removal are currently under development. In particular, adsorption is a simple and effective technology, depending on adsorbent efficiency; in addition to zeolites, activated carbon, clay minerals, biomaterials, and some industrial solid wastes have been implemented. The adsorbent material *zeolite* has vast occurrence and applications worldwide; adsorption, catalysis, building industry, agriculture, soil remediation, and energy. Global natural zeolite consumption has grown from 3.98Mt in 2009 to reach 5.5Mt in 2010 (Wang, 2010).

The existence of zeolite has been known for more than 200 years. However, its geological significance has been scientifically discovered only in the late 1950s; in the western United States, numerous volcanic tuffs in ancient saline-lake deposits as well as thick marine tuffs of Italy and Japan. As a universal constituent in vugs and cavities of trap-rock formations (basalts), it can be found in eruptive rocks and late-stage hydrothermal environments. Geologically, it may be found in sedimentary rocks, closed hydrologic systems, open hydrologic systems, low-grade metamorphic grades, and deep-sea sediments. Zeolites comprise of largest mineral groups of tekto-silicates, such that 35 different framework topologies, 40 mineral species recognized, and 100 types have been synthesized (having no natural counterparts from lab syntheses) (Mumpton, 1977).

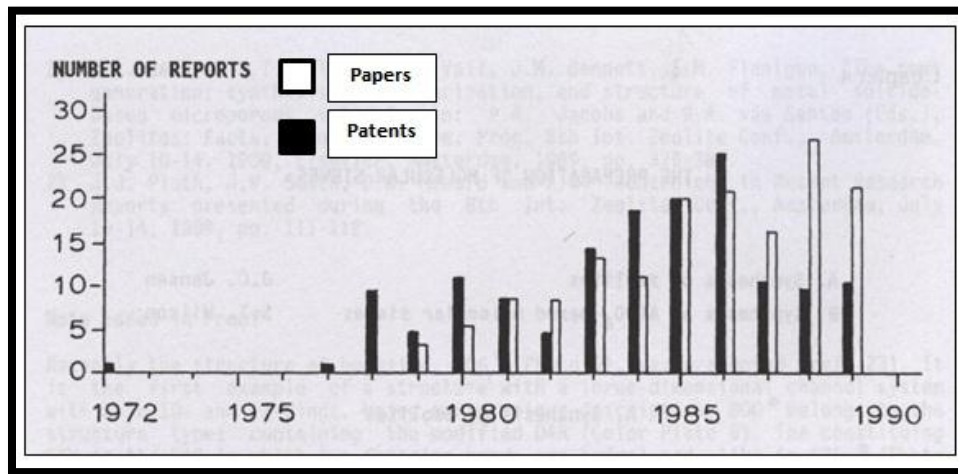


FIGURE 3.1 – THE ANNUAL NUMBER OF PAPERS AND PATENTS ON THE PREPARATION OF ZEOLITE SINCE FIRST PUBLICATION IN 1972 (MUMPTON, 1977)

As observed in Figure 3.1 above, the development of this natural mineral has vastly progressed and will continue towards a promising, sustainable future (Bekkkum, 1991).

3.1 MINERALOGY

Zeolites are defined as “crystalline, hydrated aluminosilicates of alkali and alkaline earth cations, having infinite, three-dimensional structures...further characterized by an ability to lose and gain water reversibly and to exchange constituent cations without major change of structure.” (Mumpton, 1977, pg. 2). It was discovered in 1756 by a Swedish mineralogist by the name of Fredrick Cronstedt. The word *zeolite* is translated from Greek to mean ‘boiling water’ due to its unusual frothing characteristics when heated. Cronstedt expressed it further as “...gassing and puffing up almost like borax...followed by melting...to a white glass” (Mumpton, 1977).

The formation of natural zeolites involves a reaction of mineralizing aqueous solutions with solid aluminosilicates. The main synthesis parameters are: 1) host rock and interstitial solution composition (pH – 10), 2) time (thousands of years), and 3) temperature (< 100 °C) (Bekkkum, 1991).

Both its natural or synthetic applications directly relate to the chemical compositions and crystal structures, of which are discussed in the following subsections (Mumpton, 1977).

3.1.1 CHEMICAL COMPOSITION

Zeolite is a member of the tectosilicates, which include and are similar to quartz and feldspar minerals. It consists of three-dimensional frameworks of SiO_4^{4-} tetrahedra, such that oxygen ions of each tetrahedral are shared with adjacent tetrahedral in all 4 corners (Figure 3.2) (Mumpton, 1977).

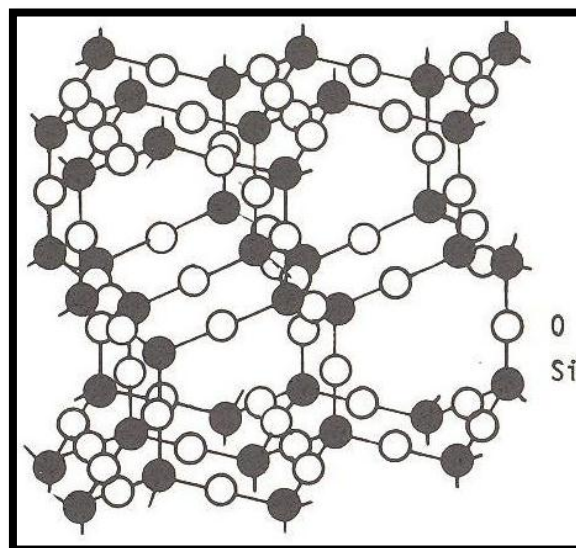


FIGURE 3.2 – THREE-DIMENSIONAL ARRANGEMENT OF SILICATE TETRAHEDRA IN TEKOSILICATES (MUMPTON, 1977)

Silicate tetrahedral structures uphold an overall Si:O ratio of 2:1. Quadrivalent silicon is replaced by trivalent aluminum, creating a positive charge deficiency to become negatively charged. A balance among charges is achieved through the addition of mono- and di-valent cations (Na^+ , Ca^{2+} , K^+). The general empirical formula of zeolite is as follows in Equation 3.1 (Mumpton, 1977; Wang, 2010):

$$M_{x/n}(\text{Al}_x\text{Si}_y\text{O}_{2(x+y)}) \cdot p\text{H}_2\text{O} \quad [3.1]$$

where M = any alkali or alkaline earth cation
(Na, K, Li and/or Ca, Mg, Ba, Sr)

n = cation valence

y/x = range of <1, 6>

p/x = range of <1,4>

Exchangeable cations are represented as the ions in the first set of parentheses within the unit-cell formula. Ions in second set are the structural cations; along w oxygen, they make up the tetrahedral framework of the structure. The ratio of the base to alumina is always equal to unit of y. The ratio of (Al+Si):O is always 1:2. In addition, the silicon ions' presence is greater than the tetrahedral aluminum ions and the SiO_2 : Al_2O_3 ratio is greater than 2:1 (Mumpton, 1977).

Ionic substitution and cation exchange negate the concept of 'coupled' substitutions of Na+Si for Ca+Al in zeolites. This mineral may be washed to produce a series of cationic forms of a single species that only vary in the nature of cations in exchange positions. The cation composition reflects the last exposed solution's composition, causing serious issues with nomenclature (Mumpton, 1977).

It is to be noted that loosely bound water makes up natural zeolites' structure, at 10-20% of the dehydrated phase. A considerable amount of water is given off continuously and reversibly on heating from room temperature to approximately 350°C. When water is removed, cations fall back into positions on the inner surface of channels and central cavities of the zeolite structure. Dehydration of zeolite is an endothermic process, causing 'activation' of the material. At a certain temperature, water temperature is dependent on $P_{\text{H}_2\text{O}}$ of the atmosphere that zeolite is exposed to (Mumpton, 1977).

3.1.2 CRYSTAL STRUCTURE

The crystal structure of zeolite possesses a considerable void space within its simple, polyhedral building blocks and within larger frameworks formed by several polyhedral. The pore sizes differ depending on the structure, channel and cavity systems, as well as effective entry. There are a wide variety of zeolites, where each group is able to screen molecules and cations by both molecular and ion sieving procedures (Mumpton, 1977).

As observed in Table 3.1 below, the framework structure of zeolite is open (specific gravity = 2.0-2.2), in comparison to quartz and feldspar which are dense and tightly packed (specific gravity = 2.6-2.7). Void volumes of dehydrated species as great as 50% are recognized; similar chemical composition but unique crystal structure and corresponding physical and chemical properties (Mumpton, 1977).

TABLE 3.1 – TYPICAL FORMULAE AND SELECTED PHYSICAL PROPERTIES OF IMPORTANT ZEOLITES (MUMPTON, 1977)

Zeolite	Typical Unit-Cell Formula	Crystal System	Void Volume (%)	Specific Gravity	Thermal Stability	Ion-Exchange Capacity (meg/g)
Analcime	$Na_{16}(Al_{16}Si_{32}O_{96}) \cdot 16H_2O$	Cubic	18	2.24-2.29	High	4.54
Chabazite	$(Na_2, Ca)_6(Al_{12}Si_{24}O_{96}) \cdot 40H_2O$	Hexagonal	47	2.05-2.10	High	3.81
Clinoptilolite	$(Na_4K_4)(Al_8Si_{40}O_{96}) \cdot 24H_2O$	Monoclinic	39	2.16	High	2.54
Erionite	$(Na, Ca_{0.5}, K)_9(Al_9Si_{27}O_{72}) \cdot 27H_2O$	Hexagonal	35	2.02-2.08	High	3.12
Faujasite	$Na_{58}(Al_{58}Si_{134}O_{384}) \cdot 240H_2O$	Cubic	47	1.91-1.92	High	2.29
Ferrierite	$(Na_2Mg_2)(Al_6Si_{30}O_{72}) \cdot 18H_2O$	Orthorhombic	--	2.14-2.21	High	2.33
Heulandite	$Ca_4(Al_8Si_{28}O_{72}) \cdot 24H_2O$	Monoclinic	39	2.10-2.20	Low	2.91
Laumontite	$Ca_4(Al_8Si_{16}O_{48}) \cdot 16H_2O$	Monoclinic	34	2.20-2.30	Low	4.25
Mordenite	$Na_8(Al_8Si_{40}O_{96}) \cdot 24H_2O$	Orthorhombic	28	2.12-2.15	High	2.29
Natrolite	$Na_{16}(Al_{16}Si_{24}O_{80}) \cdot 16H_2O$	Orthorhombic	23	2.20-2.26	Low	5.26
Phillipsite	$(Na, K)_{10}(Al_{10}Si_{22}O_{62}) \cdot 20H_2O$	Orthorhombic	31	2.15-2.20	Low	3.87
Wairakite	$Ca_8Al_{16}Si_{32}O_{96} \cdot 16H_2O$	Monoclinic	20	2.26	High	4.61
Linde A ³	$Na_{12}(Al_{12}Si_{12}O_{48}) \cdot 27H_2O$	Cubic	47	1.99	High	5.48
Linde X ³	$Na_{86}(Al_{86}Si_{106}O_{384}) \cdot 264H_2O$	Cubic	50	1.93	High	4.73

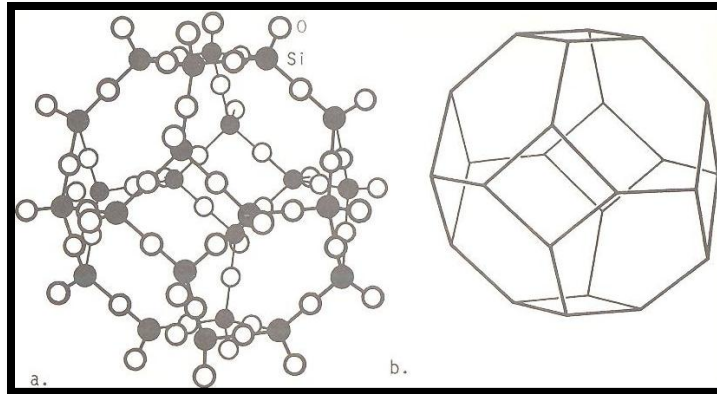


FIGURE 3.3 – SIMPLE POLYHEDRON OF SILICATE (SiO_4) AND ALUMINATE (AlO_4) TETRAHEDRA – TRUNCATED CUBO-OCTAHEDRA; A) GEOMETRICAL FORM – BALL AND PEG MODEL; B) LINE DRAWING (LINES CONNECT MIDPOINTS OF EACH TETRAHEDRON) (MUMPTON, 1977)

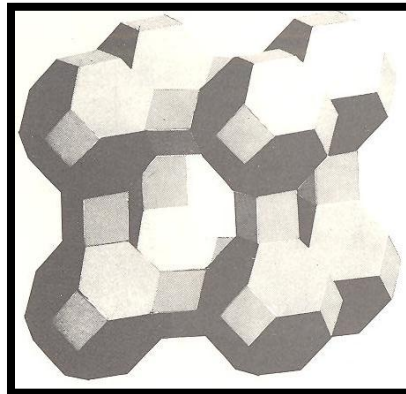


FIGURE 3.4 – ARRANGEMENT OF SIMPLE POLYHEDRA TO ENCLOSE LARGE CENTRAL CAVITIES - TRUNCATED CUBO-OCTAHEDRA CONNECTED BY DOUBLE 4-RINGS OF OXYGEN IN STRUCTURE OF SYNTHETIC ZEOLITE A (INDIVIDUAL POLYHEDRAL CONNECTIONS – FRAMEWORK STRUCTURES) (MUMPTON, 1977)

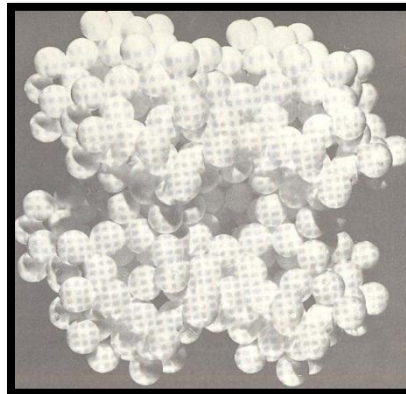
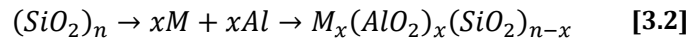


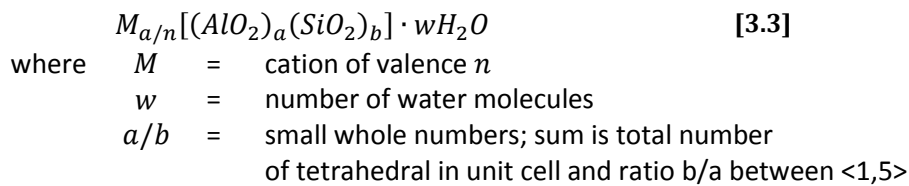
FIGURE 3.5 – SOLID-SPHERE MODEL OF CRYSTAL STRUCTURE OF SYNTHETIC ZEOLITE A (INDIVIDUAL POLYHEDRAL CONNECTIONS – SOLID-SPHERE STRUCTURES) (MUMPTON, 1977)

Figures 3.3 to 3.5 above display passage ways leading into simple polyhedral connections that are too small for all but the smallest molecules to pass. However, ports/channels up to 8 Å in diameter lead into large, three-dimensional cavities (Mumpton, 1977).

Zeolite is composed of earth cations (metal elements – sodium, potassium, magnesium, calcium, strontium, barium), which infinitely extend three-dimensional networks of SiO₄ and AlO₄. As observed in Equation 3.2, substitution of monovalent cation plus aluminum for silicon in basic formula of silica minerals is illustrated (Mumpton, 1977).



The empirical formula of zeolite becomes a crystallographic unit-cell formula, as observed in Equation 3.3 (Mumpton, 1977):



The structure of zeolite is divided into three independent components (Mumpton, 1977) (Wang, 2010):

1. Aluminosilicate framework
2. Interconnected void spaces in framework containing metal, exchangeable cations
3. Zeolitic water; water molecules which are present as an occluded phase

The primary building block framework is the tetrahedron, where its center is occupied by a silicon or aluminium atom, with four oxygen atoms at the vertices. The framework's negative charge is generated by the substitution of Si⁴⁺ by Al³⁺, offset by mono- or di-valent cations positioned together with water. The structure type is defined by the framework, being the conserved and stable of the three components. The water molecules are located within large cavities and form aqueous bridges that bond between framework and exchangeable ions, as well as among exchangeable cations (Wang, 2010).

The fundamental building units shown in Table 3.2 are described and classified based on the following (Mumpton, 1977):

1. Primary Building Unit – tetrahedron (TO₄)
2. Secondary Building Unit (SBU) – single and double rings
3. Larger Symmetrical Polyhedral – Archimedean solids

TABLE 3.2 – BUILDING UNITS IN ZEOLITE STRUCTURES (MUMPTON, 1977)

<i>Primary Building Unit – Tetrahedron (TO₄)</i>	Tetrahedron of four oxygen ions with a central ion (T) of Si ⁺⁴ or Al ⁺³
<i>Secondary Building Units (SBU)</i>	Rings: S-4, S-5, S-6, S-8, S-10, S-12 Double Rings: D-4, D-6, D-8
<i>Larger Symmetrical Polyhedra</i>	Truncated Octahedron (T.O.) or Sodalite Unit 11-Hedron or Cancrinite Unit 14-Hedron II or Gmelinite Unit

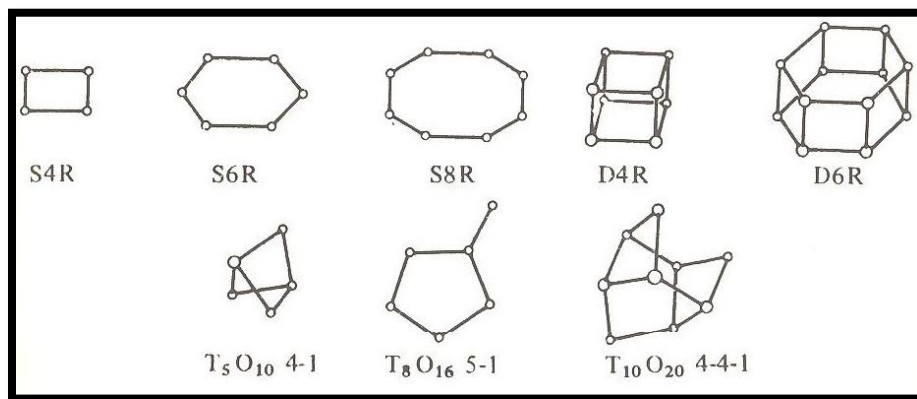


FIGURE 3.6 – ZEOLITE STRUCTURES' SECONDARY BUILDING UNITS (SBU) (MUMPTON, 1977)

It is to be noted that there are various structural unit depictions and building models (Mumpton, 1977):

1. Solid Tetrahedral Models
2. Framework Models
3. Space-Filling Models
4. Ball And Stick Models

Both the natural and synthetic structural classifications based on a combination of framework topology and Secondary Building Units (SBU) is displayed in the following Table 3.3 (Mumpton, 1977).

TABLE 3.3 - ZEOLITE GROUP - SBU - CLASSIFICATION (MUMPTON, 1977)

Group	SBU	Classification	
1	S4R	Single 4-ring (S4R)	Analcime
			Phillipsite
			Gismondine
			Laumontite
2	S6R	Single 6-ring (S6R)	Erioinite
			Offretite
			Sadolite
3	D4R	Double 4-ring (D4R)	Zeolite A
4	D6R	Double 6-ring (D6R)	Faujasite
			Chabazite
5	T_5O_{10} units	Complex 4-1, T_5O_{10} units	Natrolite
			Scolecite
			Mesolite
6	T_8O_{16} units	Complex 5-1, T_8O_{16} units	Mordenite
			Dachiardite
			Ferrierite
7	$T_{10}O_{20}$ units	Complex 4-4-1, $T_{10}O_{20}$ units	Heulandite
			Clinoptilolite*

*Research Focus - Clinoptilolite

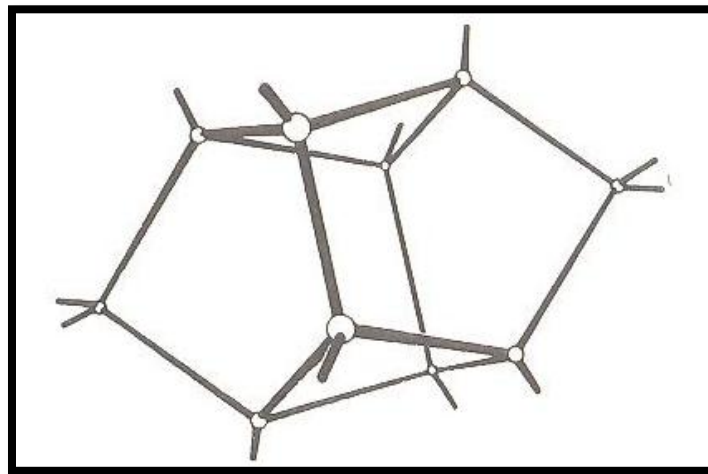


FIGURE 3.7 - GROUP 7 ZEOLITES - CONFIGURATION OF $T_{10}O_{20}$ UNITS OF TETRAHEDRA IN THE FRAMEWORK STRUCTURES (MUMPTON, 1977)

3.1.3 CLINOPTILOLITE

There are various forms of natural zeolite. The most common are clinoptilolite, mordenite, phillipsite, chabazite, stilbite, analcime, laumontite, while the rare forms include offretite, paulingite, barrerite, mazzite, and they are shown in Table 3.4 (Wang, 2010).

Zeolite	Formula	Structure Type	Symmetry
<i>Clinoptilolite</i>	$(K_2, Na_2, Ca)_3(Al_6Si_{30}O_{72}) \cdot 21H_2O$	HEU	Monoclinic, C2/m
<i>Mordenite</i>	$(Na_2, Ca)_4(Al_8Si_{40}O_{96}) \cdot 28H_2O$	MOR	Orthorhombic, Cmcm
<i>Chabazite</i>	$(Ca, Na_2, K_2)_2(Al_4Si_8O_{24}) \cdot 12H_2O$	CHA	Rhombohedral or Triclinic P1
<i>Phillipsite</i>	$K_2(Ca, Na_2)_2(Al_8Si_{10}O_{32}) \cdot 12H_2O$	PHI	Monoclinic, P2 ₁ /m
<i>Scolecite</i>	$Ca_4(Al_8Si_{12}O_{40}) \cdot 12H_2O$	NAT	Monoclinic, C _c
<i>Stilbite</i>	$Na_2Ca_4(Al_{10}Si_{26}O_{72}) \cdot 30H_2O$	STI	Monoclinic, C2/m
<i>Analcime</i>	$Na_{16}(Al_{16}Si_{32}O_{96}) \cdot 16H_2O$	ANA	Cubic 1a3d
<i>Laumontite</i>	$Ca_4(Al_8Si_{16}O_{48}) \cdot 16H_2O$	LAU	Monoclinic, C2/m
<i>Erionite</i>	$(Na_2K_2MgCa_{1.5})_4(Al_8Si_{28}O_{72}) \cdot 28H_2O$	ERI	Hexagonal P6 ₃ /mmc
<i>Ferrierite</i>	$(Na_2K_2CaMg)_3(Al_6Si_{30}O_{72}) \cdot 20H_2O$	FER	Orthorhombic, Immm Monoclinic, P2 ₁ /n

Clinoptilolite is one of the more valuable and abundant natural zeolite types and is extensively used on a global scale (Wang, 2010).

Clinoptilolite forms through various processes and natural deposits. Firstly, it is a product of devitrification (the conversion of glass to crystalline material) of volcanic glass in tuffs or consolidated pyroclastic rocks. The devitrification process involves the contact of glass with saline waters. Clinoptilolite is also discovered in volcanic rocks' vesicles (i.e. basalts, rhyolites and andesites). It is a variation of phillipsite in deep-sea sediments and of borate minerals in playa lakes. Clinoptilolite in Greek translates to *oblique feather stone*, coined as such because it was considered as the monoclinic (or obliquely inclined) phase of the mineral ptilolite (Amethyst Galleries, 2011).

Clinoptilolite is related to the zeolite types called heulandite (as part of Group 7 - T₁₀O₂₀ units). The major difference between the two is clinoptilolite's greater potassium and slightly greater silica contents. Like heulandite, its structural organization is sheet-like. The sheets are connected by bonds, of which are comparatively separated. As a true tectosilicate, oxygen is connected to either a silicon or an aluminum ion with a ratio of (Al+Si):O of 1:2 (Amethyst Galleries, 2011).

The sheets comprise of open rings of alternating eight and ten sides. These rings stack together amongst sheets to configure channels throughout the crystal structure. The channels' size determines the

molecules' or ions' size that is able to transmit through them, and providing its chemical sieve abilities. Clinoptilolite's sheet-like structure emits its physical characteristics; prominent pinacoid faces, perfect cleavage, and unique luster faces outlined in Table 3.5 (Amethyst Galleries, 2011).

TABLE 3.5 –PHYSICAL CHARACTERISTICS OF CLINOPTILOLITE (AMETHYST GALLERIES, 2011)

Characteristic	Description
<i>Colour</i>	Colourless, white, pink, yellow, reddish, pale brown
<i>Luster</i>	Vitreous to pearly on prominent pinacoid face and cleavage surfaces
<i>Transparency</i>	Transparent to translucent
<i>Crystal System</i>	Monoclinic (2/m)
<i>Crystal Habits</i>	Proportionate blocky or tabular crystals
<i>Cleavage</i>	Perfect in direct parallel to prominent pinacoid face
<i>Fracture</i>	Uneven
<i>Hardness</i>	3.5 – 4 (softer on cleavage surfaces)
<i>Specific Gravity</i>	2.2 (very light)
<i>Streak</i>	White

This zeolite category is able to absorb significant quantities of water after drying and retains its structure if heated (almost to temperature of melted glass). Associated minerals include calcite, aragonite, thenardite, hectorite, quartz, apophyllite, opal, clays, pyrite, halite, mordenite, heulandite, chabazite, analcime, erionite, ferrierite, harmotome, dachiardite, phillipsite and various borate minerals. It may be found in tuffaceous volcanic rocks of Arizona; of Hoodoo Mountains and the Yucca Mountains of Nevada; Altoona, Washington; Agate Beach and Madres, Oregon and California, USA. In addition, clinoptilolite may be found in Styria, Austria; Bulgaria; British Columbia, Canada; Ortenberg Quarry, Germany; Alpe di Siusi, Italy; Kuruma Pass, Japan; McQueens Valley and Moeraki, New Zealand as well as Chinchwad, India. The optimal field indicators include crystal habit, density, locality, water absorption, as well as heat tolerance (Amethyst Galleries, 2011).

3.2 COMMERCIAL PROPERTIES

For commercialization purposes, zeolite's properties depend on the specific crystal structure and framework, as well as cationic compositions. Both adsorption capacity and ion-exchange capacity are of primary focus in the following subsections.

3.2.1 ADSORPTION CAPACITY

Adsorption is a process where molecules from the gas phase or a solution bind in a condensed layer on a solid or liquid surface. Previous adsorption experiments determined that the quantity of gas/solution adsorbed depends on temperature, pressure and composition of the gas/solution. Adsorption isotherms are a graphical representation of the quantity adsorbed as a function of pressure of the gas/solution (Masel, 1996).

Adsorption measurements involve the analysis of molecules of different sizes, which provide direct information about dimensions of the pore system; molecules with kinetic diameters smaller than pore openings can be adsorbed and larger molecules cannot. In boundary cases, a minimum temperature of adsorption may be required. Commonly, the adsorption isotherm gives information about pore structure. This method is often applied for characterizing minerals with mesopores (2-50 nm) and macropores (>50 nm) (Bekkkum, 1991).

The adsorption process strength may be either weak or strong. Weak strength occurs in the physisorption process, such that fragile bondings of molecules to surfaces occur, through interactions of induced or permanent dipoles and/or quadrupoles (framework cations). This is a low temperature observation, non-activated process, and completely reversible. Strength is achieved through the chemisorption process; adsorption involves the transfer of chemical charges between adsorbate and surface (extra-framework cations). Through the formation of bonds, elevated temperatures persist, leading to chemical changes (Wright, 2008).

Experimental adsorption studies are categorized as follows (Wright, 2008):

1. Measurement of adsorption uptakes and associated thermodynamic parameters, such as the strength of adsorption and heterogeneity.
2. Spectroscopic analysis of adsorbate molecules
 - a. Investigate changes in vibrational and electronic energy levels of adsorbate and molecular sieve
 - b. Identify strength and chemical type of specific interactions
3. NMR and diffraction-based analysis of molecules' location in pores, determining the exact geometry of adsorbate-solid complex.

Brunauer (1945) classified behavior observed during gas-on-solid adsorption based on 5 general isotherm forms (Figure 3.8) (Masel, 1996), as follows:

- Type I: amount of gas increases with increasing pressure and then saturates at a monolayer coverage (adsorbent with small pores causing monolayer adsorption)
- Type II: amount adsorbed increases with increase in pressure, levels off, and then grows at higher pressures (multilayer adsorption)
- Type III: initially very little adsorption, but with small droplet exposure of adsorbate on the surface, adsorption increases
- Type IV and V: occurs when multilayers of gas adsorb onto porous solid's surface

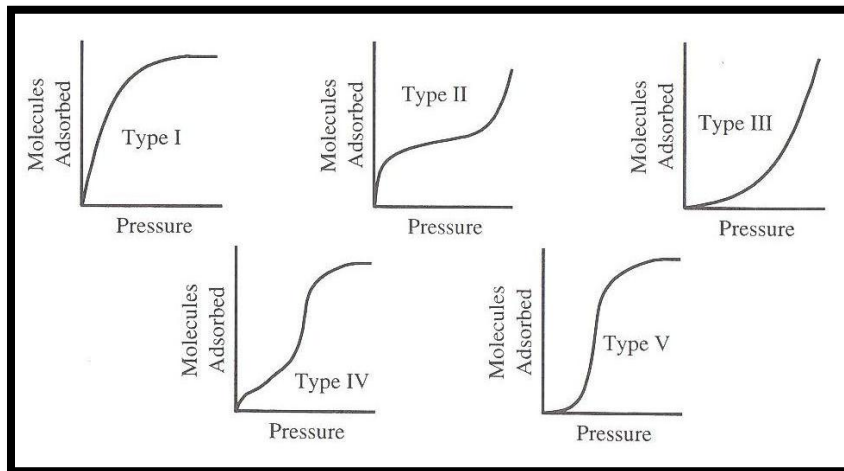


FIGURE 3.8 - ADSORPTION ISOTHERMS (MASEL, 1996)

The most significant model of mono layer adsorption is represented by Langmuir (1913, 1915, 1918). Adsorption considered ideal gas onto idealized surface, such that gas is presumed to bind at a series of distinct sites on the solid's surface, as observed in Figure 3.9 below; the block dots represent adsorption sites and white ovals represent adsorbed molecules (Masel, 1996).

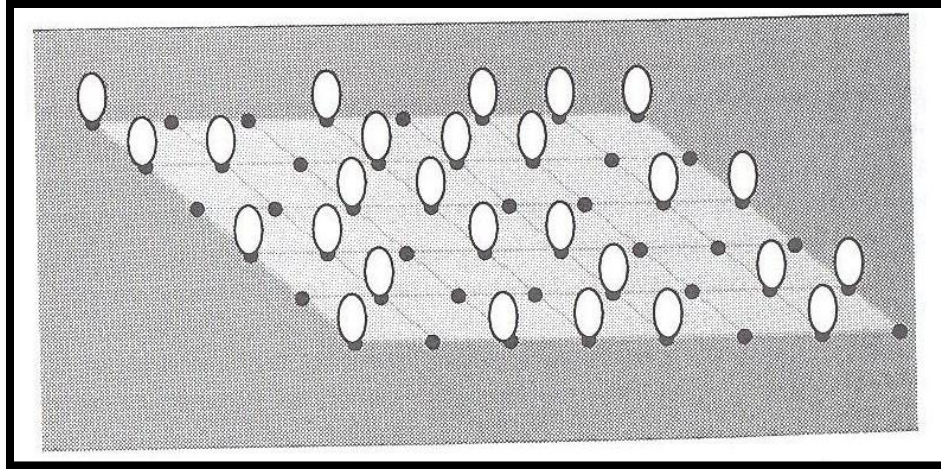
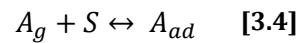


FIGURE 3.9 – LANGMUIR'S MODEL OF ADSORBED LAYER STRUCTURE (MASEL, 1996)

This model represents the adsorption process as a reaction in Equation 3.4, such that the gas molecule (A_g) reacts with an empty site (S) to yield an adsorbed complex (A_{ad}) (Masel, 1996):



At equilibrium, the rate of adsorption (r_{ad}) is equivalent to the rate of desorption (r_d) (Masel, 1996):

$$r_{ad} = k_{ad}P_A[S] \quad r_d = k_dP_A[A_{ad}]$$

$$\frac{[A_{ad}]}{P_A[S]} = \frac{k_{ad}}{k_d} = K_{equ}^A \quad [3.5]$$

where

$[A_{ad}]$	=	surface concentration of A (molecules/cm ²)
P_A	=	partial pressure of A over surface
$[S]$	=	concentration of bare sites (number/cm ²)

k_{ad}, k_d	=	constants
---------------	---	-----------

The model follows the assumption that there are a finite number of sites to hold gas, such that as pressure increases, fewer sites are accessible to capture additional adsorbate. The simplest scenario of the model is the adsorption of a single adsorbate onto a sequence of equivalent sites on the solid's surface. For derivational purposes, assumptions are as follows (Masel, 1996):

- adsorbing gas adsorbs into an immobile state
- all sites are equivalent
- each site can hold at most one molecule of A
- there are no interactions between adsorbate molecules on contiguous sites so that K_{equ}^A will be impartial to adsorbed species' coverage, $[A_{ad}]$

Through kinetic derivation, the non-competitive, non-dissociative adsorption is characterized by Langmuir Adsorption Isotherm, where θ_A is the fraction of surface sites occupied (Masel, 1996):

$$\theta_A = \frac{K_{equ}^A P_A}{1 + K_{equ}^A P_A} \quad [3.6]$$

The most straightforward deviation from the Langmuir Adsorption Isotherm occurs during rough inhomogeneous surface adsorption. As such, multiple adsorption sites are formed with heat variations among them. The multiple sites' assume each site acts independently during adsorption process and follows the Langmuir Adsorption Isotherm (Masel, 1996).

With reference to Table 3.6 below, the Freundlich Adsorption Isotherm is the most important multisite adsorption isotherm for rough surfaces.

TABLE 3.6 – COMPARISON OF ADSORPTION ISOTHERMS (MASEL, 1996)

Isotherm	Advantages	Disadvantages
<i>Langmuir</i>	Best one parameter isotherm	Ignores adsorbate/adsorbate interactions
<i>Freundlich, Toth</i>	Two parameters	No physical basis for equation
<i>Multisite</i>	Many parameters	Good for inhomogeneous surfaces; Wrong physics for single crystals
<i>Templin Fowler Slygin-Frumkin</i>	Accounts for adsorbate/adsorbate interactions in an average sense	Does not consider adsorbate layer arrangement
<i>Lattice Gas</i>	Complete description of adsorbate/adsorbate interactions for commensurate layers; Predicts adsorbed layer arrangement	Computer required to calculate isotherm; Assumes commensurate adsorption; Model parameters are difficult to determine

However, it only fits adsorption data over a limited pressure range, with little predictive value. It is represented as below, where α_F and C_F are fitting parameters (Masel, 1996).

$$\theta_A = \alpha_F P^{C_F} \quad [3.7]$$

Zeolite possesses unique adsorption properties, characterizing it as a synthetic molecular sieve. Large central cavities and access channels are filled with water molecules to form hydration spheres around the exchangeable cations at normal conditions. Conditioning is achieved when water is removed by heating the material to 350-400°C for a few hours to overnight. The molecules with effective cross-sectional diameters small enough to pass through the channels are promptly absorbed in both the dehydrated channels and cavities. Molecules that are too large to pass through the channels are excluded, giving it its *molecular sieving* property (Mumpton, 1977).

As observed in Figure 3.10, zeolites' pore-size distributions are relatively narrow due to the uniform size of oxygen rings within the framework structures. This is in contrast to other commercial adsorbents such as silica gel, activated alumina, or activated carbon (Mumpton, 1977).

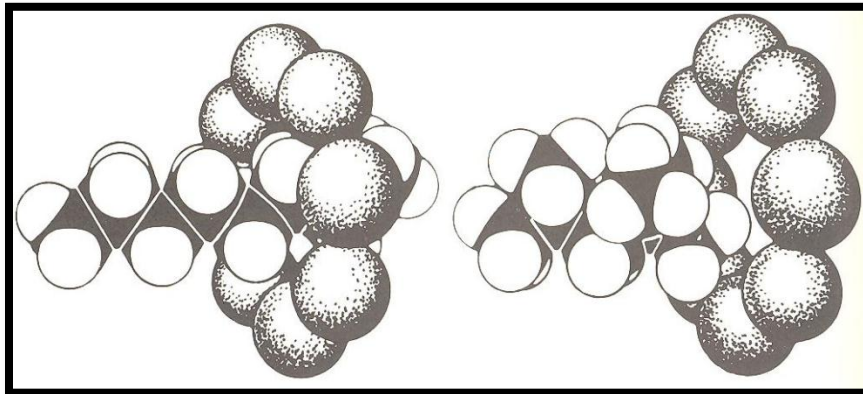


FIGURE 3.10 – SCHEMATIC ILLUSTRATION – ENTRY OF STRAIGHT-CHAIN HYDROCARBONS AND THE BLOCKAGE OF BRANCH-CHAIN HYDROCARBONS AT CHANNEL OPENINGS (MUMPTON, 1977)

Crystalline zeolites' adsorption is characterized by Langmuir-type isotherms as observed in Figures 3.11 and 3.12. The quantity adsorbed (x), relative to the quantity of complete pore-filling (x_s) is at its maximum value at very low partial pressures of adsorbent (Mumpton, 1977).

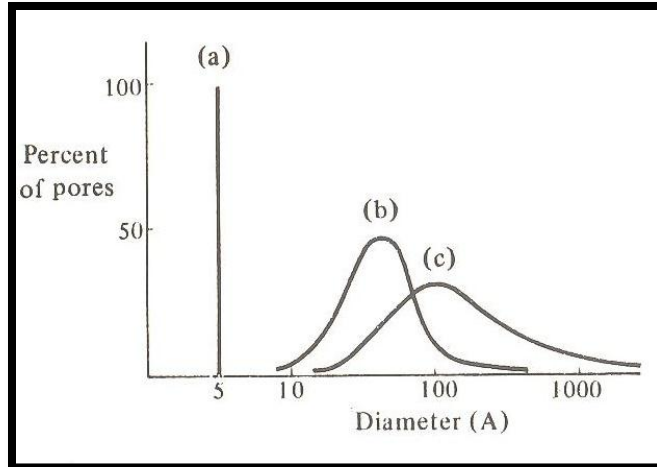


FIGURE 3.11 – PORE SIZE DISTRIBUTION IN MICRO-POROUS ADSORBENTS; A) DEHYDRATED CRYSTALLINE ZEOLITE; B) TYPICAL SILICA GEL; C) ACTIVATED CARBON (MUMPTON, 1977)

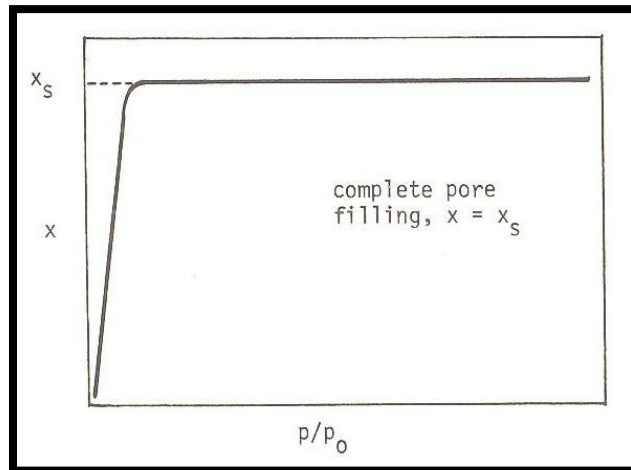


FIGURE 3.12 – LANGMUIR-TYPE ISOTHERM FOR ADSORPTION ON CRYSTALLINE ZEOLITES – NEAR SATURATION COMPLETION AT LOW PARTIAL PRESSURES OF ADSORBENT (X – AMOUNT ADSORBED AND P – PRESSURE) (MUMPTON, 1977)

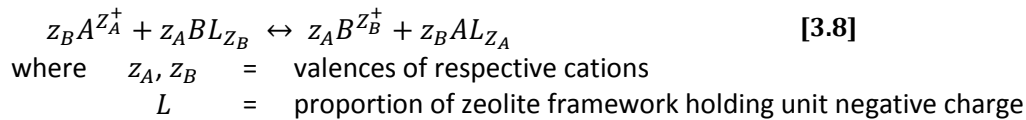
The surface area for adsorption ranges up to several hundred square meters per gram, where some zeolite types are able to adsorb up to 30% their own dry weight. Most of this surface area found within the zeolite structure and represents the inner surface of dehydrated channels and cavities; only 1% of a zeolite particles' external surface contributes to this adsorption surface area (Mumpton, 1977).

Unusual charge distributions within the dehydrated void volume are caused by the presence of cations, hydroxyl groups, and field gradients generated by substitution of aluminum for silicon in its framework. This enables many species with permanent dipole moments (i.e. H₂O, CO₂, H₂S) to be adsorbed with great selectivity (Mumpton, 1977).

3.2.2 ION-EXCHANGE CAPACITY

Ion-exchange capacity is defined as a function of degree of substitution of aluminum for silicon in the framework structure. The greater the substitution, the greater charge deficiency, such that higher number of alkali or alkaline earth cations become required for electrical neutrality (Mumpton, 1977).

A major attribute of zeolites is their ability to exchange ions with external medium through an isomorphous approach. This is expressed by the following equilibrium equation (Wang, 2010):



The behaviour is dependent upon various factors, as follows (Mumpton, 1977; Wang, 2010):

1. framework structure
2. cation species' nature (i.e. size, shape, charge)
3. anionic framework charge density
4. external electrolyte solution's ionic charge and shape
5. cation species in solution concentration
6. temperature

Zeolite's cations are exchangeable cations, due to being loosely bonded to a tetrahedral framework and may be removed or exchanged easily by washing with a strong solution of another ion. This conditioning process encourages cation sieving, which may occur if the size of cation in solution is too large to pass through entry ports into central cavities of structure (Mumpton, 1977).

Crystalline zeolites are very effective ion exchangers, with capabilities of up to 3-4 milli-equivalents (meq) per gram. They dictate its selectivity towards competing ions and different structures offer diverse sites for the same cation; in comparison to non-crystalline ion exchangers (i.e. organic resins or inorganic aluminosilicate gels) (Mumpton, 1977).

It is to be noted that hydration spheres of high field-strength ions prevent their close approach to the seat of charge in framework. In many zeolites, ions with low field strength are more tightly held and selected from solution than others (Mumpton, 1977).

The various forms of zeolite depend on the environment from which they derived from. As such, their chemical composition and cation-exchange capacity (CEC) vary; between 0.6 and 2.3 meq/g as displayed in Table 3.7 (Wang, 2010).

TABLE 3.7 – SELECTED CHEMICAL CHARACTERISTICS OF NATURAL ZEOLITE (WANG, 2010)

Zeolite	Chemical composition (%)								CEC (meq/g)
	SiO ₂	Al ₂ O ₃	Fe ₂ O ₃	CaO	MgO	Na ₂ O	K ₂ O	TiO ₂	
Turkey clinoptilolite	70.90	12.40	1.21	2.54	0.83	0.28	4.46	0.089	1.6–1.8
Iranian clinoptilolite	70.00	10.46	0.46	0.2	–	2.86	4.92	0.02	–
Cuba clinoptilolite	62.36	13.14	1.63	2.72	1.22	3.99	1.20	–	–
Brazil mordenite	67.82	14.96	0.42	1.87	0.18	0.32	4.47	0.07	2.29
Italy phillipsite + chabazite	56.42	15.8	4.08	2.42	0.86	2.35	8.14	0.004	2.12
Turkey clinoptilolite	69.72	11.74	1.21	2.30	0.31	0.76	4.14	–	1.84
Chinese clinoptilolite	65.52	9.89	1.04	3.17	0.61	2.31	0.88	0.21	1.03
Chilean clinoptilolite + mordenite	67.00	13.00	2.00	3.20	0.69	2.60	0.45	0.20	2.05
Turkey clinoptilolite	69.31	13.11	1.31	2.07	1.13	0.52	2.83	–	–
Croatia clinoptilolite	64.93	13.39	2.07	2.00	1.08	2.40	1.30	–	1.45
Iranian clinoptilolite + mordenite	66.5	11.81	1.3	3.11	0.72	2.01	3.12	0.21	1.20
Turkey clinoptilolite	64.99	9.99	3.99	3.51	1.01	0.18	1.95	–	–
Chinese clinoptilolite	68.27	7.48	1.95	2.61	1.87	0.68	1.69	–	–
Turkey clinoptilolite	70.00	14.00	0.75	2.50	1.15	0.20	2.30	0.05	–
Chinese clinoptilolite	69.5	11.05	0.08	2.95	0.13	2.95	1.13	0.14	–
Ukrainian clinoptilolite	67.29	12.32	1.26	3.01	0.29	0.66	2.76	0.26	–
Ukrainian mordenite	64.56	12.02	0.95	3.58	0.68	0.94	2.03	0.23	–
Slovakian clinoptilolite	67.16	12.30	2.30	2.91	1.10	0.66	2.28	0.17	–
Croatian clinoptilolite	55.80	13.32	1.30	5.75	0.70	3.90	2.35	–	–
Ukraine clinoptilolite	66.7	12.3	1.05	2.10	1.07	2.06	2.96	–	0.64
Australian clinoptilolite	68.26	12.99	1.37	2.09	0.83	0.64	4.11	0.23	1.20

3.3 UTILIZATION

Zeolite is widely deemed as a legitimate, distinct mineral, and used among zeolite industries, mineral collectors, and mineralogists. It is used for many applications, including chemical sieve, odor control agent, and water filter for municipal and residential drinking water, as well as agricultural wastewater; it is able to absorb toxic gases from both air and water, for both health control and odor removal purposes. Its pollution-control capabilities are due to its large pore space, high resistivity to extreme temperatures, and chemically neutral basic structure (Amethyst Galleries, 2011) (Mumpton, 1977).

Surface water, groundwater, and industrial or household wastewater contain various pollutants, which include inorganic and organic compounds, and are relatively dangerous to human beings, animals, and plants (Wang, 2010). There are various zeolite applications in practice today, as outlined in Table 3.8 (Bekkkum, 1991):

TABLE 3.8 – ZEOLITE APPLICATIONS IN PRACTICE (BEKKKUM, 1991)

<i>Adsorbents/Desiccants/ Separation Processes</i>	Drying agents, gas purification, separation processes (i.e. n-paraffins from branched paraffins, p-xylene from its isomers)
<i>Catalysts</i>	Industrial applications; petroleum refining, synfuels production, petrochemicals production
<i>Detergents</i>	Formulations of a large market, sequestering agent to substitute phosphates
<i>Miscellaneous</i>	Synthetic or natural; wastewater treatment, nuclear effluent treatment, animal feed supplements ,soil improvement

Natural and modified zeolite forms for pollutant removal for water treatment involve ammonium, heavy metal ions, inorganic anions, and organics (dye adsorption, humic substances, phenolic compounds/petroleum/surfactants/pesticides/pharmaceuticals) (Wang, 2010).

3.4 CONDITIONING

Prior to application, it is imperative that zeolite characterization occurs, given that its properties play a major role and are adapted accordingly. Figure 3.13 provides a flowchart of zeolite's lifecycle (Bekkkum, 1991).

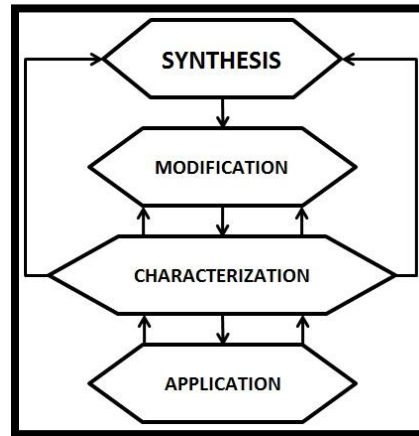


FIGURE 3.13 – POSITION OF ZEOLITE CHARACTERIZATION (BEKKKUM, 1991)

Depending on its pore dimensions, the internal zeolite surface enables metal-oxygen tetrahedral exposure. Zeolite is thereby ideal for the following modifications (Bekkkum, 1991):

1. Exchange of charge-compensating cations
2. Replacement of Si and Al in zeolite framework
3. Introduction of metal particles

The adsorption characteristics of any zeolite depend upon the chemical and structural formations of the adsorbent, including the Si/Al ratio, as well as type, number, and location of the cation. Modification imposed upon the raw natural zeolite to improve the separation efficiency, altering the hydrophilic/hydrophobic properties for the ions and/or organics' adsorption. There are two major techniques; 1) acid/base treatment, and 2) surfactant modification.

3.4.1 ACID/BASE TREATMENT

Acid washing removes impurities that block the pores, gradually eliminates cations to change into H-form, and dealuminates the structure. This two-type modification procedure forms proton exchanged zeolite; 1) ammonium exchange followed by calcination, and 2) direct ion exchange with dilute acid solution. Ammonium exchange maintains a stable structure, whereas acid treatment causes dealumination and reduction of thermal stability. Various investigations concluded that acid treatment reduces the cation-exchange capacity due to dealumination; however, it improves the capacity and Si/Al ratio offering benefits for the adsorption/separation of non-polar molecules from water flows.

3.4.2 SURFACTANT MODIFICATION

Raw natural zeolites' net negative charged framework has poor attraction towards anions, exhibiting low adsorption for organics in aqueous solution. This technique alters the surface properties through the implementation of organic surfactants. Previous investigations involved cationic surfactants, as follows:

- tetramethylammonium
- cetyltrimethylammonium (CTMA)
- hexadecyltrimethylammonium (HDTMA)
- octadecyldimethylbenzyl ammonium (ODMBA)
- n-cetylpyridinium(CPD)
- benzyltetradecyl ammonium (BDTDA)
- stearyldimethylbenzylammonium (SDBAC)
- N,N,N',N',N'-hexamethyl-1,9-nonanediammonium
- polyhexamethylene-guanidine

This modification process relies on the degree of the zeolite surfactant adsorption. Cationic surfactant sorption on a solid surface is represented by the formation of a monolayer called 'hemimicelle' (Figure 3.14). This occurs at the solid-aqueous interface through strong ionic bonds at surfactant concentrations that are equal to or less than the Critical Micelle Concentration (CMC). However, if the surfactant concentration in solution is greater than the CMC, then the hydrophobic tails of its molecules form a bilayer called 'admicelle' (Figure 3.15) (Wang, 2010).

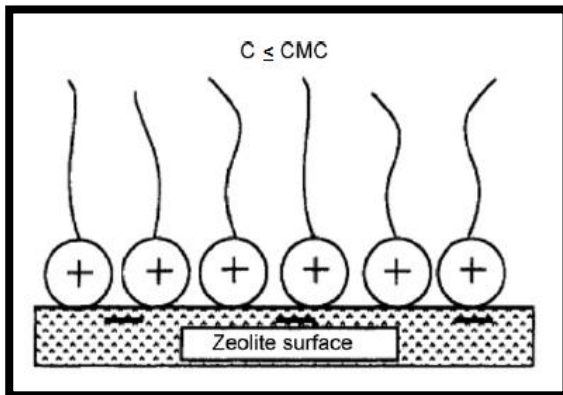


FIGURE 3.14 - HEMIMICELLE FORMATION

(WANG, 2010)

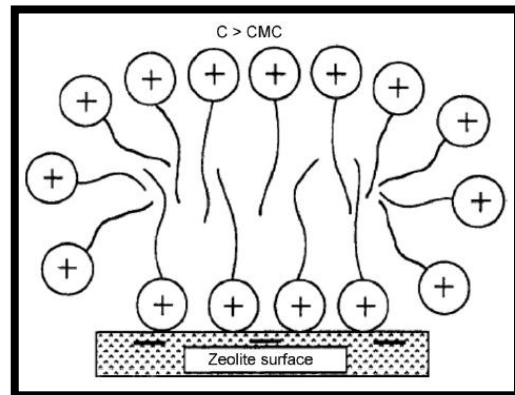


FIGURE 3.15 - ADMICELLE FORMATION

4 EXPERIMENTAL DEVELOPMENT FROM RECENT LITERATURE

This chapter of the report provides an overview of various research efforts towards phosphorus adsorption. The investigations carried out are summarized based on key parameters, modification procedures, and results. In addition, a connective table of innovative technologies is provided. The aim of this component of the report is to convey the reasoning behind the experimental procedure's final protocol.

4.1 EQUILIBRIUM ADSORPTION CAPACITY AND ISOTHERMS

The major objective of Sun (2010) was to investigate the equilibrium adsorption capacity of modified zeolite, while identifying its corresponding qualities and adsorption isotherms.

The analysis involved five major parameters: 1) zeolite adsorbent characteristics, 2) contact time, 3) dosage, 4) temperature, and 5) initial concentration. With the implementation of Scanning Electron Microscopy (SEM), the characteristics of natural, modified, and phosphorus-treated zeolite were determined. It was determined that *modified* zeolite was optimal based on the surface topography, particle size, crystal shape, porosity, and impurities. The contact time was optimal at *180 minutes (3 hours)*, such that the adsorption capacity and removal rate at equilibrium reached its maximum values. As the adsorbent dosage increased, the phosphorus adsorption decreased and removal rate increased; the ideal *solid:liquid ratio is thereby 4g:50 mL*. The temperature has a large effect on phosphorus adsorption; below *normal temperature*, the removal rate increases and below, a moderating trend emerges. Finally, with regards to the initial concentration, the preliminary adsorption capacity reaction increased quickly, then slowly, reaching a balanced state overtime. And so, the greater the quality of phosphorus concentration, the greater the adsorption capacity balance; phosphorus containing samples *of 80 mg/L at 6 hours* is ideal (0.76 mg/g).

Sun (2010) conducted batch studies, after applying the modification procedure summarized in Table 4.2 of Section 4.5. This was followed by adding 4 g of modified zeolite to 50 mL of phosphorus solution. This was stored in a polythene flask, into a thermostat shaker at 120 rpm at $25\pm 1^{\circ}\text{C}$, evaluating mass concentrations of 10, 30, 50, and 80 mg/L.

For analysis, the Langmuir and Freundlich Adsorption Isotherms' equation were used to model the adsorption capacity, and the Banerm Adsorption Kinetics Equation to represent the adsorption rate.

The phosphorus adsorption capacity was calculated by applying the following equation:

$$Q_e = \frac{(C_0 - C_e)V}{m} \left(\frac{mg}{g} \right) \quad [4.1]$$

where Q_e = phosphorus adsorbed (mg/g)
 C_0 = initial concentration of phosphorus (mg/L)
 C_e = phosphorus concentration in solution at equilibrium time (mg/L)
 V = solution volume (L)
 m = zeolite dosage (g)

Through the linearization of the Banerm Adsorption Kinetics Equation (Equation 4.2), a linear plot of $\ln \left(\ln \frac{q_e}{q_e - q} = k't^n \right)$ versus $\ln t$ given an initial concentration of 5 mg/L and corresponding constants, demonstrates it follows this model for the rate of adsorption.

$$\ln \frac{q_e}{q_e - q} = k't^n \quad [4.2]$$

where q = adsorption capacity (mg/g)
 q_e = adsorption capacity at equilibrium (mg/g)
 t = time (hrs)
 k' = constant (7.17136×10^{-7})
 n = constant (2.9217)

As a solid:liquid system, the Langmuir and Freundlich Isotherms represent the phosphorus adsorption process.

$$q_e = \frac{(q_m K_a C_e)}{(1 + K_a C_e)} \rightarrow \text{logarithmic linearization} \rightarrow \quad [4.3]$$

$$\frac{C_e}{q_e} = \frac{1}{(q_m K_a)} + \frac{C_e}{q_m} \rightarrow \frac{1}{q_e} = \frac{1}{(q_m K_a C_e)} + \frac{1}{q_m}$$

where q_e = solute adsorbed at equilibrium (mg/g)
 C_e = equilibrium solute concentration in solution (mg/L)
 q_m = saturation capacity parameter (mg/g)
 K_a = adsorption binding constant (Langmuir Constant) (L/mg)

The linearized plot of $\frac{C_e}{q_e}$ versus C_e generated a coefficient of correlation $R^2 = 0.7942$.

$$q_e = K_F C_e^{1/n} \rightarrow \text{logarithmic linearization} \rightarrow \log(q_e) = \log(K_F) + \left(\frac{1}{n}\right) \log(C_e) \quad [4.4]$$

where q_e = equilibrium adsorption capacity (mg/g)
 C_e = equilibrium solute concentration in solution (mg/L)
 K_F = Freundlich constant (Wanchun, 2011)
 n = heterogeneity factor (Wanchun, 2011)

The Freundlich Model is a modification of the Langmuir Model, as an empirical expression involving the surface's heterogeneity and exponential distribution of sites and their energies. The linearized plot of $\log(q_e)$ versus $\log(C_e)$ generated a coefficient of determination $R^2 = 0.9883$; the adsorption process was consistent with Freundlich isotherm and an n value of 1.315, such that the adsorption process was primarily chemical, accompanied by physical.

Sun concluded that the equilibrium adsorption was best fitted with the Freundlich Model and Benernm Adsorption Kinetics Equation.

4.2 ADSORPTION ISOTHERMS AND KINETICS

The research of Wanchun (2011) involved the following methods of analysis: 1) adsorption isotherm, 2) adsorption kinetics, and 3) adsorption factors.

The adsorption isotherm kinetics investigation involved adding 5 g 10-20 mesh zeolite and 300 mL of phosphorus solution of different concentrations into several 500 mL beakers. This was stirred 24 hours with a controlled magnetic stirrer at 26°C, and rotational speed 180 rpm. The phosphorus content in the supernatant fluid was then determined.

The Langmuir and Freundlich Adsorption Isotherms used to describe the adsorbent process between the liquid and solid phase, once the equilibrium stage is reached. The Langmuir theory follows the following four assumptions:

1. adsorption is a single molecular layer
2. dynamic equilibrium between adsorption and analysis
3. solid surface is uniform
4. no interaction between molecule which were adsorbed, independently of each other

The Freundlich Model is expressed through empirical method. As per Wanchun (2011), K_F indicates the adsorption capacity, such that the greater K_F , the stronger adsorption capacity. The n value indicates the adsorption intensity; less than 0.5 (easy adsorption) or greater than 2 (difficult adsorption).

Wanchan applied the following Equations 4.5 and 4.6, with their linearization, assuming the Langmuir Model such that $\frac{1}{Q_e} \sim \frac{1}{C_e}$, such that a plot of $\frac{1}{Q_e}$ versus $\frac{1}{C_e}$ was created. Also, with regards to the Freundlich model linearization, it was assumed that $\ln(q_e) \sim \ln(C_e)$ such that a plot of $\ln(q_e)$ versus $\ln(C_e)$ was created.

$$Q_e = \frac{(bQ_oC_e)}{(1 + bC_e)} \rightarrow \text{logarithmic linearization} \rightarrow \frac{1}{Q_e} = \frac{1}{bQ_oC_e} + \frac{1}{Q_o} \quad [4.5]$$

where

- Q_e = equilibrium adsorption capacity (mg/kg)
- b = Langmuir constant (0.1961 L/mg)
- Q_o = Langmuir theoretical adsorption capacity (125 mg/L)
- C_e = equilibrium concentration (mg/L)

$$Q_e = K_F C_e^n \rightarrow \text{logarithmic linearization} \rightarrow \log(Q_e) = n \log(C_e) + \log(K_F) \quad [4.6]$$

where

- Q_e = equilibrium adsorption capacity (mg/kg)
- K_F = Freundlich constant (41.29)
- C_e = equilibrium concentration (mg/L)
- n = heterogeneity factor (0.2698)

With the comparison of the linearized adsorption isotherm models, the coefficient of correlation (R^2) for Langmuir and Freundlich were 0.9362 and 0.849, respectively. As the optimal fit, the Langmuir Model calculated the theoretical adsorption maximum capacity on natural zeolite as 125 mg/L.

An adsorption kinetics curve was generated by plotting q_t (mg/kg) versus t (h) from the quasi-second order kinetic equation below:

$$\frac{t}{q_t} = \frac{1}{kq_e^2} + \frac{1}{q_e} \quad [4.7]$$

where

- q_t = adsorption capacity at time t (mg/kg)
- t = time (hrs)
- q_e = equilibrium adsorption capacity (mg/kg)
- k = two kinetic rate constant (kg/h/mg)

At an initial concentration of 5 mg/L, the phosphorus adsorption increased rapidly within the first 0.5 hours, stabilized between 0.5-0.8 hours, and declined beyond 0.8 hours due to analysis limitations.

Four experimental factors were analyzed by adding various zeolite quantities (g, mesh) and 300 mL of phosphorus solution into several 500 mL beakers, stirred for 4 hours, and the phosphorus content in supernatant fluid was then determined. All parameters were altered and repeated accordingly. The four key factors from Wanchun (2011) examined are: 1) initial concentration, 2) zeolite size, 3) adsorbent dosage, and 4) pH. With an initial concentration of 5 mg/L, the phosphorus removal rate reached its maximum up to 18.93%. At low concentration range, removal rate increased with increasing initial concentration; then removal rate decreased with increasing initial concentration but maintained high removal rate. The smaller the zeolite particle size, the larger the specific surface area, and zeolite thereby becomes more conducive to phosphorus exchange. It becomes favourable to phosphorus to travel to zeolite's internal pore structure, adsorbed on its surface. A smaller zeolite diameter corresponds to a higher removal rate; with a particle size reduced less than 20 mesh, removal rate increased (yet not a significant impact). With a zeolite dosage of more than 3 g, removal rate did not increase with increasing dosage, but rather slightly decrease to stable state. At an initial of pH <5, the phosphorus removal decreased with increasing pH. This is due to zeolite's surface with a positive charge and exists in HPO_4^{2-} and H_2PO_4^- . In solution, zeolite adsorbs phosphate ions easily carrying opposite charges. At a greater pH value, a large number of PO_4^{3-} , Ba^{2+} , Ca^{2+} replace out in solution to produce phosphate precipitation. Therefore, the phosphorus removal slightly increased.

4.3 ZEOLITE MODIFICATION AND REGENERATION

Li (2011) continued with the modification process to prepare Silicate-Carbon Modified Zeolite (SCMZ); this conditioning improves the ion-exchange and sorption properties as well as purity. An innovative filter material was prepared by shaping modified zeolite powder into a cylindrical shape (D=4mm, H=8mm)

Li's (2011) experimental design of adsorption analysis is represented in Figure 4.1 below, with a comparative column test:

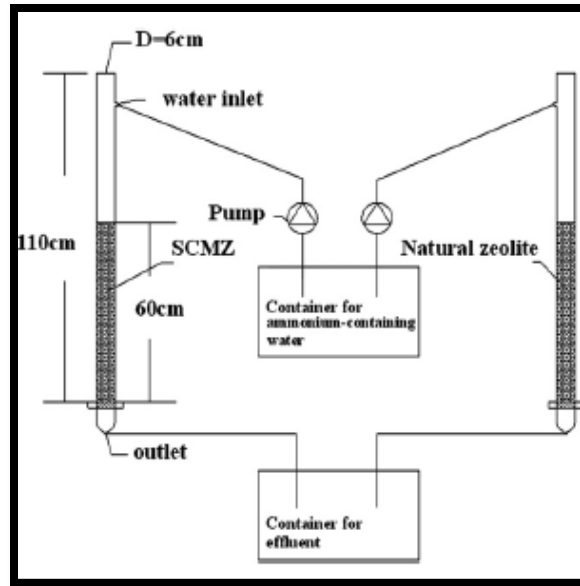


FIGURE 4.1 – ADSORPTION ANALYSIS EXPERIMENTAL DESIGN (LI, 2011)

Zeolites' surface-morphology characterization was observed through Scanning Electron Microscopy. Li (2011) determined that SCMZ possesses a rough surface, porous structure, and distinct channels/cavities. Consequently, natural zeolite has small channels/cavities with a smoother surface. With greater number of channels/cavities, a larger surface area is available for ammonium adsorption and ion exchange to occur. Through X-Ray Diffraction, it was determined that SCMZ possesses thermal stability such that no transformation occurred towards the crystalline structure after modification. The thermo-gravimetric process involved heating at 10 K/minute and N₂ gas exposure. After modification, micro-porosity encouraged porosity to increase, capsuling more water than natural zeolite. SCMZ weight-loss ratio was 61% at 340°C.

The effect of pH was analyzed through the column, at a flow rate of 10 m/hour, initial ammonium concentration of 5 mg/L, and pH adjustments of 5.0, 7.0, and 9.0. Overall, pH had a slight impact on the ammonium adsorption of zeolite. A rising trend and breakthrough time were observed; a steady pH of 5.0-9.0 was maintained, such that the SCMZ was affected greater than natural zeolite.

The effect of initial ammonium concentration was investigated at a flow rate of 10 m/hour, pH of 7.0, and initial concentrations adjusted to 2.5, 5, and 10 mg/L. It was determined that at fluctuated initial concentrations, the SCMZ column removed ammonium effectively but during a longer timeframe. Also, the breakthrough time of both zeolites reduced, with increased initial concentrations. This confirms that the high ammonium concentration would load the zeolite and accelerate breakthrough. Also, with greater initial concentration, adsorption capacity of zeolite increases; that being greater for SCMZ.

The filtration rate effect was evaluated through the column, at an initial ammonium concentration of 5 mg/L, pH of 7.0, and flow rate adjustments of 8, 10, and 12 m/hour. As the filtration rate increased, the removal efficiency breakthrough time reduced; due to the hydraulic retention time and contact between water and zeolite reduction. Also, the adsorption capacity decreased. Overall, the ammonium-removal efficiency and adsorption capacity was 2.5-3 times greater for SCMZ than natural zeolite.

The regeneration of zeolite is necessary, as the removal efficiency decreases with prolonged operation. Li (2011) applied three regenerative methods, as summarized in Table 4.1; at a pH of 7.0, initial ammonium concentration of 5 mg/L, and filtration rate of 10 m/hour.

TABLE 4.1 - ZEOLITE REGENERATION (LI, 2011)

Zeolite Regeneration Methods	Steps
<i>Heating Regeneration</i>	Breakthrough SCMZ was calcined in a muffle furnace at 200 °C for 24 hours
<i>Acid Regeneration</i>	Breakthrough SCMZ was treated with 1.0 mol/L HCl solution for 24 hours, repeatedly rinsed with tap water, and dried at 45 °C for 4 hours
<i>NaCl Regeneration</i>	Breakthrough SCMZ was treated with 2.0 mol/L NaCl solution for 24 hours, repeatedly rinsed with tap water, and dried at 100 °C for 4 hours

Of these three methods, the NaCl Regeneration method was superior as displayed in Figure 4.2, close to the fresh zeolite state. This process was applied three times at 2 mol/L NaCl solution and is expressed in the following equation; the Na⁺ substitutes the NH₄⁺ that zeolite adsorbed, such that zeolite's ammonium-removal ability is restored.

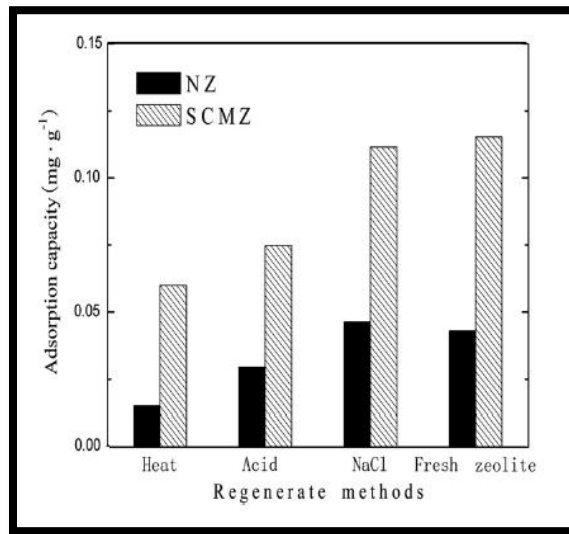


FIGURE 4.2 - ADSORPTION CAPACITY-ZEOLITE REGENERATION METHODS COMPARISON (LI, 2011)

4.4 PELLET COMPOSITION

In addition to operative conditions, the pellet composition is critical to this project's investigation. Zeolite is created from polycrystalline powders, within a particle size range of 1-10 μm . Consequently, it must be formed into granules, spheres, or extrudates before adsorption applications. This reduces the likelihood of a pressure drop and develops mechanically strong particles. Pelletization is achieved by employing natural clays such as bentonite, attapulgite, and kaolin. These clays are considered as inorganic binders, combined at 15-20% of the zeolite pellet (Jasra, 2003). Seidel also supports Jasra's claim, stating that a by mass ratio of 80% zeolite crystals to 20% binder material was ideal. This is further optimized with a binder composition as 80% kaolinite and 20% bentonite clays (similar to natural clay material) (Seidel, 1993).

These pellets are exposed to high-temperature treatment to terminate the clay's surface area and activity; yield apt mechanical stability and maintain high sorption properties. This formation of zeolite pellets generates meso/macro-pores within the pellet; transforming the absorbent attributes of the reactant molecules (Jasra, 2003).

Jasra explored the following procedure:

- Cation Exchange Procedure (Modification)
- Pellet Formation
 - 20 wt% clay binder was combined with zeolite powder
 - Added distilled water to form mixed powder into paste
 - Kneading of mixture
 - Hand extruded with 1.5 mm diameter die
 - Air-dried for 12 hours
 - Oven dried at 383 K (109.85 °C) for 6 hours
 - Calcined in air at 873 K (599.85 °C) for 6 hours (to destroy clay surface area)

It is imperative to select the appropriate binder, obtain proper blending and granulation conditions, and know the binders' influence on zeolite pellets' sorption and catalytic properties (Jasra, 2003). The binder material greatly influences the mechanical properties and adsorption abilities of the final molecular sieve product. The objective was to develop the following qualities of the final optimized pellets (Seidel, 1993):

- zeolite-binder mixture ductility
- high mechanical stability
- minimal static and dynamic adsorption influences of zeolite properties
- adequate binder thermal, hydrothermal, and chemical stability during sorption process
- low catalytic activity

4.5 DEVELOPMENT SUMMARY

The following Tables 4.2 and 4.3 are a summary of key investigators' research efforts that were employed to this project.

TABLE 4.2 – ZEOLITE MODIFICATION MATERIALS OVERVIEW

References	Factors/ Parameters	Chemicals	Phosphorus Solution
<i>Sun (2010)</i>	Zeolite Absorbent Characteristics Contact Time Dosage Temperature Initial Concentration	1 mol/L NaOH solution Dionized Water 20% MgCl ₂ solution KH ₂ PO ₄ salt	Added KH ₂ PO ₄ to distilled water; Stored in reagent bottle
<i>Wanchun (2011)</i>	Initial Concentration Zeolite Size Adsorbent Dosage pH	KH ₂ PO ₄ salt	Dissolved KH ₂ PO ₄ salt (analytical purity) into distilled water
<i>Li (2011)</i>	Zeolites' Characterization pH Initial Concentration Filtration Rate Regenerative Methods	2 mol/L NaCl solution Na ₂ SiO ₃ Ammonium chloride (99.5%) Mercuric iodide (99%) Potassium iodide (99%) Hydrochloric acid (36%) Sodium chloride (99%) Potassium sodium tartrate (99%) Powdered activated carbon	NA
<i>Bear River Zeolite (2011)</i>	NA	Quaternary Amine ('quat')	NA

TABLE 4.3 – ZEOLITE MODIFICATION PROCEDURES

References	Steps
<i>Sun (2010)</i>	<ol style="list-style-type: none"> 1. Natural zeolite soaked in 1 mol/L NaOH solution on dynamic condition at 35°C for 1 hour 2. Washed with dionized water 3. Soaked in 20% MgCl₂ solution on dynamic condition at 35°C for 48 hours 4. Roasted at 500°C in muffle furnace for 3 hours 5. Cooled to normal condition
<i>Wanchun (2011)</i>	No modification – Natural zeolite analysis
<i>Li (2011)</i>	<p><i>Silicate-Carbon Modified Zeolite (SCMZ)</i></p> <ol style="list-style-type: none"> 1. Natural zeolite (clinoptilolite) was ground and sieved to specified optimum size D=74 µm. 2. The clinoptilolite powder was repeatedly washed with tap water and dried at 100°C for 4 hours. 3. 1,000 g of the dry zeolite was dispersed into 1 L sodium chloride solution; 2 mol/L solution with tap water and 12 hour stirring. 4. The sample was repeatedly washed with tap water and then dried at 100°C for 4 hours. 5. The dried sample was ground and sieved to 74 µm again, and designated as sample A. 6. Sample A, Na₂SiO₃ and powdered activated carbon were mixed at weight/weight ratio of 100:9:2, and mixed evenly 7. 10% tap water (weight/weight ratio) was added and stirred again. 8. The mixture was shaped into a cylinder (D=4 mm, H=8 mm) by an extrusion method, and dried at 100°C for 2 hours and calcined in a muffled furnace at 500 °C for 2 hours, and the SCMZ filter was obtained. <p><i>NaCl Regeneration</i></p> <ol style="list-style-type: none"> 1. Breakthrough SCMZ was treated with 2.0 mol/L NaCl solution for 24 hours, repeatedly rinsed with tap water, and dried at 100°C for 4 hours. 2. Process applied three times at 2 mol/L NaCl solution; zeolite's ammonium-removal ability is restored.
<i>Bear River Zeolite (2011)</i>	<p><i>Surface Modified Zeolite</i></p> <ol style="list-style-type: none"> 1. 1,200 g of 14 x 30 mesh natural zeolite was dried at 100°C for 2 hours. 2. 907.2 g of dried (Step 1) 14 x 30 mesh zeolite was measured. 3. 145.2 g of quaternary amine solution was combined with Step 2 materials. 4. Mixture was set aside to dry for two days.
<i>Jasra (2003)</i>	<ol style="list-style-type: none"> 1. Mixture – zeolite crystals (80 mass %) + Binder material (20 mass %) + Water <ol style="list-style-type: none"> a. Optimum binder composition as 80% kaolinite and 20% bentonite b. Calcination temperature range of 823 to 923 K c. Pelletization by employing natural clays 2. Cation Exchange Procedure (Modification) 3. Pellet Formation

Various characterization techniques are applied to modified zeolite, in order to quantitatively identify changes made within this material upon treatment; I.R., N.M.R., X-Ray Diffraction, Electron microscopic and surface sensitive techniques (ESCA, AUGER, SIMS). The effects of a modification technique on zeolite's attributes are most affectively examined through adsorption and catalytic properties (Bekkkum, 1991). Table 4.4 outlines the technologies that were taken under consideration through various research efforts.

TABLE 4.4 – TECHNOLOGY ANALYSIS COMPARISON

Technology for Analysis	Brief Description	References
<i>Scanning Electron Microscopy</i>	Scanning Electron Microscopy (SEM) produces magnified images and in situ chemical information from virtually any type of specimen. The following three aspects are fundamental to comprehend: 1) microscopy and analysis process, 2) sample preparation, and 3) information interpretation based on form/structure relation to image and identity, validity, and locations.	Echlin (2009) Sun (2010)
<i>pH Meter</i> (Fischer Scientific: accumet Basic AB15 pH Meter)	To determine the acidity of a given solution based on the pH scale, such that 7.0 is natural, <7.0 is acidic, and > 7.0 is basic.	Wanchun (2011)
<i>Thermometer</i>	To establish the temperature of an environment, material, or solution	Wanchun (2011)
<i>X-Ray Diffraction (XRD)</i>	Crystallography involves the analysis of natural minerals' external appearance, based on how crystals are built from small components to form a unit cell of identical structural units. This data is systematized by relating geometry and space group theory.	Li (2011)
<i>Thermogravimetry (TG)</i>	Within a controlled heated or cooled environment, a substance weight measured as a function of time or temperature is recorded. Applications include (in)organic chemistry, polymer chemistry, minerals and applied sciences.	Keattch (1975) Li (2011)

Zeolite stability is an important requirement under operative conditions. For example, thermal stability towards amorphization and dealumination with regards to X-Ray Diffraction; analyzing zeolite before and after certain thermal treatment or reaction conditions in order to determine changes in degree of crystallinity, crystal structure or number of framework aluminum atoms that have occurred (Bekkkum, 1991).

Zeolite morphology and particle size are very influential properties, such as the effects on the kinetics of adsorption or ion exchange. SEM is the most versatile technique to study these distributions (Bekkkum, 1991). It is an experimental technology that is applied to determine the structure (crystal morphology and size) of a sample. Images are obtained from low-energy secondary electrons (<50 eV) that the sample emits as a reaction to the narrow electron beam rastered across its surface. Secondary electron intensity is irritable to surface orientation such that the image generated indicates topography. Commonly, surface coating by a layer of conducting metal is applied to create a conductive surface and avoid charging (Wright, 2008).

5 EXPERIMENTAL DESIGN

This chapter of the report delivers the various aspects of the experimental work conducted. This includes the key parameters assessed, materials and methods employed, pellet design as well as optimization and final apparatus procedures.

5.1 PARAMETERS

Based on extensive literature review, various key factors were analyzed in this research to determine the optimal pellet type and removal process. These parameters are included in Table 5.1.

TABLE 5.1 – EXPERIMENTAL PARAMETERS

#	Parameter	Characteristic
1	Pellet Composition	Clay Type (PHG+B, EPK, Bentonite) Zeolite Gradation (4x8, 8x40, 14x40) %Clay:%Zeolite
2	Contact Time	7.5-15 minutes 15-45 minutes 15-180 minutes
3	Influent Concentration	6-18 mgP/L (Septic tank effluent)
4	Effluent Concentration	Meeting TP meter range of 0.02-1.1 mgP/L and MOE Standards
5	Furnace Exposure	100°C and 600°C at 6 hours, 12 hours, or 24 hours
6	Effluent pH	Neutral (pH = 7)
7	Removal Efficiency	Contact Time to Removal Concentration (minutes:mgP/L)

5.2 MATERIALS AND METHODS

5.2.1 OPTIMIZATION TESTING UNIT

A small testing unit was constructed in order to assess the various pellet types. Taking a segment of one layer of the apparatus (Figure 5.1), the removal efficiency relative to initial concentration and contact time was the basis for analysis and optimization. Figure 5.2 provides a view of the final product.

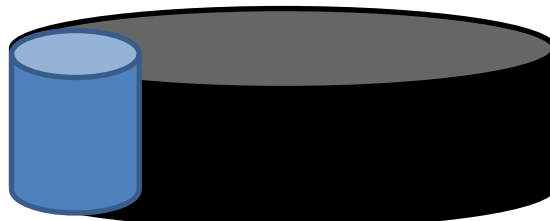


FIGURE 5.1 – OPTIMIZATION TESTING UNIT SEGMENTATION OF APPARATUS



(a) Leakage Testing



(b) Final Product

FIGURE 5.2 - OPTIMIZATION TESTING UNIT

The following outlines the process for the fabrication of the testing unit.

1. Two (2) 15.24cmx15.24cm x10cm PVC plates were cut, as a base.
2. Four (4) 15.24cmx7.62cmx10cm PVC plates were cut, as elevating legs.
3. Two (2) elevating legs were affixed on along the edge of one (1) base with PVC contact cement. This was repeated again to form a second unit.
4. For each supportive component (2 legs and base), a 7.62 cm diameter by 15.24 cm height PVC (schedule 40) pipe was attached on the center of the base with PVC contact cement.
5. A 6.35 mm diameter hole was drilled and threaded in the center of the pipe, on the base.
6. To ensure proper adhesion, the pipe was PVC welded to the base.
7. A 6.35 mm male adapter was threaded into the hole, where a 6.35 mm in diameter plastic tubing was attached. A pincher was added half way along the tubing to control flow during testing.
8. Each unit was tested for leakages, by sealing the tubing with the pincher and filling the pipe with tap water. Small leaks were indicated.
9. All leakages were corrected with an additional application of the PVC contact cement.
10. Each unit was rinsed with tap water.

5.2.2 PELLET COMPOSITION AND FORMATION

5.2.2.1 ORIGINAL VIRTUAL ENGINEERS PROCEDURE

At the preliminary stages of pellet development, Virtual Engineers (VE) original technique was employed. The concise version of the procedure employed is as follows:

1. Eight (8) clay lumps of approximately 200 g were formed; to total the 1,600 g mass indicated in the VE laboratory notes.
2. The clay lumps were combined with another VE Material, and set aside in a metal bowl.
3. The zeolite was weighed at 147.5 g, and retained in another metal bowl.
4. The clay was rolled out to an approximate $\frac{3}{4}$ inch diameter cylinder, and $\frac{3}{4}$ inch spheres were extracted.
5. The sphere was flattened, and zeolite particles were inserted to span across the center by approximately 1 cm. The sphere was sealed and reshaped.
6. The remaining zeolite was weighed at 123.2 g.
7. 134 pellets were formed, and allowed to air dry for 2 days
8. The pellets were placed on the furnace tray and inserted into the preheated furnace at approximately 600°C (3.5 Setting).

It is to be noted that within moments of being inserted, the original VE pellets exploded due to extreme heat exposure. The temperature effects are expressed in Figure 5.3.



5.2.2.2 MODIFIED VIRTUAL ENGINEERS PROCEDURE

The following outlines the procedure used to form the VE pellets, and adjusted in such a way that a melon baller was employed to ensure uniform pellet formation.

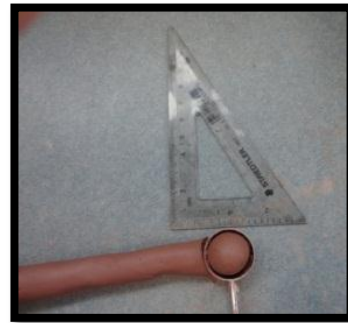
1. Eight (8) clay lumps of approximately 200 g were formed.
2. The clay lumps were combined with another VE Material, and set aside in a metal bowl.
3. The zeolite was weighed at 147.5 g, and retained in another metal bowl.
4. Each clay ball was rolled out into an approximate $\frac{3}{4}$ inch diameter cylinder.
5. With reference to Figure 5.4:
 - a. With melon baller of interior volume of a $\frac{3}{4}$ inch sphere, the clay was extracted.
 - b. The clay was removed from the melon baller.
 - c. The small clay mass was flattened.
 - d. Zeolite particles were inserted to span across the center by approximately 1 cm (2-3 particles).
 - e. The small clay mass was sealed and reshaped to form a sphere.
6. The remaining zeolite was weighted at 123.2 g.
7. 134 pellets were formed, and air dried for 24 hours.
8. The pellets were placed on the furnace tray and inserted into the preheated furnace at approximately 100°C (LOW Setting), dehydrated for 24 hours.
9. The furnace was increased to approximately 400°C (2 Setting), and one hour later to approximately 600°C (3.5 Setting), allowing for calcination for 24 hours.
10. The furnace was turned off and allowed to come to room temperature before removal, and stored in open sealable plastic bags.



(a) Workbench Set-Up



(b) Clay ball rolled out into $\frac{3}{4}$ in diameter cylinder and clay extracted with melon baller



(c) Clay removed from melon baller



(d) Clay flattened and zeolite particles inserted



(e) Clay spheres formed as encapsulated pellets



(f) Air dry



(g) Furnace exposure

FIGURE 5.4 - MODIFIED VE PROCEDURE

5.2.2.3 PELLET OPTIMIZATION PROCEDURE

It is to be noted that Jasra’s procedure (described in Section 4.4) employed a powder form of zeolite. Due to material limitations and porosity objectivity (coarser zeolite), the amount of clay was modified based on feasibility; overall clay incorporated into the mix was 80% of zeolite, but still analyzing Jasra’s two clay combination of bentonite and kaoline (hydrous aluminum silicate). The materials employed are as follows in Table 5.2:

TABLE 5.2 – PELLET OPTIMIZATION MATERIALS

#	Material	Characteristics	Product Name	Chemical Name	Composition
1	<i>Brenntag Canada Inc.</i>	Bentonite	Bentonite/ Volclay	Montmorillonite	90-100% Bentonite 1-10% Silica, Crystalline, Quartz
2	<i>Edger’s Minerals</i>	Kaoline	EPK Kaoline	Kaolinite	96-99.9% Kaolinite 0.1-4% Crystalline Silica
3	<i>Bear River Zeolite</i>	Fine Gradation	8x40 Mesh		
		Finer Gradation	14x40 Mesh		
4	<i>DDW</i>				

Bentonite clay, Kaoline clay, Bear River Zeolite (8x40 and 14x40) gradations, and DDW of various ratios as indicated in Appendix A were investigated. The following procedure outlines the procedure to form a different pellet, based on various clay types and ratios, as well as zeolite gradations and ratios.

1. In a medium steel bowl, 43.8 g of zeolite and 35 g of clay were added. These bowl contents were mixed to become evenly distributed.
2. Beginning with a clay:water ratio of 1:4, DDW was added to the bowl at 2 to 4 increments until measurable workability was achieved into paste consistency.
3. The paste was kneaded and formed into a 1-2 in diameter cylinder.
4. With reference to Figure 5.5:
 - a. With melon baller of interior volume of a ¾ inch sphere, the paste was extracted.
 - b. The paste was removed from the melon baller.
 - c. The paste mass was reshaped to form a sphere of ¾ in diameter.
5. The pellets were air dried for 24 hours.
6. The pellets were placed on the furnace tray and inserted into the preheated furnace at approximately 100°C (LOW Setting), dehydrated for 24 hours.
7. The furnace was increased to approximately 400°C (2 Setting), and one hour later to approximately 600°C (3.5 Setting), allowing for calcination for 24 hours.
8. The furnace was turned off and allowed to come to room temperature before removal, and stored in open sealable plastic bags.



(a) Bench Set-Up and Materials



(i) Zeolite



(ii) Clay – Bentonite and Kaoline



(iii) Dry ingredients combined

(b) Measurement of Dry Ingredients

FIGURE 5.5 - OPTIMIZATION PELLET PROCEDURE



(c) Water added to workability, forming paste and kneaded



(d) Pellets extracted from paste with mullon baller



(e) Formed 3/4 inch diameter spheres with palm of hands



(f) Air dry

FIGURE 5.5 – OPTIMIZATION PELLET PROCEDURE CONTINUED



(g) Pre-Furnace Exposure



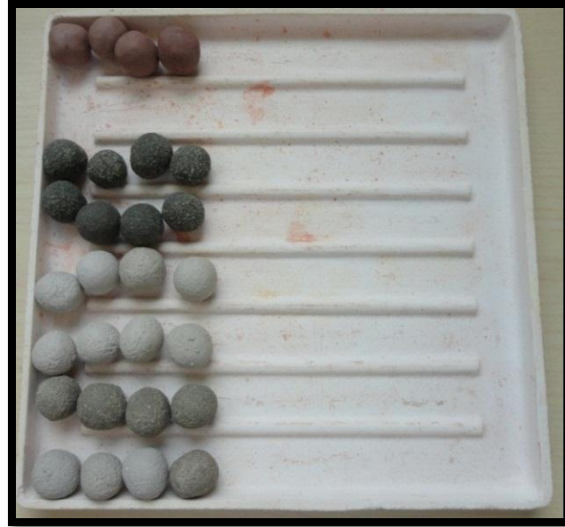
(h) Post-Furnace Exposure

FIGURE 5.5 - OPTIMIZATION PELLET PROCEDURE CONTINUED

The Modified VE and Pellet Optimization Procedures outlined above are based on various works, such as Seidel (1993) and Jasra (2003); determining that a gradual exposure to temperature monitoring be employed. All seven (7) pellet types were formed, and 4 pellets of each type were analyzed for temperature effects, as in Figure 5.6.



(a) Air Dry



(b) Pre-Furnace Exposure



(c) Post-Furnace Exposure

FIGURE 5.6 – PELLET COMPOSITION, FORMATION AND TEMPERATURE MONITORING

All pellet types withstood the gradual temperature exposure. Consequently, approximately 100 pellets of each type were formed for the pellet optimization stage of the experiment, as outlined in Appendix B.

5.2.3 PELLET SACK DEVELOPMENT

A simple and cost effective method was determined to hold the mass quantity of the optimized pellets at each of the five removal levels; burlap. A Janome 4235 Sewing Machine with the following settings were applied:

- Tension - 2
- Stitch - C (zigzag)
- Length - 2.5
- Width - 5

Figure 5.7 and 5.8 below provides a schematic of the approximate configuration; these sacks were prepared to be filled and sealed prior to inserting them into the apparatus.

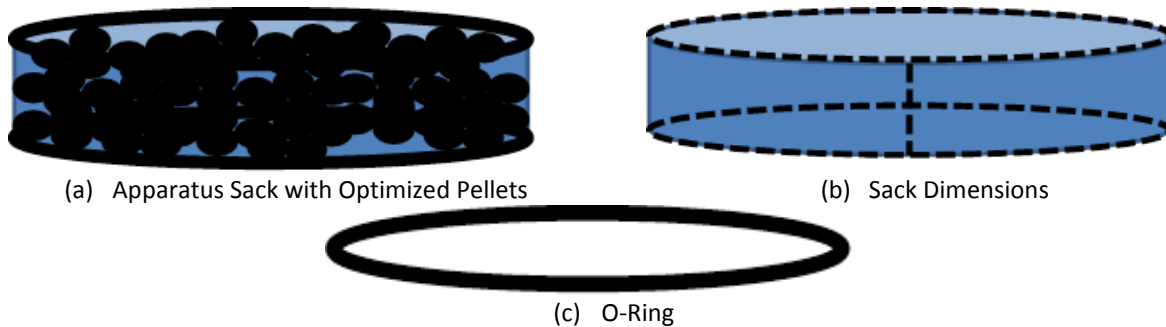


FIGURE 5.7 – APPARATUS SACK CONFIGURATION

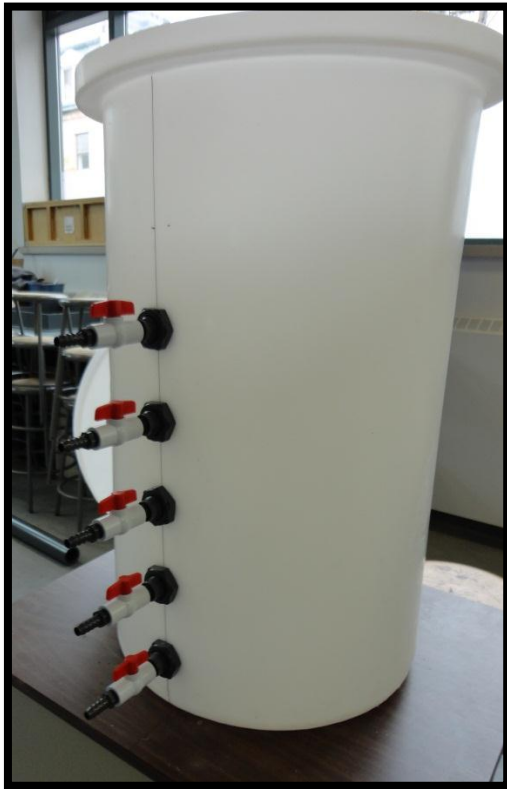


FIGURE 5.8 – PELLET SACK DEVELOPMENT

Five burlap cylindrical sacks were assembled, with approximate cylindrical dimensions of 5 inch height and 22 inch diameter with sewing margins taken into account. To divide each layer, 400 Series O-Rings at 22 inch outer diameter were employed from HighTech Seals.

5.2.4 APPARATUS PROTOTYPE

With reference to Figure 5.9 below, the apparatus prototype was assembled and prepared for testing. The apparatus tank was configured for the optimized pellets to be inserted into each sack, and each sack placed at its respected layer. The sampling posts are positioned below each sack layer to draw effluent for testing.



(a) Apparatus Tank



(b) Sampling Port Outlet



(c) Sampling Port Inlet

FIGURE 5.9 - APPARATUS DEVELOPMENT

Figure 5.10 is the AutoCAD schematic employed to construct the prototype.

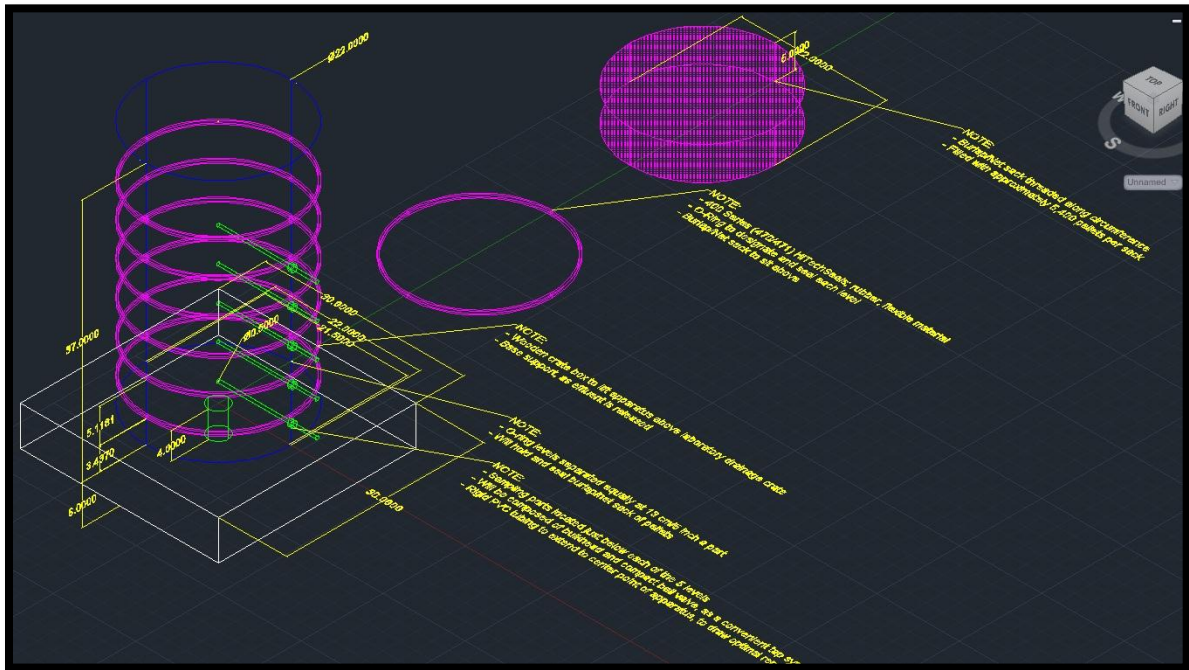


FIGURE 5.10 – SCHEMATIC DRAWING

5.2.5 DEIONIZED DISTILLED WATER (DDW)

Based on extensive reliance on purified water, a large quantity of DDW was obtained from the Ryerson University – Chemistry and Biology Department. Approximately 700 L was extracted, and transported to the testing location in a 720L tank. Figure 5.11 visually outlines the actions taken.



(a) Filling 20 L carboy with DDW



(b) Chemistry and Biology Department Filter System



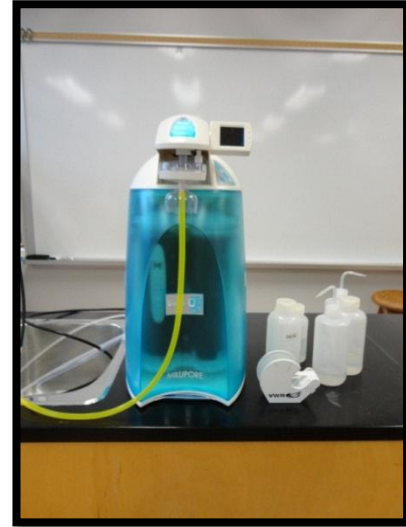
(c) Filling 720 L tank with DDW

FIGURE 5.11 – DDW LOADING AND TRANSPORTATION

It is to be noted that DDW was also supplied from the Ryerson University – Civil Engineering Department from a lab scale machine to rinse glassware following acid soaking. The machine located in the Environmental Engineering Laboratory operates at 18 ohms resistivity. However, prior to pre-optimization testing, it was discovered that the resistivity and subsequent purity was reduced due to filter replacement. And so, all subsequent testing was conducted with the DDW supplied from the neighbouring department to ensure the quality of the experimental results.



(a) Display Screen



(b) Machine Unit

FIGURE 5.12 – CIVIL ENGINEERING LAB SCALE DDW MACHINE

5.2.6 CLEANING PROCEDURE

5.2.6.1 TANK

To account for any additional impurities, both the DDW tank and apparatus tank were thoroughly rinsed with tap water then DDW. Its sides were wiped down in a circular motion from base to top. Its base was filled to approximately 1 inch in height and the tank was swirled. No detergent was applied due to phosphate sensitivity.

5.2.6.2 TESTING UNIT

To account for any additional impurities, each testing unit was thoroughly rinsed with tap water then DDW, three consecutive times each. Between each subsequent influent concentration exposure, the unit was rinsed with tap water then DDW.

5.2.6.3 GLASSWARE AND SAMPLE BOTTLES

With reference to Spec-20, phosphate adsorbs to glass surfaces.



(a) Soaking basin



(b) Sulfuric acid bath of submerged glassware

FIGURE 5.13 – GLASSWARE AND SAMPLE BOTTLE PREPARATION

Consequently, all glassware and sample bottles (polyethylene containers) were soaked overnight in a 10% sulfuric acid bath (approximately 20L basin as in Figure 5.13), rinsed three times in tap water, and rinsed three times in DDW. All samples were stored in a dark cupboard for testing, to follow for no more than 24 hours.

5.3 DESIGN STAGES

This section of the report provides overview of the protocol developed in order to determine the optimal pellet type. For the calculative stage of this project, the following equations were employed; pellet volume (5.1), pellet surface area (5.2), burlap sack volume (5.3), burlap sack surface area (5.4), stock volume (5.5), DDW volume (5.6).

$$V_p = \frac{4\pi r_p^3}{3} \quad [5.1]$$

$$A_p = \pi r_p^2 \quad [5.2]$$

Where

V_p	=	pellet volume (in ³)
A_p	=	pellet surface area (in ²)
r_p	=	pellet radius (in)
D_p	=	pellet diameter (in)

$$V_{bs} = H_{bs}\pi r_{bs}^2 = \frac{H_{bs}\pi D_{bs}^2}{4} \quad [5.3]$$

$$A_{bs} = \pi r_{bs}^2 \quad [5.4]$$

where

V_{bs}	=	burlap sack volume (in ³)
A_{bs}	=	burlap sack surface area (in ²)
H_{bs}	=	burlap sack height (in)
r_{bs}	=	burlap sack radius (in)
D_{bs}	=	burlap sack diameter (in)

$$V_{stock} = \frac{V_{sump} \times C_{sump}}{C_{stock}} \quad [5.5]$$

$$V_{DDW} = V_{sump} - V_{stock} \quad [5.6]$$

where

V_{stock}	=	stock solution volume (L)
C_{stock}	=	stock solution concentration (20 mg P/L)
V_{sump}	=	sump solution volume (L)
C_{sump}	=	sump solution concentration (Ci mg P/L)
V_{DDW}	=	DDW volume (L)

This project was a three stage process:

1. Pre-Optimization
2. Optimization
3. Final Apparatus

At Ryerson University, Stages 1 and 2 were conducted in the Environmental Engineering Lab (MON412), and Stage 3 in the Hydraulics Engineering (MON106) and Structures Lab (ENGLG26).

For the preliminary stages 1 and 2 of the experiments, the testing unit was constructed with the characteristics in Table 5.3.

TABLE 5.3 – TESTING UNIT PROPERTIES

Height [H _{tu}]	Diameter [D _{tu}]	Volume [V _{tu}] (in ³)
13 cm (5.12 inch)	7.62 cm (3 inch)	592.9 cm ³ (36.18 in ³)

According to Song (2008), two random packing factors occur; close (RCP) and loose (RLP). Their respective maximum density Atomic Packing Factors (APF) are 64% (RCP) and 55% (RLP). The medium of these values was selected at 60%, such that (Callister, 2007):

$$APF = \frac{V(\text{atoms in unit cell})}{V(\text{total unit cell})} = 0.60 \quad [5.7]$$

With the assumption of a 60% atomic packing factor, the volume of the pellets (V_p) to occupy the volume of the testing unit (V_{tu}) would be as follows:

$$V_p = 0.60 \times V_{tu} = 355.8 \text{ cm}^3 (21.71 \text{ in}^3)$$

In order to determine the most feasible pellet size, various extraction and pelletizing methods were explored, such as a pelletizing machine, truffle moulds, and measuring spoons. From the preliminary testing of the VE original procedure, 6 pellets formed by hand were randomly selected to measure their diameters, as indicated in Table 5.4.

TABLE 5.4 – RANDOMLY SELECTED ORIGINAL VE PELLETS

Pellet	Diameter		Volume	
	cm	in	cm ³	in ³
1	2	0.787	4.20	0.256
2	1.75	0.689	2.80	0.171
3	2	0.787	4.20	0.256
4	1.75	0.689	2.80	0.171
5	1.5	0.591	1.77	0.108
6	2	0.787	4.20	0.256
Average	1.833	0.722	3.23	0.197

Various measuring spoons were analyzed as well, converting the volume of half a sphere, and translating it to its corresponding diameter of a complete sphere as expressed in Table 5.5:

TABLE 5.5 – MEASURING SPOON ANALYSIS

Measurement	Diameter		Volume	Half of Volume	Radius-Half of Volume	Diameter- Half of Volume	
	cm	in	in ³		in	in	cm
1/4 Teaspoon	2	0.787	0.256	0.128	0.312	0.625	1.59
1/2 Teaspoon	2.5	0.984	0.499	0.250	0.391	0.781	1.98
1 Teaspoon	3	1.18	0.863	0.431	0.469	0.937	2.38
1 Tablespoon	4	1.57	2.04	1.02	0.625	1.25	3.17

As indicated in Tables 5.4 and 5.5, the average Original VE pellet and ½ teaspoon measuring spoon diameters are 0.722 inches (1.83 cm) and 0.781 inches (1.98 cm), respectively. These values bound a ¾ inch pellet diameter volume.

For repeatability purposes, a melon baller was purchased of corresponding diameter-volume. All calculations that followed correspond to a ¾ inch pellet diameter volume.

To determine the number of pellets to fill the testing unit, the corrected pellet volume was employed such that the volume of a ¾ inch diameter pellet is 0.221 in³ as follows:

$$\#Pellets = \frac{V_p}{V_{p=0.75inch}} = \frac{21.707 \text{ in}^3}{0.221 \text{ in}^3} \approx 100$$

$$Void\ Space = V_{tu} - \#Pellets \times V_p = 14.5 \text{ in}^3 = 0.237 \text{ L}$$

This void space corresponds to the sump volume for experimentation; a 25% safety factor was applied, such that 0.296 L was carried through testing. In order to account for time and economic factors to the experiment, specific initial influent concentrations and contact times (converted to flow rate) were selected. A septic tank’s effluent (apparatus influent) concentration of phosphorus ranges approximately from 7-20 mgP/L (EPA, 2012, University of Minnesota, 2010).

The following outlines the testing procedure for each pellet type. Figure 5.14 displays the various components to this test; captions (a) and (b) pertain specifically to the Pre-Optimization stage.

1. As per subsection 5.2.6, the testing unit was cleaned and filled with 100 pellets.
2. The pellets were rinsed once with DDW to reach a saturated surface dry moist surface.
3. The testing unit was filled with an overall influent volume of 500 mL, to fully submerge the pellets to the designated contact time.
4. 30 mL cleaned sample bottles were filled with the influent, effluent and blank.
5. The pellets and testing unit were thoroughly rinsed with tap water.
6. The pellets were set aside on a tray to dehydrate in air for a minimum of 48 hours.
7. With reference to Appendix F, the MC500 Colorimeter testing procedure was employed and all results were recorded.



(a) Influent Preparation



(b) Pellet Testing Set-Up



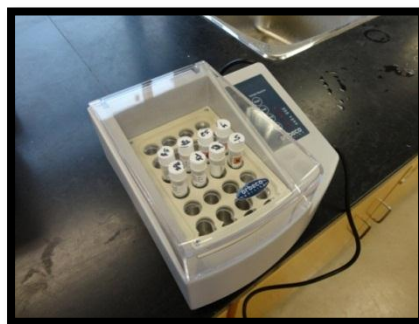
(c) Pellet Submersion



(d) Pellet Air Dehydration

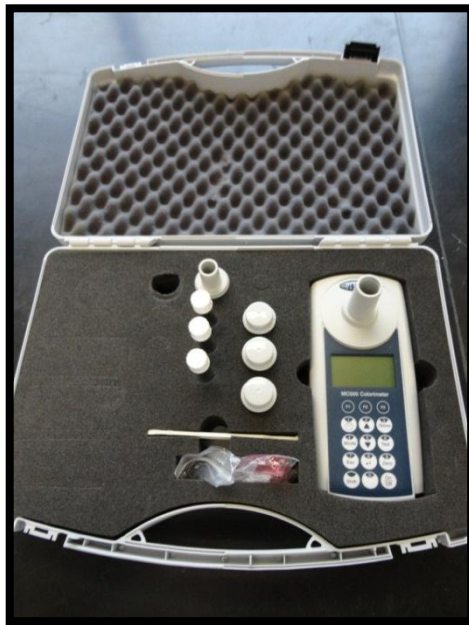


(e) Total Phosphorus Reagent Set



(f) Orbeco Hellige – TR125 Reactor

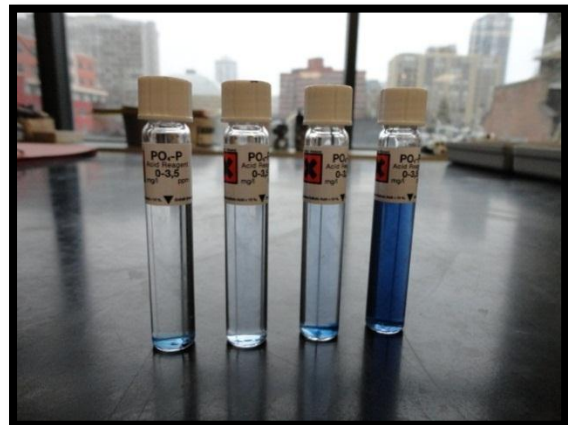
FIGURE 5.14 – STEPS OF THE LABORATORY BENCH SCALE TESTING



(g) Orbeco Hellige – MC500 Colorimeter



(h) MC500 Colorimeter Testing Set-Up



(i) Sample results of various concentrations

FIGURE 5.14 – STEPS OF THE LABORATORY BENCH SCALE TESTING CONTINUED

The following subsections outline the actions taken and the decisions made over the course of each of the three design stages.

5.3.1 PRE-OPTIMIZATION

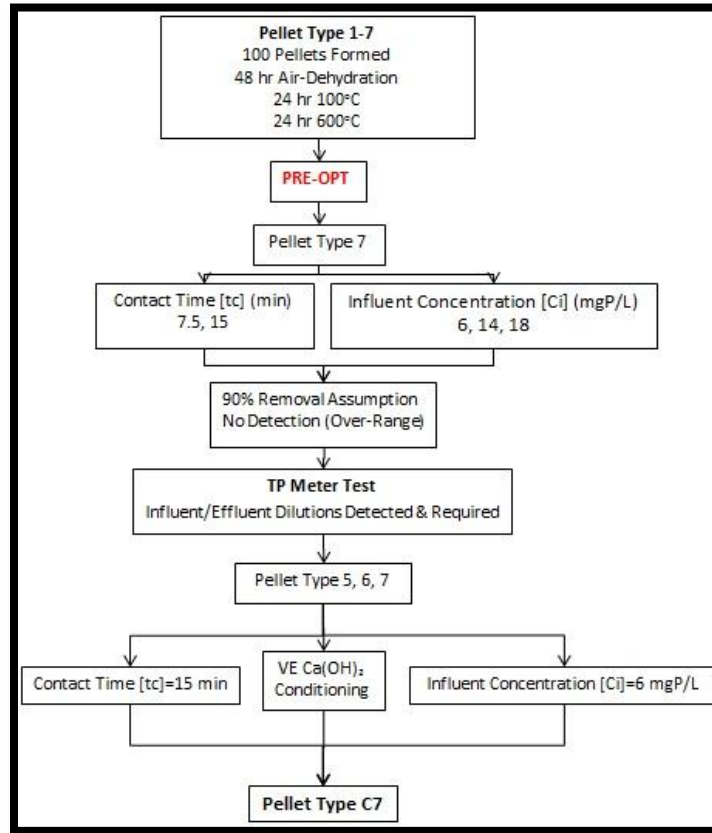


FIGURE 5.15 – PRE-OPTIMIZATION PROCESS

As indicated in Figure 5.15, the lower, middle and upper bounds of initial influent concentrations were analyzed. Given that only two contact times were explored at this stage, the samples were extracted at these times rather than regenerating the testing unit with influent. The design is as indicated in Table 5.6.

TABLE 5.6 – PRE-OPTIMIZATION STOCK-SUMP DETERMINATION

Sump Volume						
V_{sump} (L)	0.296					
Stock Solution		Sump Solution		Influent Concentration [C _i] (mg P/L)	V_{stock} (L)	V_{DDW} (L)*
V_{stock} (L)		V_{sump} (L)	0.300	6	0.0900	0.210
C_{stock} (mg P/L)	20	C_{sump} (mg P/L)	C _i	14	0.210	0.0900
				18	0.270	0.0300
				TOTAL	0.570	0.330

*DDW Volume = Sump Volume – Stock Volume

Therefore, for one pellet type, the volume of stock at 20 mg p/L and volume of DDW required is 570 mL and 330 mL, respectively. Correspondingly, for this stage accounting for all 7 pellet types, the total amount of stock and DDW required is 3.99 L and 2.31 L, respectively.

The experimental design was modified due to the constraints of the TP meter. In addition, the pellets were conditioned to observe the effects on the removal efficiency. As conducted by VE, a calcium hydroxide solution was applied to conduct surface modification to the pellets. The procedure for two pellet types is as follows:

1. With a sulfuric acid cleaned and thoroughly rinsed 1 L graduated cylinder, the VE ratio of 500 mg Ca(OH)_2 to 3L tap water was mixed to a 800 mL quantity (at 167 mg/L concentration).
2. Using a scale, 133.4 mg of hydrated lime (Ca(OH)_2) was weighed.
3. With a 100 mL volumetric flask, 400 mL of tap water was measured and added to the 1 L graduated cylinder.
4. The measured calcium hydroxide was added to the 1 L graduated cylinder.
5. The 1 L graduated cylinder was covered with plastic wrap and inverted three times.
6. Step 3 followed by step 5 was repeated.
7. The pellets were added to the graduated cylinder, such that they are fully submerged.
8. The pellets were left unsettled for 30 minutes (Figure 5.16).
9. The conditioning solution was thoroughly drained.
10. The pellets were rinsed with tap water once, and prepared for testing.



FIGURE 5.16 – PRE-OPTIMIZATION PELLET CONDITIONING PROCEDURE

5.3.2 OPTIMIZATION

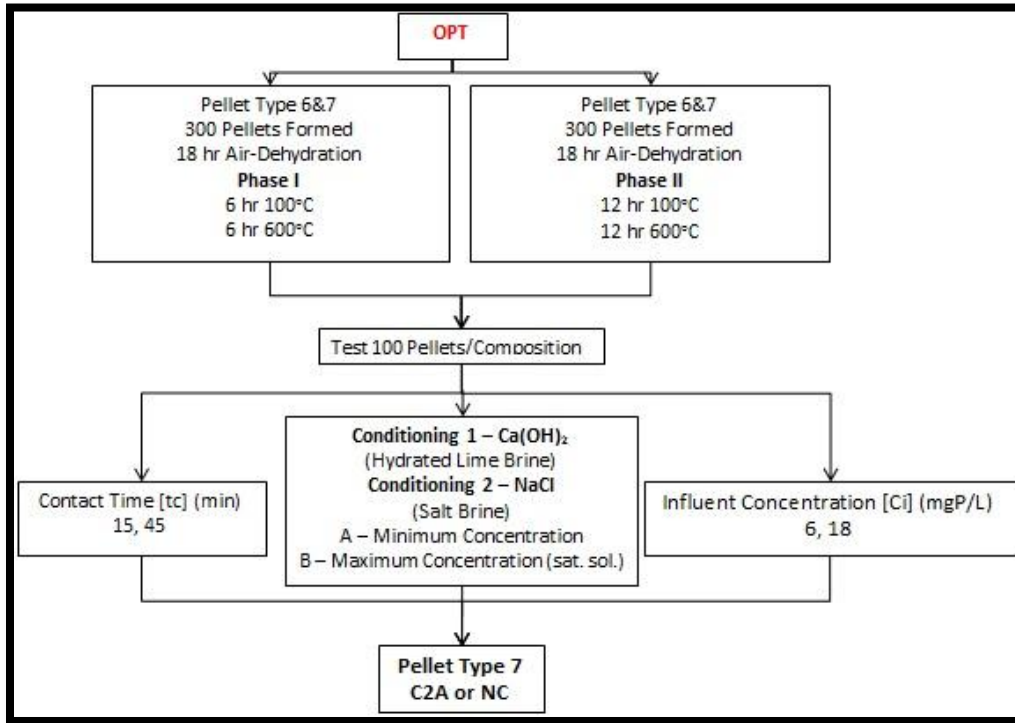


FIGURE 5.17 - OPTIMIZATION PROCESS

Following the discoveries of Pre-Optimization, an informing meeting was scheduled between the researcher’s efforts and that of Virtual Engineers. It was discussed that an important factor from the mass production perspective is the furnace time. The pre-optimization pellets were exposed to 100°C for 24 hours, and 600°C for 24 hours. This places a strain on energy consumption. As a result, the furnace time became another parameter. In addition, the further exploration of conditioning versus as-received pellet form was discussed. This stage (Figure 5.17) investigated the effects of conditioning concentration, as well as furnace time against the minimum and maximum influent concentrations at two different contact times.

Approximately 300 pellets of both Type 6 and Type 7 were formed; such that 100 non-conditioned, 100 conditioned with Calcium Hydroxide (Ca(OH)₂) (C1) and 100 conditioned with Sodium Chloride (NaCl) (C2). The pellets were exposed to the furnace times of 6 hours at 100°C and 600°C (Phase I), and 12 hours at 100°C and 600°C (Phase II). The pellets conditioned were exposed to a low (A) and high (B) concentration or maximum solubility of each brine solution. The pellets were submerged in a minimum and maximum influent, 6 mgP/L and 18 mgP/L, respectively. The effluent was drawn at two different contact times; 15 and 45 minutes. Tables 5.7 and 5.8, and Figure 5.17 provide a summary of the actions taken at this stage.

TABLE 5.7 – PHASE I PELLET DETERMINATION

Pellet Type	Furnace Time (hrs/°C)	Influent Concentration [Ci] (mgP/L)	Pellet Conditioning		Contact Time [Tc] (min)
6I (14x40 Zeolite Clay Mixture)	6/100	6	Non-Conditioned		15
7I (VE – 4x8 Zeolite Encapsulate)	6/600	18	Calcium Hydroxide (Ca(OH) ₂) – Lime Brine (1)	Minimum Concentration (A) C1 – 50% C2 – 2 mol/L	45
			Sodium Chloride (NaCl) – Salt Brine (2)	Maximum Concentration (B) (100%)	

TABLE 5.8 – PHASE II PELLET DETERMINATION

Pellet Type	Furnace Time (hrs/°C)	Influent Concentration [Ci] (mgP/L)	Pellet Conditioning		Contact Time [Tc] (min)
6II (14x40 Zeolite Clay Mixture)	12/100	6	Non-Conditioned		15
7II (VE – 4x8 Zeolite Encapsulate)	12/600	18	Calcium Hydroxide (Ca(OH) ₂) – Lime Brine (1)	Minimum Concentration (A) C1 – 50% C2 – 2 mol/L	45
			Sodium Chloride (NaCl) – Salt Brine (2)	Maximum Concentration (B) (100%)	



(a) Glassware and Sampling Bottle Set-Up



(b) Stock stirring



(c) Conditioning Set-Up



(d) Conditioning stirring



(e) Pellet soaking in conditioning brines



FIGURE 5.18 – OPTIMIZATION PHASE PROCEDURES

5.3.2.1 HEAT TREATMENT

As per Jasra's research efforts (2003), the furnace time was analyzed. Approximately 300 pellets of Types 6 and 7 were formed (as per subsection 5.2.2.2 and 5.2.2.3) and their ratios are outlined in Appendix D. With regards to the Type 7 pellets, they were air-dried for 18 hours; however, their furnace times were modified. As opposed to the 24 hours at 100°C and 600°C as in the pre-optimization stage, Phase I exposed the pellets to these temperatures for 6 hours each, and Phase II at 12 hours each. This significantly reduced the energy consumption required. With digital thermometer calibration (Figure 5.19), the heating and cooling rate was approximated and outlined in Table 5.9.

TABLE 5.9 - HEATING-COOLING RATE

Heating Temperature	Time Frame (hours)
Room Temperature (20°C) to Low Setting (100°C)	1
Low Setting (100°C) to 3.5 Setting (600°C)	2
3.5 Setting (600°C) to Room Temperature (20°C)	3

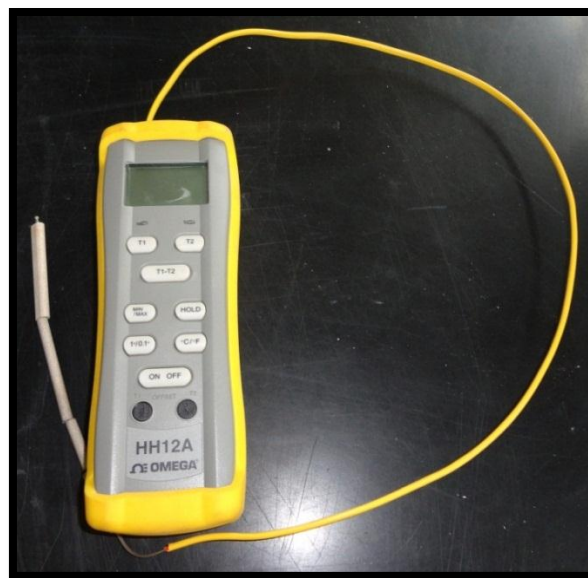


FIGURE 5.19 - MUFFLE FURNACE TEMPERATURE VERIFICATION - OMEGA HH12A

It is to be noted that 6 pellets of ¾ inch diameter were employed during the optimization stage of final composition, in order to observe the effects of moisture, as follows:

- | | | |
|----------------------|---|------|
| 1. Moist Mass (g) | = | 38.0 |
| 2. Air-Day Mass (g) | = | 35.4 |
| 3. Oven-Dry Mass (g) | = | 29.4 |

Therefore, this three stage dehydration process provided an approximate moisture loss of 1.43 g or 22.63%, per pellet.

5.3.2.2 OPTIMIZATION CONDITIONING

In order to explore the ion-exchange capacity of clay and zeolite, the pellets were conditioned with two cation-rich brines. Conditioning 1 (C1) involved calcium hydroxide (Hydrated Lime Brine) and Conditioning 2 (C2) contained sodium chloride (Salt Brine). Two concentrations were analyzed; minimum (A) and maximum (B) solubility at approximately 20°C were diluted with 500 mL of DDW. A 1 L beaker was employed, such that half the solvent was added, followed by the solute, and the remaining solvent. The brine was placed on a rotational bed for 45 minutes at 120 rpm. For each pellet type, 100 pellets were rinsed once with DDW to wash off any debris and then submerged in the brine, and allowed to soak for approximately 24 hours. Prior to testing, the pellets were rinsed once with DDW. Table 5.10 provides an overview of the conditioning employed, followed by Table 5.11 with the solute to solvent calculations.

TABLE 5.10 – CONDITIONING DETERMINATION

Conditioning	Concentration	
	Minimum [A] (mg/L)	Maximum [B – saturated solution] (mg/L)*
C1 – Calcium Hydroxide (Hydrated Lime)	50% Saturated Solution	1.65
C2 – Sodium Chloride (Salt)	2 mol/L (Li, 2011) (Kesraoul-Oukl, 1993)	360

*(Cheney Lime & Cement Company, 2012)

TABLE 5.11 – CONDITIONING BRINE CALCULATIONS

Brine Parameters	Conditioning Brine	
	C1	C2
Solute Solubility at 20°C (g/L)	1.65	360
Solute Molecular Mass (g/mol)	74.09268	58.4428
Solvent Volume (L)	0.5	
Mass Solute at Saturated Solution [A] (g) sat sol.	0.825	180
Solute Molecular Weight at 2 mol/L (g/L).	NA	116.8856
Solute Mass at 2 mol/L (g)	NA	58.4428
Solute Mass at 50% Saturate Solution (g)	0.4125	NA

5.3.3 FINAL APPARATUS

For prototype purposes, a High-Density Polyethylene (HDPE) tank with 22 inch diameter and 36 inches in height was employed as the shell of the apparatus. Based on these dimensions, 5 sampling levels were analyzed and the optimal pellet type was extracted with the following burlap sack layer dimensions of Table 5.12.

TABLE 5.12 – BURLAP SACK PROPERTIES

Height [H_{bs}]	Diameter [D_{bs}]	Volume [V_{bs}]
13 cm (5.12 in)	55.88 cm (22 in)	31,882 cm ³ (1945.56 in ³)

During the pre-optimization and optimization stages of the project, a ¾ inch diameter pellet was employed. This pellet diameter was scaled up to a 1 inch diameter for the final apparatus. If the ¾ inch pellets were carried through to the final stage, approximately 26,000 pellets would be required as opposed to the approximate 12,000 1 inch pellets that were formed this improved the mass production feasibility and met scheduled time restrictions. This was scaled up to 1 inch to account for scheduling (Figure 5.20).

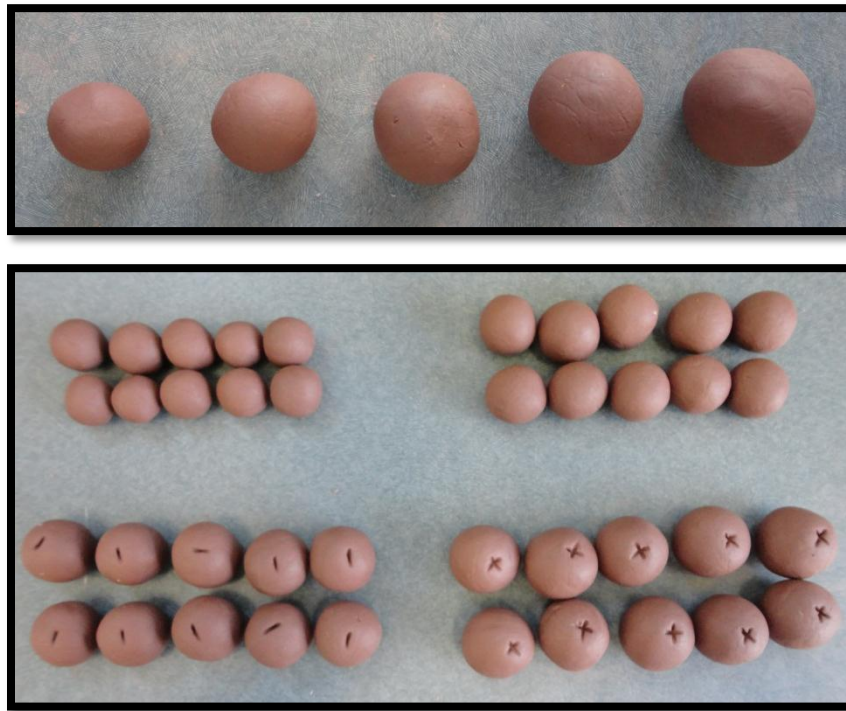


FIGURE 5.20 – PELLET FORMATION SCALE-UP

To determine the volume of 1 inch diameter pellets to be held in one sack, the 60% APF is employed.

$$V_p = 0.60 \times V_{bs} = 1167.337 \text{ in}^3 \text{ (19.13 L)}$$

$$\#Pellets/Layer = \frac{V_p}{V_{p=1inch}} = \frac{1,167.337 \text{ in}^3}{0.524 \text{ in}^3} \approx 2,229$$

$$Void \text{ Space} = V_{bs} - \#Pellets \times V_p = 778.224 \text{ in}^3 \text{ (12.75 L)}$$

$$Percent \text{ Void} = \frac{Void \text{ Space}}{V_{bs}} \approx 40\%$$

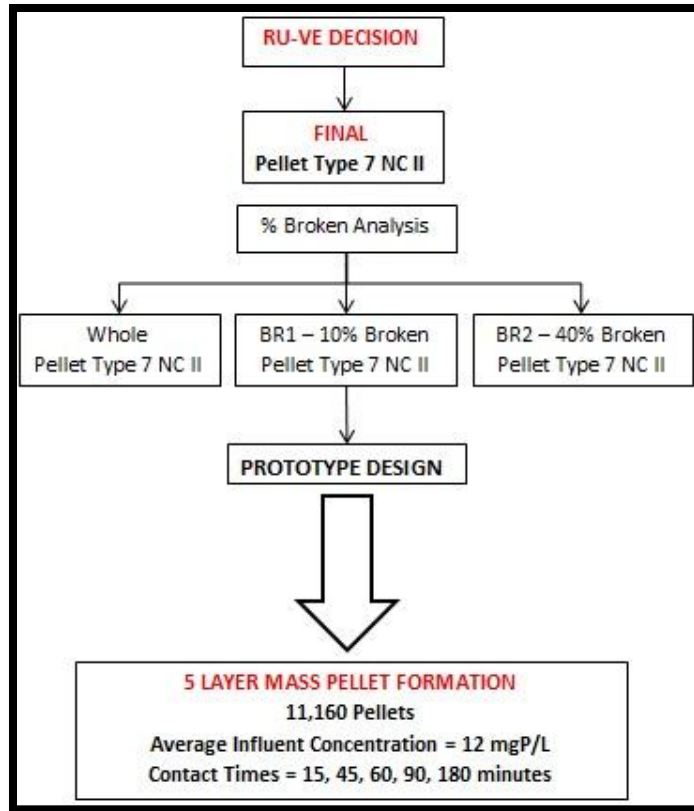


FIGURE 5.21 - FINAL APPARATUS PROCESS

Therefore, for all five burlap sack layers, approximately 11,145 pellets of final, optimized composition were formed. Working with a two week time frame and a team of 5 to 6 representatives of the project, a daily minimum quota of a 1,860 pellet batch were formed over the course of 6 formation days. Each batch was placed into the furnace in five equal layers, maximizing its capacity. The intermediate analysis outlined in Figure 5.21 is discussed further in Chapter 6 and 7 to follow.

Figure 5.22 is a view of the large scale furnace employed for the pellets heat treatment.



(a) Pellet Batch Heat Treatment Set-up



(b) Euclid Kiln

FIGURE 5.22 – APPARATUS PELLET HEAT TREATMENT

Values shown in Table 5.10 were used to calibrate the kiln for final pellet production, as outlined in Table 5.13. Segments 1 and 2 involve a heating rate and maintained for 11 and 12 hours respectively. Segment 3 involved a cooling rate and then turned off.. It is to be noted that these segments are approximated, and were dependent upon how much internal kiln volume employed by the pellets.

TABLE 5.13 – FURNACE/KILN CALIBRATION

	Segment	Rate (°C/hr)	Maintain (hr)
1	Room to 100°C	100	11
2	100°C to 600°C	250	12
3	600°C to Room	200	Off

As a result, the cooling rate of segment 3 required approximately 8 hours rather than 3 hours, where 1 hour prior to extracting the batch, the furnace was turned off and the door was opened to ensure gradual temperature reduction.

Aside from the pellets that were enclosed in the unit, other elements to the design were taken into consideration; sample piping, O-rings, and drainage gravel. The following table outlines their dimensions and corresponding volumes.

TABLE 5.14 – APPARATUS ELEMENTS

<i>PVC Sample Piping</i>		<i>HighTech Seal 470 O-Ring</i>		<i>King 1/2 Gravel</i>	
Outer Diameter (in)	0.840	Inner Diameter (in)	20.955	Gravel Bag Mass (kg) (Loose Compaction)	30
Inner Diameter (in)	0.622	Cross-Section (in)	0.275	Gravel Bag Loose Compaction Volume (m ³)	0.0210
Outer Height (in)	7.087	Outer Diameter (in)	21.505	Gravel Tank Volume [V _g] (22in dia.x 10cm) (in ³)	1496.585
Inner Height (in)		Height (in)	67.560	Average Gravel Void Volume [V _{gv}] (in ³)	653.367 (≈ 43.657%)
Tubing Volume [V _t]=V _{out} -V _{in} (in ³)	1.774	O-Ring Volume [V _o] (in ³)	4.013		
Total Tubing Volume (5)	8.870	Total O-Ring Volume (5)	20.064		

With the logical assumption that the burlap sack materials' volume is negligible, the total void volume is calculated as follows:

$$\begin{aligned}
 V_{void} &= V_{tank} - (V_{pellets} + V_{sample\ tubing} + V_{O-ring}) + V_{gravel-voids} \\
 &= 13,685 - [(11,160 \times 0.524) + 8.870 + 20.064] + 653.367 \\
 &= 8463 \text{ in}^3 \\
 &= 138.760 \text{ L}
 \end{aligned}$$

As a static, saturated system, the corresponding flow rate is determined by applying selected contact times to this void volume; as shown in Equation 5.8 and Table 5.15.

$$Q = \frac{V_v}{t_c} \quad [5.8]$$

where

- Q = flow rate (m³/s, L/s, L/min)
- V_v = void volume (in³, m³, L)
- t_c = contact time (min, s)

TABLE 5.15 – CONTACT TIME TO FLOW DETERMINATION

<i>Contact Time [t_c]</i>		<i>Flow [Q]</i>
(min)	(s)	(m ³ /s)
15	900	1.543E-04
45	2700	5.142E-05
60	3600	1.296E+07
90	5400	2.571E-05
180	10800	1.286E-05

Based on the optimization analysis of minimum and maximum influent concentrations (6 and 18 mgP/L, respectively), the median concentration of 12 mgP/L was selected for final analysis in addition to the contact times outlined in Table 5.15.

To determine the influent stock for final analysis, a 25% safety factor was applied to the calculated apparatus void volume; obtaining 175 L. Table 5.16 outlines the dilution calculations employed. It is to be noted that a 4 L stock was formed, with the addition of the 210 mL of the 10,000 mgP/L concentrated solution to form a concentration of 525 mgP/L. This was diluted in the influent tank to obtain the required 12 mgP/L testing value, as follows:

1. The 10,000 mgP/L concentrated solution was measured at 210 mL, and added 3.79 L DDW into a 4 L beaker.
2. The solution was placed on a rotational mixer for 1 hour at approximately 100 rpm.
3. A 4 L 525 mgP/L stock was created.
4. DDW at 86L was added into the influent tank.
5. The concentrated stock was added into influent tank.
6. The remaining 85 L of DDW was added into influent tank.
7. A 175 L 12 mgP/L solution was created.
8. The influent solution was circulated through the pump as a continuous system, for approximately 15 minutes, to ensure thorough distribution.

TABLE 5.16 – APPARATUS STOCK-SUMP DETERMINATION

Dilution 1 (10,000 mgP/L to 100 mgP/L)				
<i>V_{stock} (L)</i>	0.210	<i>V_{dil1} (L)</i>	21.0	<i>V_{ddw1} (L)</i>
<i>C_{stock} (mgP/L)</i>	10,000	<i>C_{dil1} (mgP/L)</i>	100	
Dilution 2 (100 mgP/L to 20 mgP/L)				
<i>V_{dil1} (L)</i>	21.0	<i>V_{dil2} (L)</i>	105	<i>V_{ddw2} (L)</i>
<i>C_{dil1} (mgP/L)</i>	100	<i>C_{dil2} (mgP/L)</i>	20.0	
Dilution 3 (20 mgP/L to 12 mgP/L)				
<i>V_{dil2} (L)</i>	105	<i>V_{ddw3} (L)</i>	70.0	
<i>C_{dil2} (mgP/L)</i>	20.0	<i>C_{dil3} (mgP/L)</i>	12.0	

Figure 5.23 provides a visualization of the set-up arrangement for the final testing of the apparatus.



(a) Drainage Layer – Gravel



(b) Pellet Burlap sack, Sampling Port, O-Ring



(c) Influent Tank – Apparatus



(d) Pump

FIGURE 5.23 – APPARATUS CONFIGURATION

6 RESULTS

This chapter of the report provides an overview of the results obtained from carrying out the experiments.

6.1 PRE-OPTIMIZATION RESULTS

The preliminary stage of the experiments began with testing the Type 7 pellet (VE design), at 6, 14, and 18 mgP/L influent concentrations. These concentrations were analyzed at 7.5 and 15 minute contact times. All readings indicated over-range for the TP meter; beyond the upper bound of its 0.02-1.1 mgP/L range (Appendix C Table C.1). Consequently, both the 20 mgP/L stock and 6 mgP/L influents were tested through various 50% dilutions, all of which were detectable (Appendix C Table C.2). Tables 6.1 and 6.2 display the dilutions applied to the influent and effluent of subsequent experiments, based on a 20 mgP/L stock created from a 10,000 ppm phosphorus reagent (as in Figure 6.1).



FIGURE 6.1 – CONCENTRATED PHOSPHORUS SOLUTION

TABLE 6.1 – INFLUENT DILUTION

		4-50% Dilutions (DF=0.0625)	5-50% Dilutions (DF=0.03125)	6-50% Dilutions (DF=0.015625)
<i>Influent</i>	Concentration (mgP/L)	6	12	18
	Volume (mL)	0.95	0.50	0.25
<i>Diluted Influent</i>	Concentration (mgP/L)	0.375	0.375	0.28125
	Volume (mL)	15.2	16.0	16.0
DDW (mL)*		14.25	15.50	15.75

TABLE 6.2 – EFFLUENT DILUTION

		3-50% Dilutions (DF=0.125)	4-50% Dilutions (DF=0.0625)	5-50% Dilutions (DF=0.03125)
<i>Effluent</i>	Concentration (mgP/L)	6	12	18
	Volume (mL)	1.9	0.95	0.50
<i>Diluted Effluent</i>	Concentration (mgP/L)	0.75	0.75	0.5625
	Volume (mL)	15.2	15.2	16.0
DDW (mL)*		13.30	14.25	15.50

*DDW Volume = Diluted Volume – Influent Volume

This was followed by the analysis of the Type 6 pellet at the minimum influent concentration (6 mgP/L) and maximum contact time (15 and 30 minutes); once again, with a 90% removal assumed and no dilutions employed, all readings were undetectable by the TP meter (Table C.3). This was followed by the analysis of both the influent and effluent of Type 6 and 7 pellets, with minimum influent concentration (6 mgP/L), and maximum contact time (15 minutes) (Table C.4). At this stage, the influent and effluent were exposed to 4 and 3 50% dilutions as in Table 6.1 and 6.2, respectively. Subsequently, these same pellets were conditioned with calcium hydroxide (Hydrated Lime); there was a successful reading with dilutions (Table C.5). Pellet Type 5 analysis was conducted, following the same procedure for Types 6 and 7 (Tables C.6 and C.6). Table 6.3 provides a summary of the Pre-Optimization results, which is based on an influent concentration of 6 mgP/L for a contact time of 15 minutes; all others are tabulated in Appendix C.

TABLE 6.3 – PRE-OPTIMIZATION PELLETT RESULTS SUMMARY

Pellet Type		TP Removal	
		(mgP/L)	(%)
5	Non-conditioned	2.32	29.42
	Conditioned	1.08	15.24
6	Non-conditioned	0.68	9.93
	Conditioned	0.52	7.18
7	Non-conditioned	1.16	16.56
	Conditioned	2.36	30.87

6.2 OPTIMIZATION RESULTS

Following the pre-optimization stage, parameters 2 through 6 in section 5.1 were further analyzed. It is to be noted that the primary parameter for pellet selection was based upon the TP removal. As to be discussed in chapter 7, the pH parameter was recorded and should be investigated in future research.

Pre-Optimization confirmed that dilutions were required to receive TP Meter detection due to the reading restraints of the narrow range (0.02-1.1 mgP/L). Tables 6.1 and 6.2 of section 6.1 were employed to the influent and effluent, respectively, of the optimization stage as well.

It is to be noted that when the pellets were exposed to the influent and minimum conditioning brines (C1A and C2A), a distinct sizzling sound occurred due to gas formation, and the pellets began to expand. In particular, when Pellet Type 7 was exposed to Phase I, the pellets began to ‘explode’ and fell apart (Figure 6.2). This is most likely due to the compact, dense attribute of the pellets. Consequently, Phase I analysis proceeded, utilizing all pellet fragments in the experiments. The surface area and contact points were greater, which may have skewed the results in its favour with greater phosphorus removal. This fragmentation would compromise the pellet integrity. Consequently, it was decided that Phase II furnace exposure be observed, thereby ensuring a more stable pellet composition.



FIGURE 6.2 – PELLET TYPE 7 PHASE I CA – EXPANSION OBSERVATION

Pellet types 6 and 7 were formed, for both Phase I and II furnace exposures, and carried through for experimentation. Table 6.4 provides a summary of the DDW blank pH and TP concentrations, the values of which were an average of each pellet type and each phase that were applied to all influent and effluent dilutions.

TABLE 6.4 – PHASE BLANK SUMMARY

Pellet Type	Phase	pH	Total Phosphorus Concentration (mgP/L)
6	I	5.30	0.06
	II	5.71	0.08
7	I	5.24	0.07
	II	5.50	0.06

To be discussed in chapter 7, the final pellet type selected was the non-conditioned (NC) Type 7 (VE), Phase II (12 hour furnace exposure). This selection was based on the minor difference in overall phosphorus removal, taking into account the environmental and economic impacts of conditioning. With reference to Table E.13 of Appendix E, this pellet type was recreated and tested once again, and its results demonstrated consistency.

TABLE E.13 – NON-CONDITIONED TYPE 7II – SURFACE AREA ANALYSIS

	Code*	pH	Total Phosphorus Concentration (mgP/L)	Removal	
				(mgP/L)	(%)
<i>Influent</i>	NC:6	5.29	6.72		
	NC:18	5.21	19.12		
<i>Effluent</i>	NC:6:15	10.49	4.92	1.8	27
	NC:6:45	10.8	4.12	2.6	39
	NC:18:15	9.24	14.48	4.64	24
	NC:18:45	10.32	11.44	7.68	40

*NC (Non-Conditioned):# (Theoretical Influent Concentration):# (Contact Time)

Furthermore, when pellet disassembly was experienced earlier in the optimization stage, it was decided to analyze the effects of percent broken (BR) to whole pellets (Figure 5.21 of subsection 5.3.3) . As a result, whole pellets, 10% broken (BR1) and 40% broken (BR2) were analyzed with the same influent concentrations and contact times (Figure 7.13). Results are displayed in Appendix E, Table 14; with an average blank P concentration and pH of 0.08 mgP/L and 5.06, respectively.



FIGURE 6.3 – PELLET SURFACE AREA DEVELOPMENT (10% LEFT AND 40% RIGHT)

TABLE E.14 – NON-CONDITIONED BR1&2 TYPE 7II – SURFACE AREA ANALYSIS

	Code*	pH	Total Phosphorus Concentration (mgP/L)	Removal	
				(mgP/L)	(%)
<i>Influent</i>	BR:6	5.69	6.96		
	BR:18	5.41	23.92		
<i>Effluent</i>	BR:1:6:15	10.84	5.40	1.56	22
	BR:1:6:45	11	4.44	2.52	36
	BR:1:18:15	10.22	15.28	8.64	36
	BR:1:18:45	10.74	12.72	11.2	47
	BR:2:6:15	10.66	4.16	2.8	40
	BR:2:6:45	10.93	3.88	3.08	44
	BR:2:18:15	9.98	12.56	11.36	47
	BR:2:18:45	10.73	10.00	13.92	58

*BR (Brown):# (% Broken):# (Theoretical Influent Concentration):# (Contact Time)
BR1=10%; BR2=40%

6.3 FINAL APPARATUS RESULTS

Overall, 11,547 pellets were formed, and 11,285 pellets survived the extreme heat. This crude, hand-formed technique resulted in an approximately 98% production; a strong performance and promising outcome for the industrial setting following the commercialization phase of the project.

With reference to Appendix E, Table 15, the results for each of the five apparatus layers are displayed, with an average blank P concentration and pH of 0.07 mgP/L and 5.95, respectively.

TABLE E.15 – FINAL APPARATUS TEST

	Code*	pH	Total Phosphorus Concentration (mgP/L)	Removal	
				(mgP/L)	(%)
<i>Influent</i>	INF	5.84	13.21		
<i>Effluent</i>	A:15	9.21	7.29	5.92	45
	B:15	8.90	7.53	5.68	43
	C:15	8.58	7.85	5.36	41
	D:15	8.64	8.17	5.04	38
	E:15	7.86	9.29	3.92	30
	A:45	9.50	5.77	7.44	56
	B:45	9.47	5.77	7.44	56
	C:45	9.32	6.01	7.20	55
	D:45	9.34	6.65	6.56	50
	E:45	8.89	7.53	5.68	43
	A:60	9.83	5.21	8.00	61
	B:60	9.76	5.29	7.92	60
	C:60	9.66	5.77	7.44	56
	D:60	9.65	5.69	7.52	57
	E:60	9.12	7.53	5.68	43
	A:90	10.00	4.73	8.48	64
	B:90	9.95	4.73	8.48	64
	C:90	9.83	4.73	8.48	64
	D:90	9.83	5.29	7.92	60
	E:90	9.40	5.53	7.68	58
A:180	10.16	3.93	9.28	70	
B:180	10.17	3.93	9.28	70	
C:180	10.15	3.61	9.60	73	

*Letter (Layer) :# (Contact Time)

It is to be noted that two influent samples were drawn; at the top of the solution (INF:TOP) as well as at the outlet of the influent tank (INF:BOT). The results indicate that a consistent concentration was achieved, through circulation of the solution by the pump prior to testing to obtain an average influent concentration of 13.21 mgP/L.

As indicated in Figure 6.4, the effluent was drawn from each of the five burlap sack layers, following a purging volume of approximately 60 mL; accounting for the tubing located within the tank as well as on the exterior as the valve.

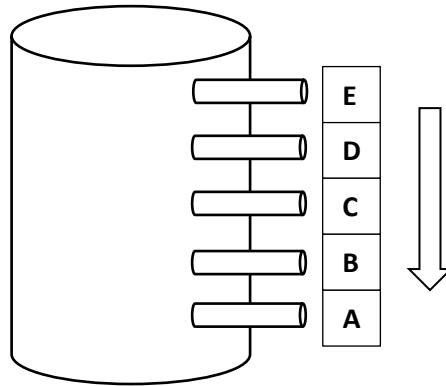


FIGURE 6.4 – EFFLENT SAMPLING ARRANGEMENT

It is important to note that prior to testing, the tank was evaluated for leaks and a caulking/silicone (DAP-AlexPlus Acrylic Latex) was applied to the gasket-tank base connection and allowed to dry for 24 hours. Shortly after the influent was pumped into the apparatus tank, the valve at its base began to leak, due to a poor threading-gasket connection. As a result, prior to each contact time sampling, a sample of leakage flow was drawn to fill a 50 mL graduated cylinder to provide an average rate of approximately 3.656 mL/s (13.667 second filling time), as outlined in Table 6.5 below. ‘Bursting’ sounds were heard which indicated that the pellets within the system began to disassemble to a small degree; percent broken was undeterminable. This accounts for the variability in leakage rate.

TABLE 6.5 – LEAKAGE RATE TEST

Sampling Time (min)	Average Time to Fill 50 mL (s)
<i>Start</i>	15
<i>15</i>	15
<i>45</i>	7
<i>60</i>	10
<i>90</i>	10
<i>180</i>	25

Although approximately 40 L (18% of the total tank volume of 224 L) sample discharged based on the approximate leakage rate during the 3 hour contact time analysis, this may be considered negligible; effluent concentrations of each layer were consistent at each contact time, the purging volume and sampling volume all contributed to this occurrence.

7 ANALYSIS

This chapter of the report takes the findings presented in chapter 6 and interprets them, from the pre-optimization, optimization, and final apparatus analyses.

7.1 PRE-OPTIMIZATION ANALYSIS

Based on a TP removal at a 6 mgP/L influent and 15 minute contact time, the findings tabulated in Appendix C are displayed in Figure 7.1. Pellet Types 1 to 4 were not carried through to the quantitative analysis stage. These pellets were only formed for qualitative purposes; to observe the workability. Given that Types 1 to 4 were only of one clay type (Bentonite and Kaoline) rather than a blend (Types 5 and 6), the overall composition was brittle and consequently not considered ideal for mass production.

Pellet Types 5 and 6 were very porous compared to Type 7. Notably, Types 6 and 7 were exposed to more influent cycles than Type 5, during the preliminary stages of TP Meter detections; in order to refine the dilution calculations. As observed, non-conditioned pellet Type 5 performed similar to that of conditioned pellet Type 7. Based on the coarser, zeolite gradation used to compose Type 5, the fluid dispersion was greater, such that the influent traversed through the material; as opposed to the denser pellets Type 6 and 7. However, Type 5 removal reduced once conditioned. For comparative purposes, the more compact pellets were carried further into analysis (Types 6 and 7), concluding that conditioned pellet Type 7 produced the highest removal efficiency from the pre-optimization perspective.

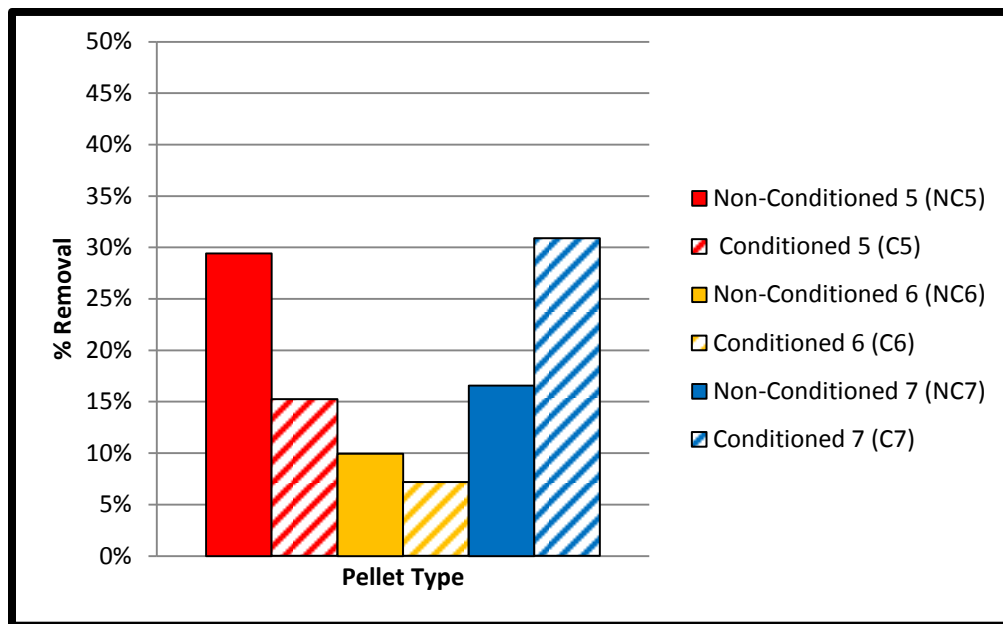


FIGURE 7.1 - PRE-OPTIMIZATION PELLETT ANALYSIS

7.2 OPTIMIZATION ANALYSIS

This section provides a key insight into determining the ideal pellet type, with regards to the parameters indicated in section 5.1.

7.2.1 CONTACT TIME

As observed in Figure 7.2, removal provided by both Types 6 and 7 are optimal non-conditioned (NC) and minimum conditioned Salt Brine (C2A). Pellet Type 7 is great among the two.

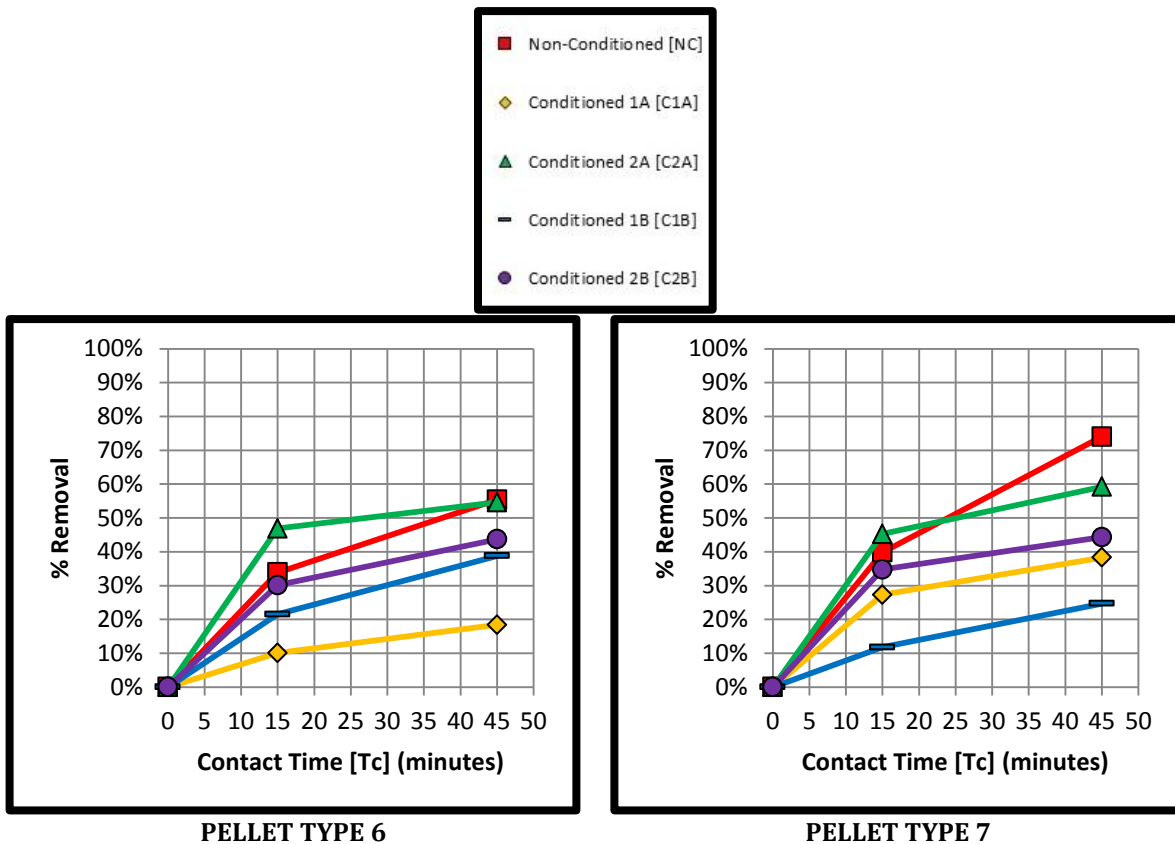
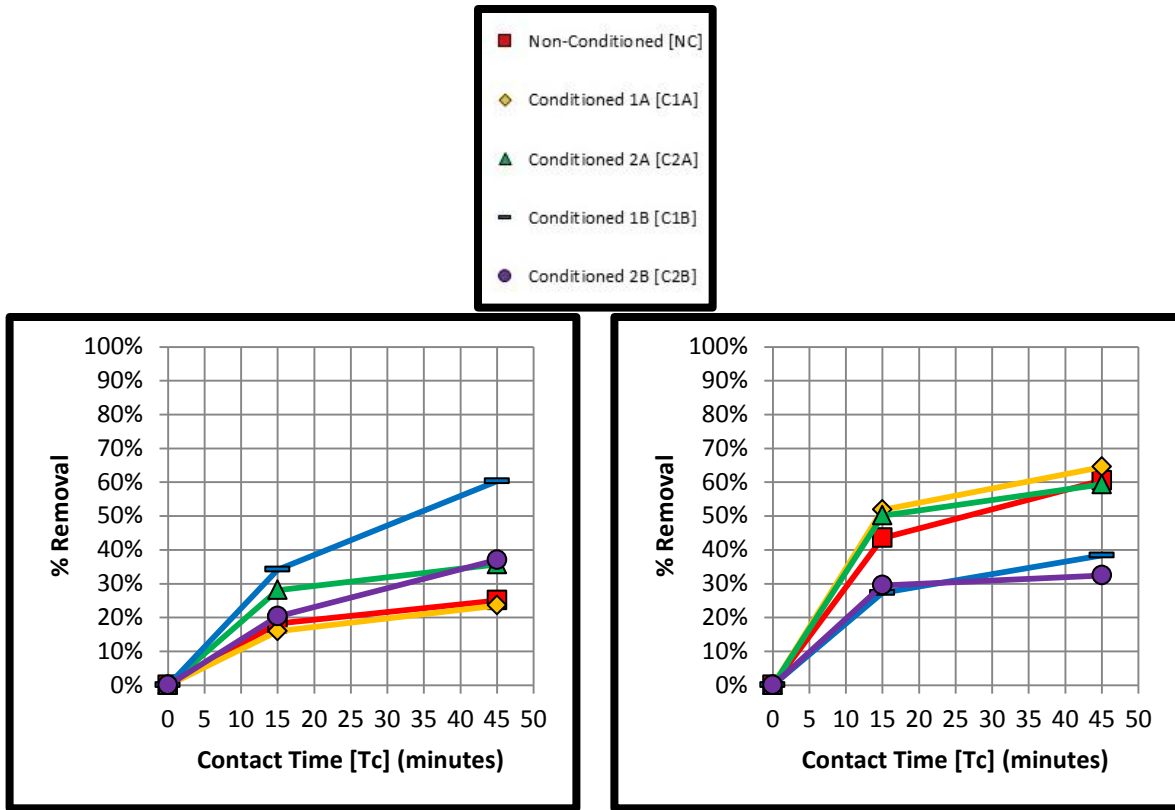
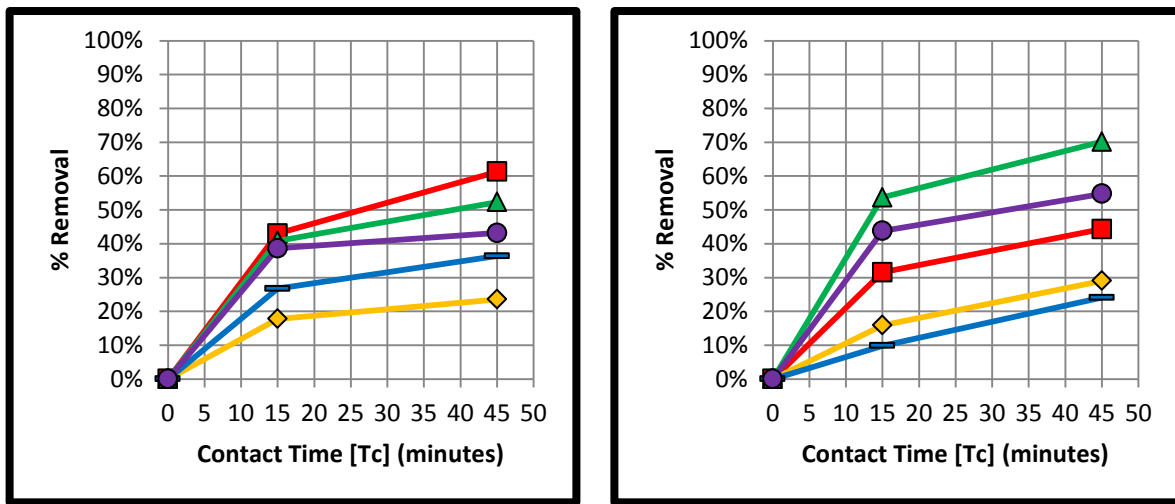


FIGURE 7.2 - PHASE I - 6 MGP/L INFLUENT



PELLET TYPE 6
PELLET TYPE 7
FIGURE 7.3 - PHASE I - 18 MGP/L INFLUENT

Figure 7.3 indicates that Pellet Type 6 is greatest with the Hydrated Lime Brine at maximum concentration (C1B), whereas Type 7 is more or less equivalent whether non-conditioned or exposed to either conditioning solution at minimum concentration (C1A, C2A). Both pellet types' removals are close in value.



PELLET TYPE 6
PELLET TYPE 7
FIGURE 7.4 - PHASE II - 6 MGP/L INFLUENT

As observed in Figure 7.4, as in Phase I, Pellet Type 6 is optimal non-conditioned (NC) and in the Salt Brine at minimum concentration (C2A). For Type 7, the removal is greatest with an exposure to the Salt Brine at either concentration (C2A, C2B). Pellet Type 7 at C2A exposure is great among the two.

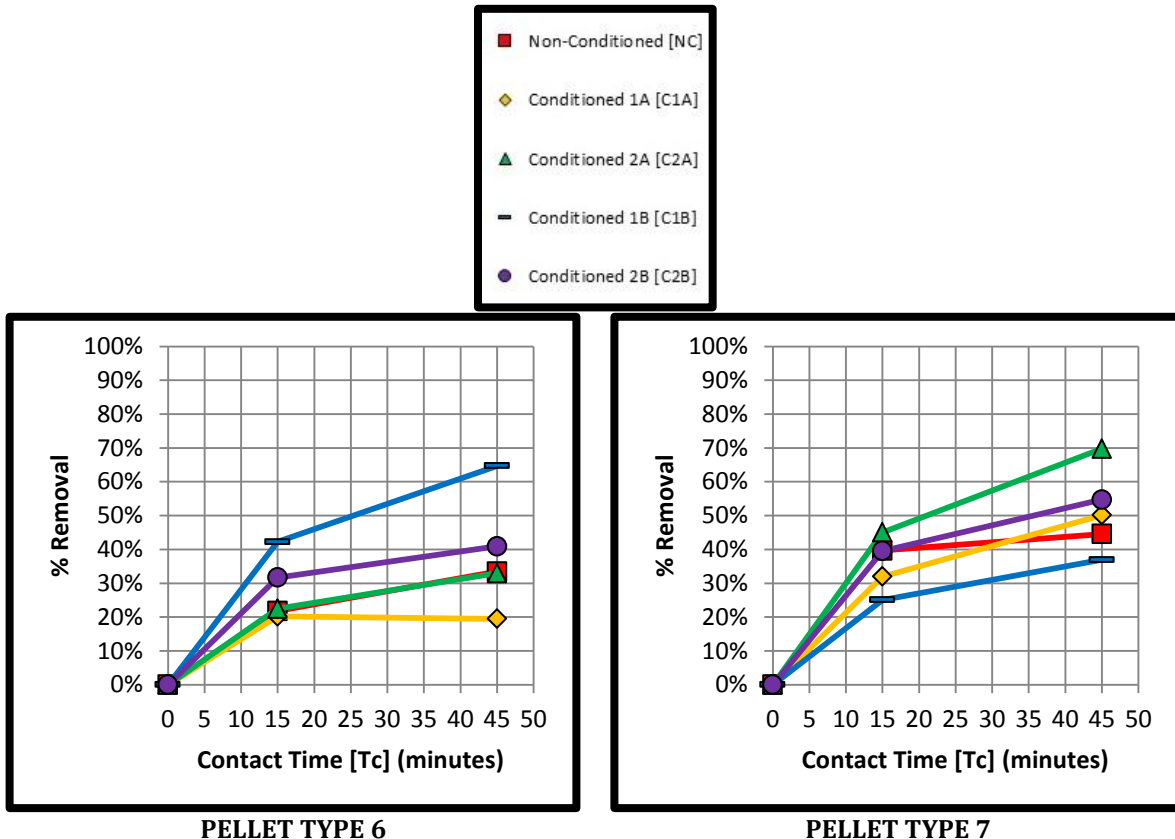


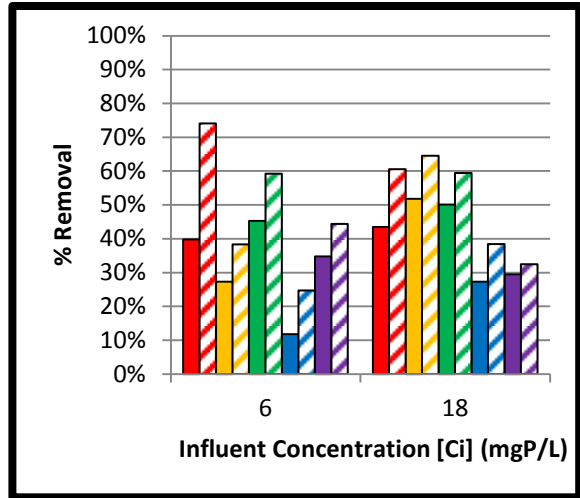
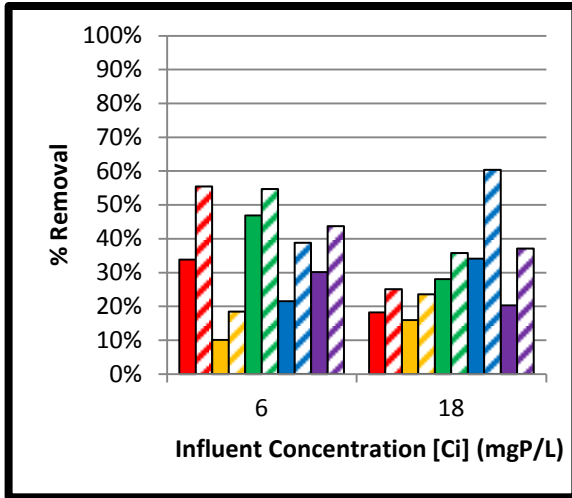
FIGURE 7.5 - PHASE II - 18 MGP/L INFLUENT

Finally, as in Figure 7.5, Pellet Type 6 in phase II is optimal as in phase I; at a maximum Calcium Hydroxide solution concentration (C1B). For Type 7, the removal is greatest with once again the Salt Brine at minimum concentration, closely followed by its maximum concentration.

7.2.2 INFLUENT CONCENTRATION

As observed in Figures 7.6 and 7.7, Pellet Type 7 overall removal is greatest among the two, taking into account the various contact times and furnace exposures.

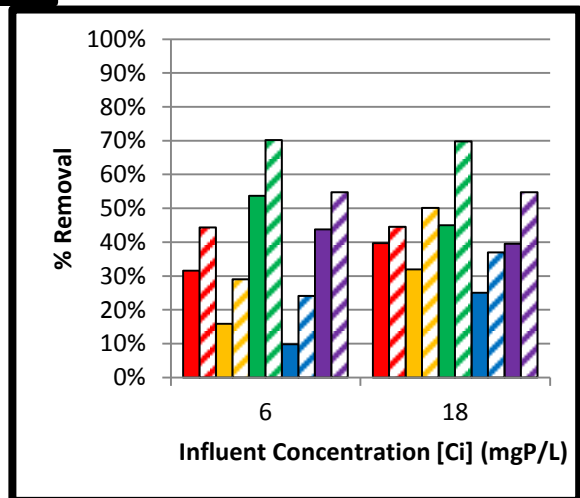
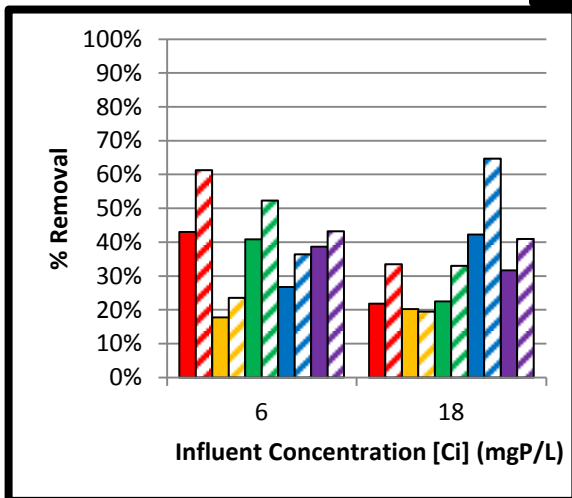
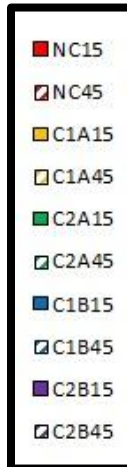
A key observation of the influent concentration results is that the removal was consistent, given the wide range of 6 to 18 mgP/L. This supports the conclusion that the septic tank effluent concentrations were addressed most effectively.



PELLET TYPE 6

PELLET TYPE 7

FIGURE 7.6 - PHASE I INFLUENT ANALYSIS

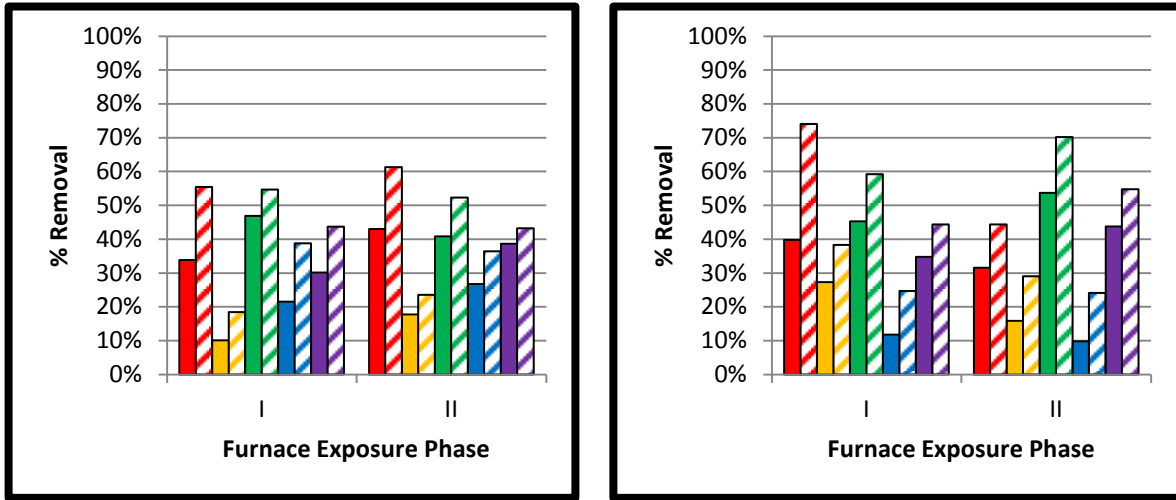


PELLET TYPE 6

PELLET TYPE 7

FIGURE 7.7 - PHASE II INFLUENT ANALYSIS

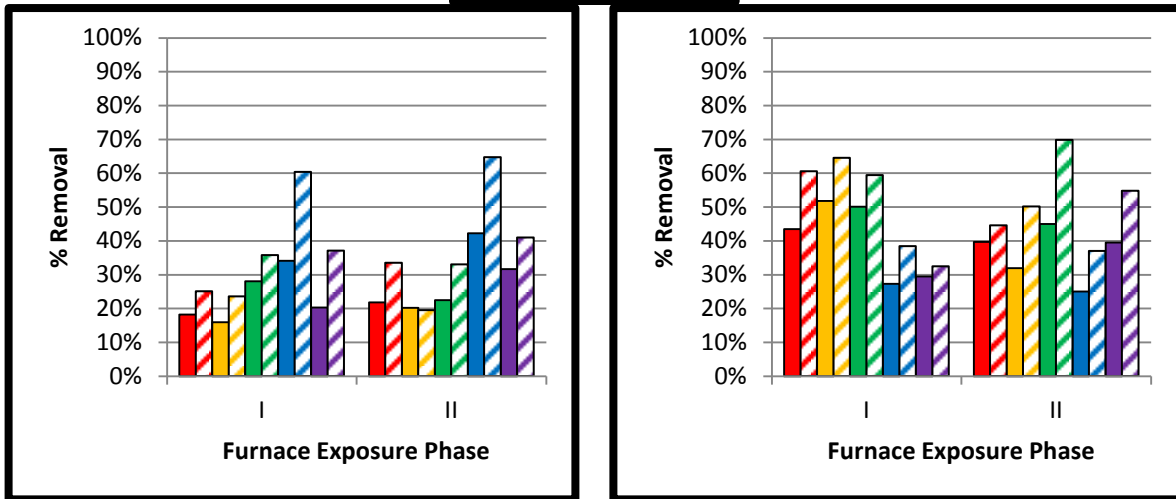
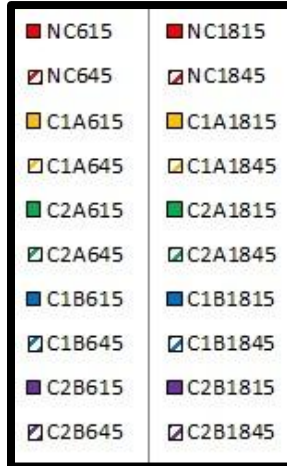
7.2.3 FURNACE EXPOSURE



PELLET TYPE 6

PELLET TYPE 7

FIGURE 7.8 - FURNACE EXPOSURE - 6 MGP/L INFLUENT



PELLET TYPE 6

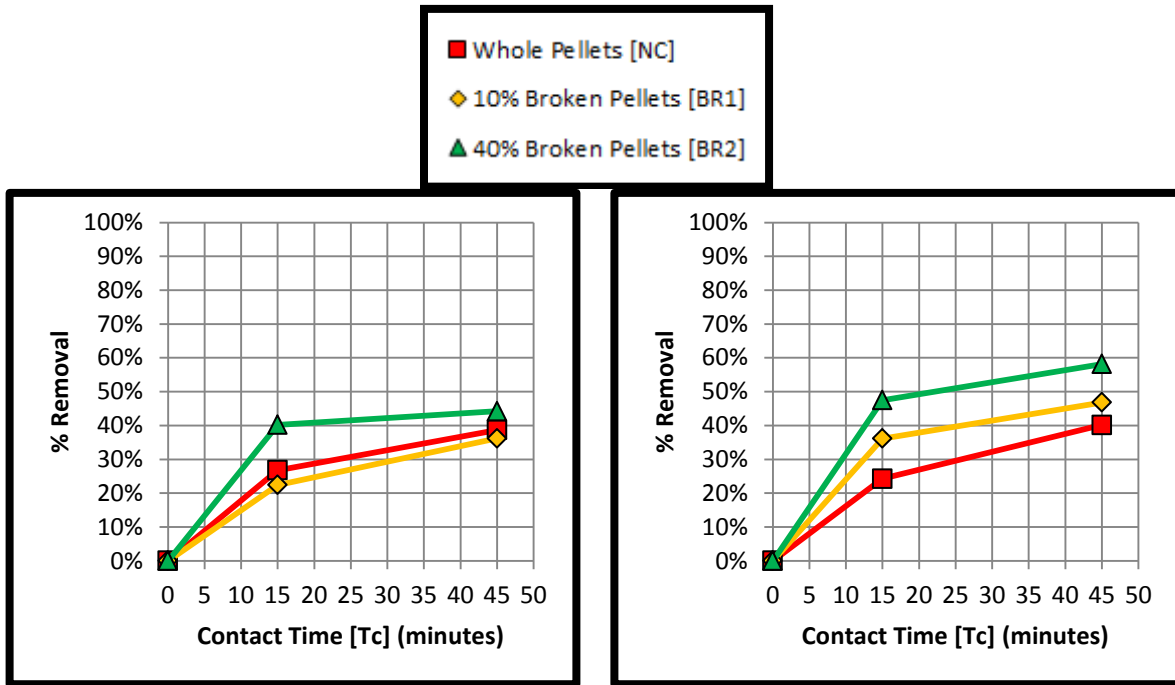
PELLET TYPE 7

FIGURE 7.9 - FURNACE EXPOSURE - 18 MGP/L INFLUENT

As observed in Figures 7.8 and 7.9, the Phase II furnace exposure removal is slightly greater among the various contact times and influent concentrations.

7.2.4 SURFACE AREA

As discussed in section 6.2, the percentage broken to whole pellets was analyzed.



6 MGP/L INFLUENT CONCENTRATION
18 MGP/L INFLUENT CONCENTRATION
FIGURE 7.10 - PELLET TYPE NC7II - CONTACT TIME ANALYSIS

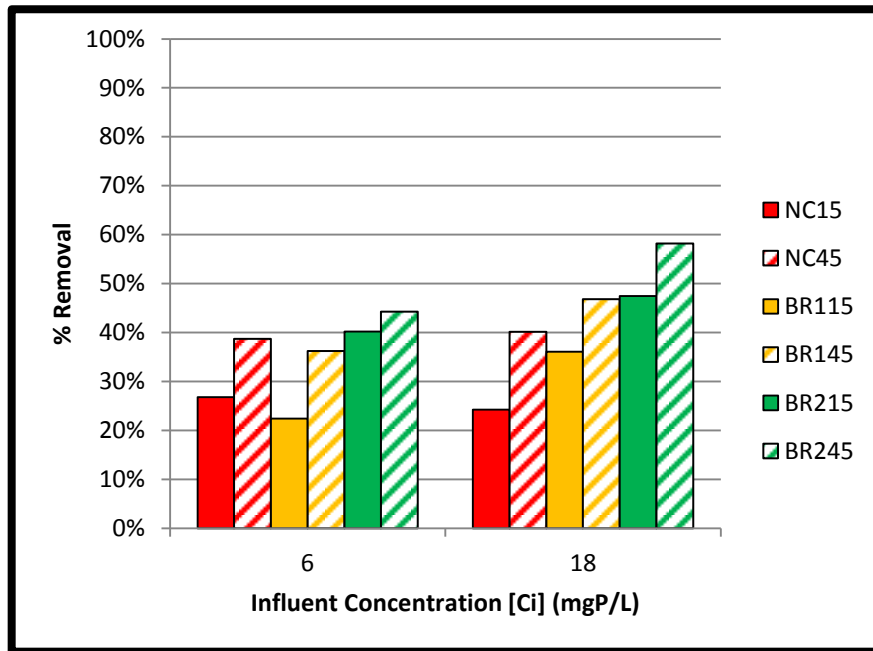


FIGURE 7.11 - PELLET TYPE NC7II - INFLUENT ANALYSIS

Subsection 7.2.1 results are verified, with an approximate removal of phosphorus as 45% for NC7II at 45 minutes contact time (Figure 7.10). As anticipated, as the surface area increases, the removal increases

(Figure 7.11). This optimization parameter demonstrates an innovative approach to the overall experimental design; the changes were made during the course of testing. This displays a greater insight into the media's future behaviour, under the given conditions.

7.2.5 OPTIMIZATION ANALYSIS SUMMARY

This subsection provides an overview of the major findings from the optimization stage. Table 7.1 outlines the percent removal at 45 minutes is outlined. For review, NC, C1A, C2A, C1B, and C2B refer to non-conditioned (as received), minimum (A) Lime (1) and Salt (2) Brines, and maximum (B) Lime (1) and Salt (2) Brines, respectively.

With the *contact time* parameter analysis at the minimum and maximum influent concentrations and *furnace exposures*, it was determined that the non-conditioned (NC) or minimum Salt Brined (C2A) pellets performed superior, with pellet type 7 as optimal; presumably due to greater surface contact and overall ion exchange. The *influent concentration* parameter analysis determined that again Pellet Type 7 had a slight advantage in overall removal. The *furnace exposure* parameter reveals that Phase II removal is slightly greater, but also ensures a more stable product. Following a progress meeting, the final pellet composition was decided as Type 7 NCII taking into account economic and environmental impacts of conditioning, verifying an optimization removal of 45% at the 45 minute contact time.

TABLE 7.1 – OPTIMIZATION 45 MINUTE PERCENT REMOVAL ANALYSIS

	Phase I		Phase II			Phase I		Phase II	
Ci (mgP/L)	6	18	6	18	Ci (mgP/L)	6	18	6	18
<i>Pellet Type 6</i>					<i>Pellet Type 7</i>				
<i>NC</i>	55	25	61	33	<i>NC</i>	74	60	44	45
<i>C1A</i>	18	24	24	19	<i>C1A</i>	38	65	29	50
<i>C2A</i>	55	36	52	33	<i>C2A</i>	59	59	70	70
<i>C1B</i>	39	60	36	65	<i>C1B</i>	25	38	24	37
<i>C2B</i>	44	37	43	41	<i>C2B</i>	44	32	55	55

7.3 FINAL APPARATUS ANALYSIS

7.3.1 ANALYSIS BREAKDOWN

This subsection of the report provides the steps taken to draw the final conclusions of TP removal, based on the pre-optimization and optimization phases' results to determine the final pellet type – VE.

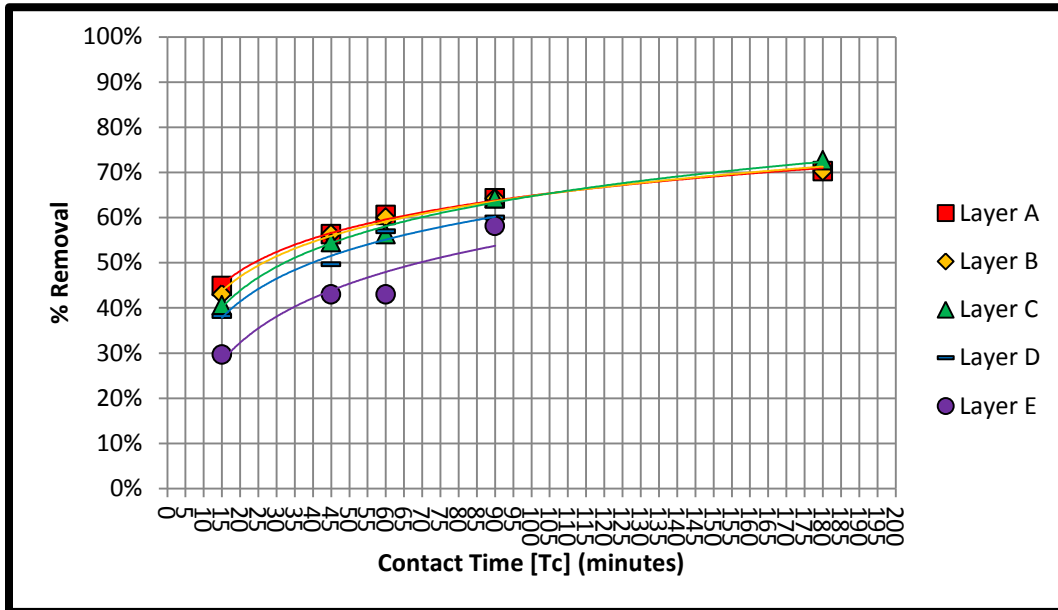


FIGURE 7.12 – FINAL APPARATUS ANALYSIS – LOGARITHMIC

TABLE 7.2 – APPARATUS LAYERS' R² VALUES

Layer	Trend-line Function		
	Linear	Polynomial (2)	Logarithmic
A	0.5394	0.8428	0.9948
B	0.5394	0.8428	0.9932
C	0.6136	0.8680	0.9927
D	0.7486	0.9178	0.9755
E	0.8510	0.9145	0.8845
Layer C Equation	$y = 0.0031x + 0.2773$	$y = -4E-05x^2 + 0.0098x + 0.1252$	$y = 0.1298\ln(x) + 0.0496$

The logarithmic trend-line best represents the percent removal to contact time correlation; all other trend-lines' R² values have been tabulated in Table 7.2 and the logarithmic correlation graphically represented in Figure 7.12. The percent removal of each layer were based on an average contact time of 15, 45, 60, 90, 180; the time required to fill the tank with the 12 mgP/L influent was brought to the median of these determined times.

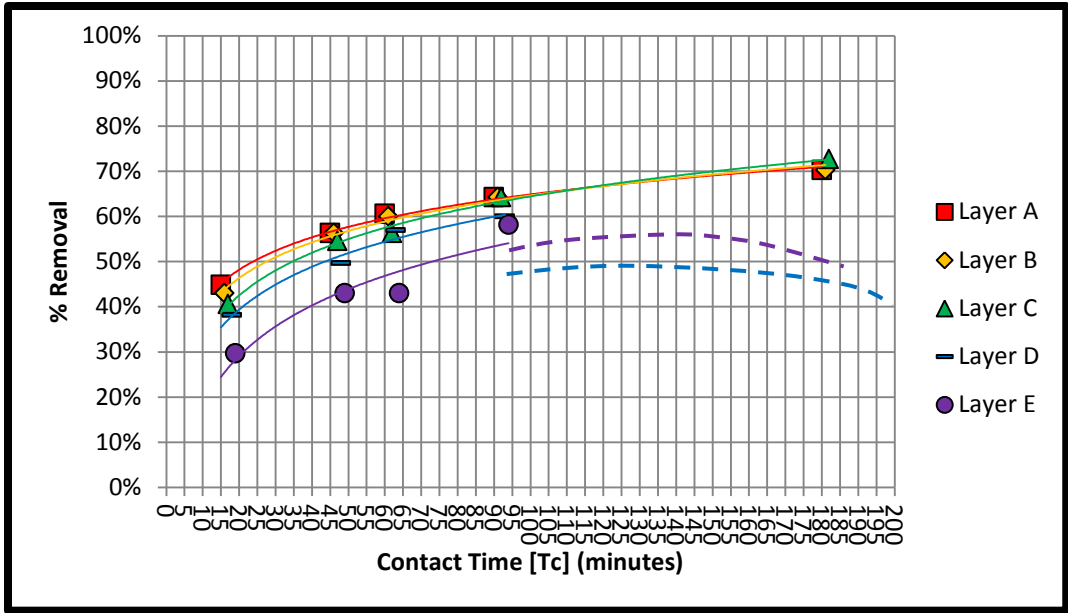


FIGURE 7.13 – FINAL APPARATUS ANALYSIS – INFLUENT TIME APPLIED

TABLE 7.3 – INFLUENT TIME APPLIED APPARATUS LAYERS' R² VALUES

Layer	Trend-line Function - Logarithmic
A	0.9948
B	0.9917
C	0.9937
D	0.9768
E	0.8952
Layer C Equation	$y = 0.1362\ln(x) + 0.0173$

By applying the approximated time required to fill each apparatus layer (1 minute/layer), the lag between sampling times was accounted for (Figure 7.13). As a result, a stronger logarithmic correlation is observed based on Layer C's R² values; from 0.9927 of Table 7.2 to 0.9937 of Table 7.3.

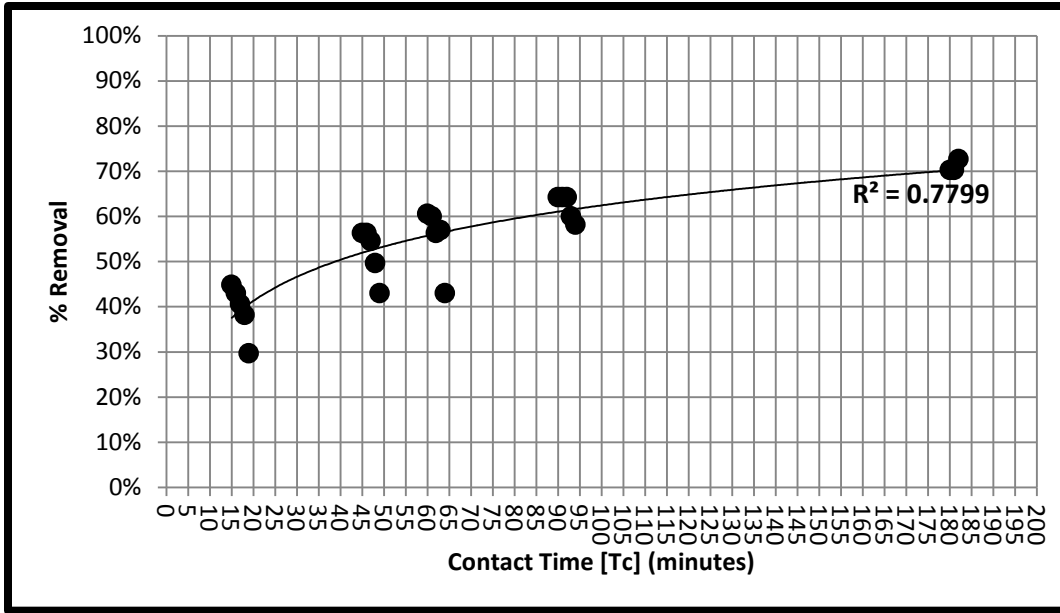


FIGURE 7.14 – FINAL APPARATUS ANALYSIS – OVERALL CORRELATION

Figure 7.14 once again applies this 1 minute lag time between layer sampling, providing an inclusive view of the correlation between percent removal and contact time, with an R^2 value of 0.7799. This coefficient of correlation is not strong, largely due to the limited and skewed data of the top two layers D and E. Therefore, Figure 7.15 below displays a more pronounced correlation between percent removal and contact time, such that layers D and E are removed to produce a R^2 value of 0.972.

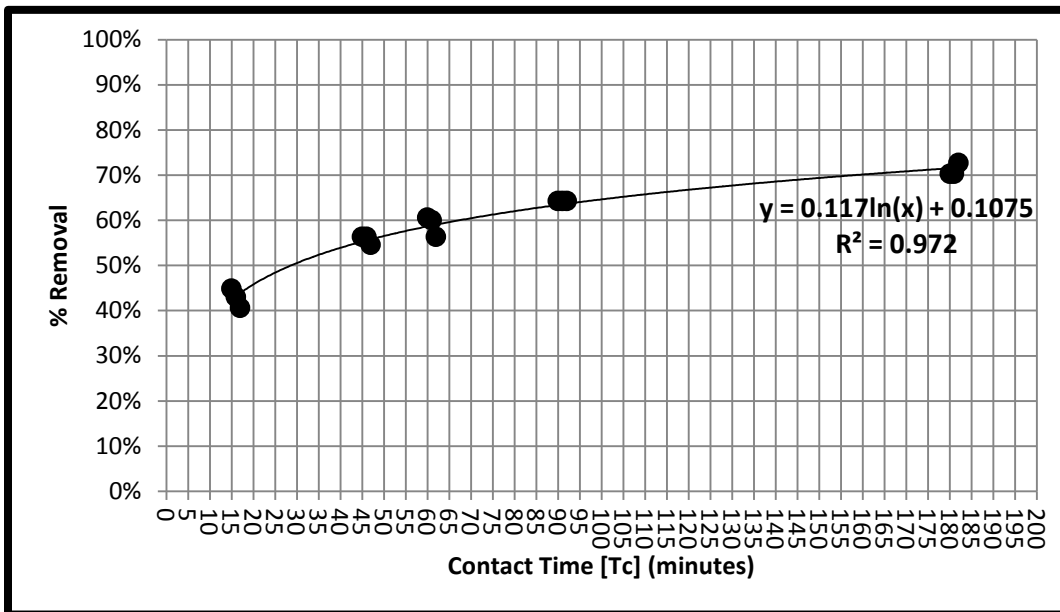


FIGURE 7.15 – FINAL APPARATUS ANALYSIS – OVERALL CORRELATION CORRECTED

Based on a median septic tank effluent (apparatus influent) concentration of 12 mgP/L, it is concluded that the removal rate plateaus to approximately 72% with an optimal contact time of 3 hours. The results show that the layers' percent removal values were relatively close at each given contact time, thereby supporting the assumption that 5 layers would not have been a requirement. Consequently, the final apparatus configuration should enable the influent to traverse through the system for the determined 3 hour time period prior to discharge.

It is to be noted that the trend-line generated and displayed on Figure 7.15 is representative of the testing range specified; a 15 minute to 180 minute (3 hour) contact time. Based on this logarithmic trend-line equation of $y = 0.117\ln x + 0.1075$, it was determined that at a extrapolated 12 hour (720 minutes) contact time, approximately 88% removal is achieved, as follows:

$$y = 0.117\ln x + 0.1075 \rightarrow \% \text{ Removal} = 0.117\ln(T_c) + 0.1075$$

$$\% \text{ Removal} = 0.117\ln(720) + 0.1075 = 0.8773 \rightarrow 88\% \text{ Removal}$$

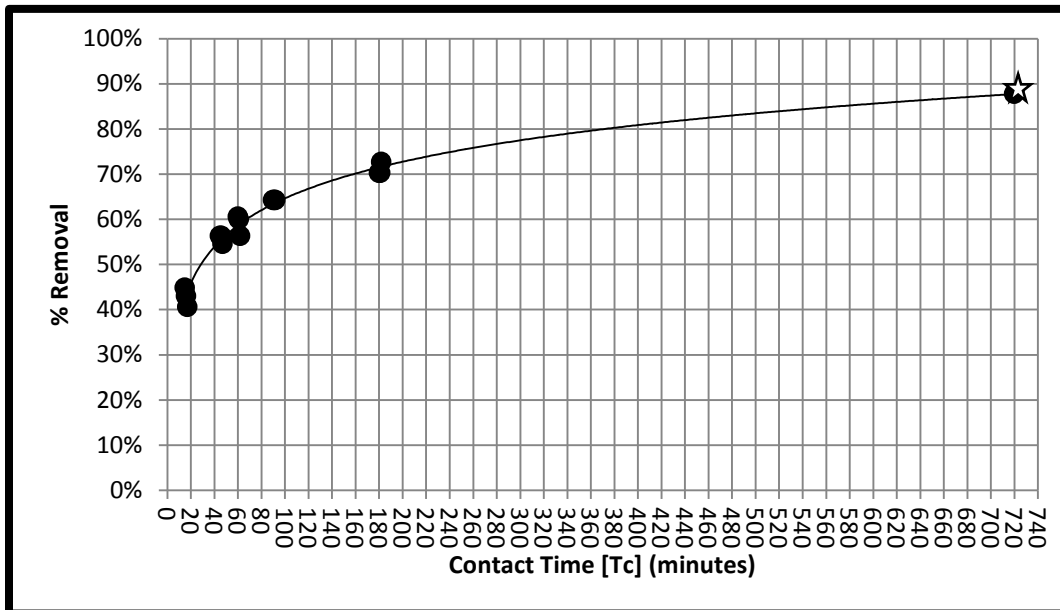


FIGURE 7.16 – FINAL APPARATUS ANALYSIS – EXTRAPOLATION

This theoretical finding is displayed in Figure 7.16, to fit the experimentally determined removal values with the 1 minute influent time and layer correction applied. This 12 hour contact time is representative of the field conditions, such that discharge from the apparatus' outlet would occur over this time cycle. Given that an 88% removal is theoretically achievable, this presents promising results for the treatment process.

7.3.2 EXPERIMENT-LITERATURE ASSESSMENT

To further evaluate the findings of Sun (2010), Equation 4.1 (Phosphorus Adsorption Capacity) is applied as follows:

1. Based on an average zeolite particle per pellet value of 0.1425 g, and 2,232 pellets per layer, the average amount of natural, non-conditioned zeolite dosage is approximately $m = 318 \text{ g}$ per apparatus layer.
2. With assumption of an APF of 60%, the void space per layer based on 2,232 pellets per layer is approximately $V = 776 \text{ in}^3 = 12.7 \text{ L}$.
3. With reference to Appendix E Table E.15, applying Equation 4.1 to Layer C (middle layer), the initial concentration and equilibrium concentration are $C_0 = 13.21 \text{ mgP/L}$ and $C_e = 3.61 \text{ mgP/L}$, respectively.
4. Equation 4.1 determines a phosphorus adsorption capacity of:

$$Q_e = \frac{(C_0 - C_e)V}{m} = \frac{(13.21 - 3.61) \times (12.7)}{(318)} \approx 0.383 \text{ mg/g}$$

This concludes that for every gram of zeolite, 0.383 mg of phosphorus is adsorbed by this system.

As discussed in chapter 4, the Langmuir Adsorption Isotherm represents the process between a solid-liquid system once an equilibrium state is reached. The Freundlich Adsorption Isotherm is an empirical representation, involving surface heterogeneity and exponential site energy distributions. The results of Sun (2010) are further analyzed by applying Equations 4.3 and 4.4 to Layer C, as follows:

Langmuir Equation

$$q_e = \frac{q_m K_a C_e}{1 + K_a C_e} \rightarrow \frac{C_e}{q_e} = \frac{1}{q_m K_a} + \frac{C_e}{q_m}$$

$$q_e = \frac{(1.796 \text{ mg/g})(0.011 \text{ L/mg})(3.61 \text{ mgP/L})}{1 + (0.011 \text{ L/mg})(3.61 \text{ mgP/L})} \approx 0.0686 \text{ mg/g}$$

Freundlich Equation

$$q_e = K_F C_e^{1/n} \rightarrow \log(q_e) = \log(K_F) + \left(\frac{1}{n}\right) \log(C_e)$$

$$q_e = (0.032) \left(3.61 \frac{\text{mgP}}{\text{L}}\right)^{\left(\frac{1}{1.315}\right)} \approx 0.0849 \text{ mg/g}$$

By applying Equations 4.3 and 4.4 to Layers A, B, and C at equilibrium time (3 hours), the following Figure 7.21 and 7.22 plots were determined from Table 7.3.

TABLE 7.4 - LINEARIZATION OF ADSORPTION ISOTHERM VALUES

		Langmuir (Equation 4.3)		Freundlich (Equation 4.4)		
Layer	Ce (mgP/L)	Qe (mg/g)	Ce/Qe (g/L)	Qe(mg/g)	logQe	logCe
A	3.930	0.074	52.806	0.091	-1.043	0.594
B	3.930	0.074	52.806	0.091	-1.043	0.594
C	3.610	0.069	52.628	0.085	-1.071	0.558

The findings of Sun (2010) developed the linearization plots of the Langmuir and Freundlich isotherms to be $y=0.5567x+49.838$ ($R^2=0.7942$) and $y=0.7603x-1.4899$ ($R^2=0.9883$), respectively. The linearization of this project's equilibrium data provide the Langmuir and Freundlich isotherms to be $y=0.5568x+50.618$ and $y=0.7605x-1.4949$, respectively. In addition to creditable correlation based on trend-line equations and coefficients of correlation, Figures 7.17 and 7.18 were generated to display the final apparatus experimental results along the results of Sun's research.

It is to be noted that the values plotted for Sun are approximated by recreating the research paper's original copy, for demonstrative purposes. As discussed in section 4.1 of this report, Sun analyzed a broader range of mass influent concentrations, between 10 and 80 mgP/L. This exceeds the specified influent concentrations applied for this research project, ranging from 6 to 18 mgP/L. As a result, the narrower testing range is displayed on the lower bound of both figures, but still remains along the trendline.

Overall, this concludes a well-represented data correlation, supporting that the adsorption process was consistent with the Freundlich Adsorption Isotherm.

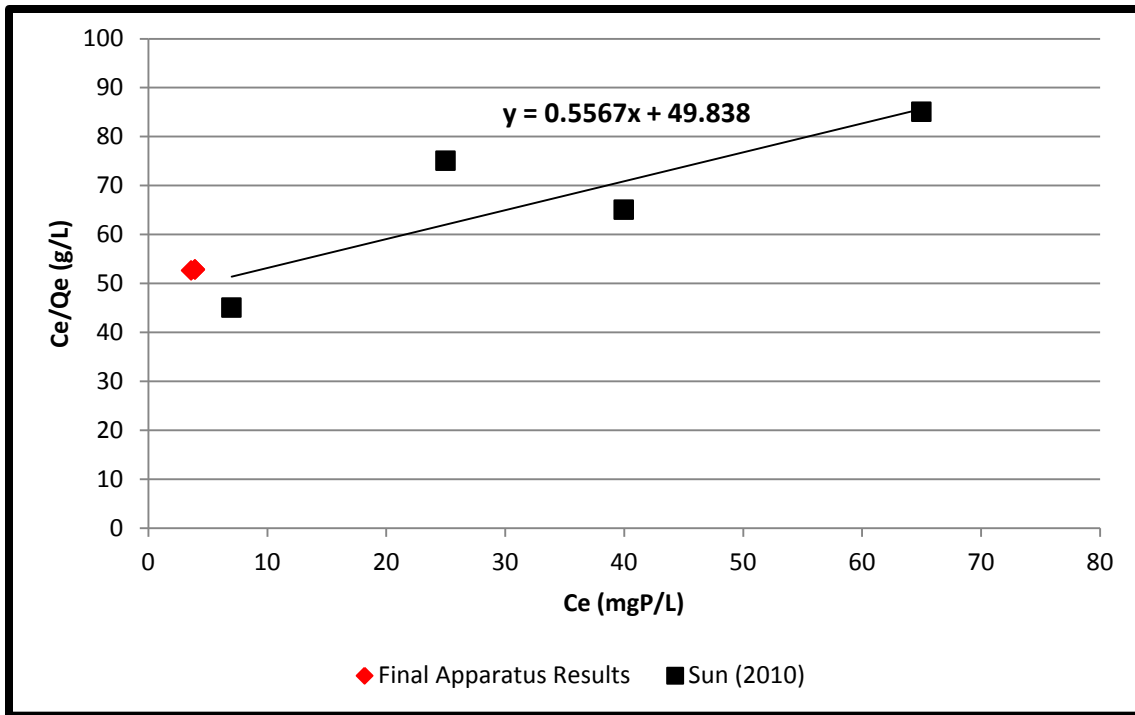


FIGURE 7.17 - LINEARIZATION OF ADSORPTION ISOTHERM BY LANGMUIR ISOTHERM

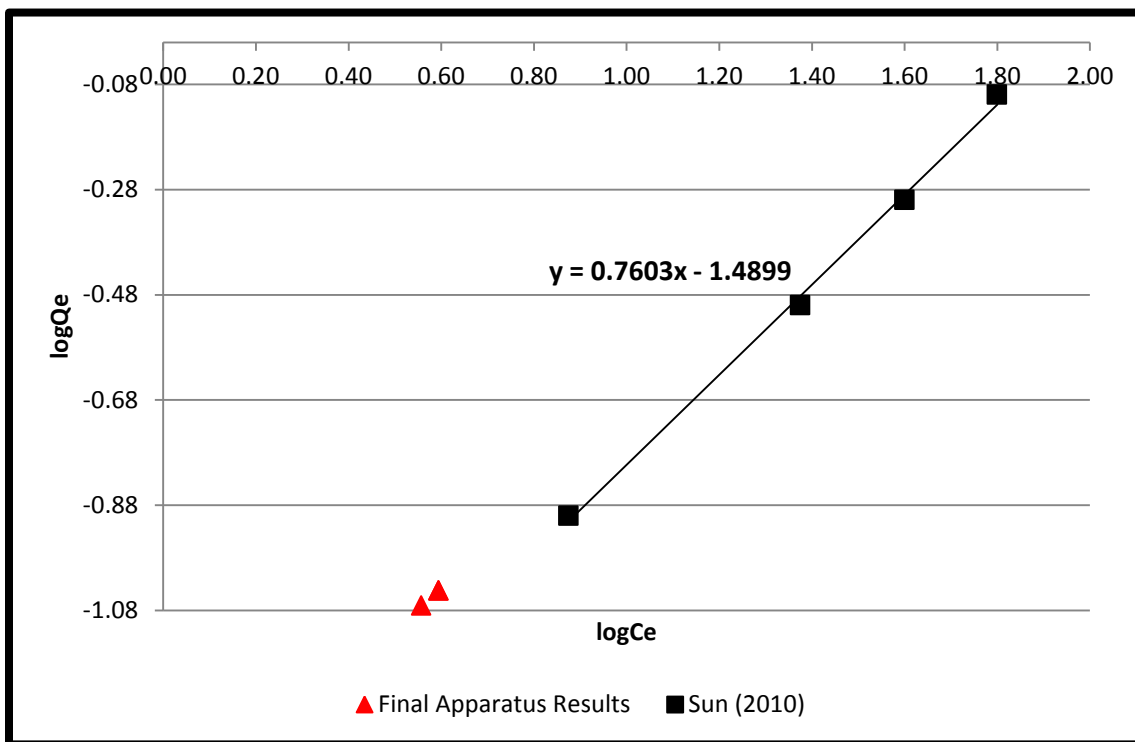


FIGURE 7.18 - LINEARIZATION OF ADSORPTION ISOTHERM BY FREUNDLICH ISOTHERM

7.4 LIMITATIONS

Phosphorus concentration sensitivity was a major factor in this researched. As outlined in subsection 5.2.6 of this report, strict cleanliness was critical. As a result, effluent dilutions were required following testing outlined in Appendix F. In addition, the detection range of the colorimeter employed for testing was very narrow (0.2-1.1 mgP/L); once again, dilutions were essential.

With reference to Appendix E, the final apparatus pH values indicate a gradual increase from a range of 8 to 10.5. Given that TP removal was the primary factor in the analyses against pellet media composition and size, influent concentration, contact time to overall removal efficiency; further investigation is required into pH stabilization.

Finally, it is to be noted zeolite was secondary in the VE Pellet composition, such that a majority was clay. As a result, the analyses drawn from the equilibrium state of the apparatus are variable to the true nature of phosphorus removal. The undisclosed, true pellet configuration must be further analyzed based on the material ratios, in order to draw the necessary conclusions for life-cycle analysis, as discussed in chapter 8.

8 CONCLUSIONS AND RECOMMENDATIONS

The overall objective of this research project was to further the developing of a cost-effective, efficient, and affordable on-site Total Phosphorus (TP) removal unit; fulfilling the technical aspect of the OCE contract through system advancement and efficiency evaluation. Employing chemical adsorption technology, the clay-zeolite media was analyzed for a pilot unit to demonstrate the TP removal capacity from an artificial influent, simulating domestic wastewater effluent concentrations. The analysis to overall removal efficiency was based on media composition and formation, conditioning, influent concentration, and contact time exposure.

Through this three stage process (Pre-Optimization, Optimization, and Final Apparatus), the analyses determined that Pellet Type 7 with Salt Brine conditioning solution at minimum concentration (C2A) and Phase II (12 hour furnace exposure) provided the greatest removal efficiency of 70%. However, the 25% removal efficiency difference (subsection 7.2.5) among the non-conditioned and conditioned results was not substantial to account for the significant future impacts. As a result, from an economic and environmental perspective, the as-received (non-conditioned) Pellet Type 7 was deemed optimal for final mass fabrication. Consequently, the final pellets formed were based on the non-conditioned Type 7 (VE) composition, at Phase II furnace exposure, scaled up from $\frac{3}{4}$ to 1 inch diameter.

The final results show that a maximum removal of approximately 72% is achieved after a 3 hour contact time observation. This supports the conclusion made by Sun (2010), such that the adsorption capacity and removal rate at equilibrium reached its maximum values with an optimal contact time of 180 minutes (3 hours). Therefore, the final apparatus configuration must ensure that the influent traverses through the pellets for this timeframe. In addition, subsection 7.3.2 confirms Sun's research in that the Freundlich isotherm best represents this adsorption process with comparable linearization plots. It is important to note that a strong theoretical removal of 88% is achievable with a contact time extrapolation to 12 hours (simulating field conditions). Based on the septic tank effluent range of 6 to 20 mgP/L, this theoretical removal would present a maximum concentration of 2.4 mgP/L and would contribute to the Ontario Ministry of the Environment phosphorus reduction strategy compliance limit of 0.30 mgP/L.

There were key observations made during Stage 2 (Optimization). With regards to the influent concentration analysis (subsection 7.2.2), the septic tank effluent concentration range was applied to the pellets with a minimum and maximum concentration of 6 and 18 mgP/L, respectively. The investigation demonstrated that the extreme influent bounds provided similar removals. This indicates an effective system. Another significant observation pertains to surface area (subsection 7.2.4), and the actions taken to demonstrate innovation. The pellet disassembly experienced when removed from the small scale furnace, placed in the conditioning brines, and into the influent solutions for testing brought about creative thought. The 10% and 40% broken of the final pellet composition (non-conditioned Pellet Type 7 Phase II furnace exposure) provided a greater insight of the future behaviour of the pellets; a 40% removal with whole pellets versus 47% and 58% removal at 10% and 40% broken, respectively, with a 18 mgP/L influent concentration at a 45 minute contact time. This assists the consumer in their understanding of the media product, such that if disassembly is experienced over the course of its service life, the overall removal improves.

This research's outcome compared favourably to other technologies outlined in section 2.5, as a more simplistic, environmentally conscious and affordable system. In addition to being a readily-available solution to the phosphorus dilemma, such as SorbtiveMedia and PhosLock, the pellets formed possess a fairly neutral discharge of which to be further analyzed pending field testing results. The VE Pellet technology faces a balance of removal efficiency with cost-effective and affordability for its consumer.

There are various recommendations that can be drawn from this research. It should be noted that all pellets were analyzed based on a first time influent to pellet exposure, where further observation is suggested of consecutive contact. To develop a stronger sense of the efficiency of the pellets' TP removal, field testing must be conducted prior to mass fabrication. Environmental conditions such as moisture and humidity, and free-thaw cycles should be analyzed. The field testing should also look into the life-cycle analysis element of the apparatus, and to determine at what point would the media need to be either regenerated or replaced. With regards to regeneration, the conditioning brine disposal must be taken into consideration and how this would adversely affect the environment. In terms of replacement, the spent pellet material must be studied with the possibility for further use, such as fertilizer and its effects on the environment (i.e. leaching into the soil, and subsequently into the waterways). Once the provided concerns above are addressed, this on-site removal unit will become a contender for its target market.

The research work presented has contributed a *sustainable* impact. *Social* benefits include creating a new market sector for employment opportunity. The design is such that the treatment unit components would be cost-effectively fabricated in an industrial setting, adsorbent media internally manufactured and processed, and system elements outsourced. The *economic* advantage is the major goal; to commercialize this unique removal product as a readily available and affordable alternative to on-site TP control of effluent discharge to the target market, including sewage treatment plants, residential dwellings, and urban application for phosphorus attenuation from storm water. The *environmental* benefits are addressing the Ministry of Environment concerns for the development of a TP reduction strategy to restore, improve and protect our environment.

APPENDIX A – PELLET TEST COMPOSITION AND FORMATION

TABLE A.1 – TYPE 1 PELLET TEST

Material		Quantity	
		Trial 1	Trial 2
Zeolite – 8x40 (g)		43.8	43.8
Clay	Bentonite (g)	35	35
	EPK (g)	0	0
DDW (g)		9.8+25.9+2.2=37.9	24.3+4.0=28.3
Quantity (#)		0	20

TABLE A.2 – TYPE 2 PELLET TEST

Material		Quantity
Zeolite – 14x40 (g)		43.9
Clay	Bentonite (g)	35
	EPK (g)	0
DDW (g)		26.6+3.7=30.3
Quantity (#)		19

TABLE A.3 – TYPE 3 PELLET TEST

Material		Quantity	
		Trial 1	Trial 2
Zeolite – 8x40 (g)		44	43.8
Clay	Bentonite (g)	0	0
	EPK (g)	35	35.6
DDW (g)		29.0	11.1+4.8+5.4
Quantity (#)		0	16

TABLE A.4 – TYPE 4 PELLET TEST

Material		Quantity
Zeolite – 14x40 (g)		43.8
Clay	Bentonite (g)	0
	EPK (g)	35.2
DDW (g)		11.2+4.8+5.4=21.4
Quantity (#)		17

TABLE A.5 – TYPE 5 PELLET TEST

Material		Quantity
Zeolite – 8x40 (g)		43.8
Clay	Bentonite (g)	7.6
	EPK (g)	28.0
DDW (g)		12.2+8.9+6.8=27.9
Quantity (#)		16

TABLE A.6 – TYPE 6 PELLET TEST

Material		Quantity
<i>Zeolite – 14x40 (g)</i>		43.8
<i>Clay</i>	<i>Bentonite (g)</i>	7.1
	<i>EPK (g)</i>	28.9
<i>DDW (g)</i>		18.5+4.0+0.9=23.4
<i>Quantity (#)</i>		17

TABLE A.7 – PELLET TEST COMPOSITION AND FORMATION SUMMARY

<i>Pellet Type</i>	<i>Quantity (#)</i>	<i>Appearance</i>	<i>Total Water to Measurable Workability (g)</i>
VE	44	red brown	N/A
1	20	dark grey	28.3
2	19	dark grey	30.3
3	16	light tan	21.2
4	17	light tan	21.4
5	16	light grey	27.9
6	17	light grey	23.4

APPENDIX B - PRE-OPTIMIZATION PELLET COMPOSITION AND FORMATION

TABLE B.1 - TYPE 1 PELLET PRE-OPTIMIZATION

Material		Batch Quantity		
		1	2	3
<i>Zeolite – 8x40 (g)</i>		87.5	87.5	43.9
<i>Clay</i>	<i>Bentonite (g)</i>	70	70.3	35
	<i>EPK (g)</i>	0	0	0
<i>DDW (g)</i>		42+10.4=52.4 +3.5=55.9 +8.8=64.7	51.6+20.6=72.2 +1.3=73.5	23.7+13.5=37.2
<i>Total DDW (g)</i>		175.4		
<i>Quantity (#)</i>		41	41	20
<i>Total Quantity (#)</i>		102		

TABLE B.2 - TYPE 2 PELLET PRE-OPTIMIZATION

Material		Batch Quantity		
		1	2	3
<i>Zeolite – 14x40 (g)</i>		87.5	87.5	87.5
<i>Clay</i>	<i>Bentonite (g)</i>	70	70	70
	<i>EPK (g)</i>	0	0	0
<i>DDW (g)</i>		55.7+7.1=62.8	62.7	62.3
<i>Total DDW (g)</i>		187.8		
<i>Quantity (#)</i>		40	40	21
<i>Total Quantity (#)</i>		101		

TABLE B.3 - TYPE 3 PELLET PRE-OPTIMIZATION

Material		Batch Quantity			
		1	2	3	4
<i>Zeolite – 8x40 (g)</i>		87.5	87.5	87.5	11.7
<i>Clay</i>	<i>Bentonite (g)</i>	0	0	0	9.5
	<i>EPK (g)</i>	70	70	70	0
<i>DDW (g)</i>		35.2+4.7+2.2=42.1	34.8+5.7+1.4=41.9	36.4+4.6+1=42	4.0+2.1=6.1
<i>Total DDW (g)</i>		132.1			
<i>Quantity (#)</i>		31	33	32	4
<i>Total Quantity (#)</i>		100			

TABLE B.4 – TYPE 4 PELLET PRE-OPTIMIZATION

Material		Batch Quantity			
		1	2	3	4
Zeolite – 14x40 (g)		87.7	87.5	87.5	11.7
Clay	Bentonite (g)	0	0	0	0
	EPK (g)	70.4	70.0	70.3	9.3
DDW (g)		42.8	40.7	45.9	3.1+4.2=7.3
Total DDW (g)		136.7			
Quantity (#)		32	34	32	3
Total Quantity (#)		101			

TABLE B.5 – TYPE 5 PELLET PRE-OPTIMIZATION

Material		Batch Quantity		
		1	2	3
Zeolite – 8x40 (g)		87.5	87.5	87.5
Clay	Bentonite (g)	14	14	14
	EPK (g)	56	56	56
DDW (g)		51.3+5.7=57	50.1+5.4=55.5	51.5+3.5=55
Total DDW (g)		167.5		
Quantity (#)		35	35	35
Total Quantity (#)		105		

TABLE B.6 – TYPE 6 PELLET PRE-OPTIMIZATION

Material		Batch Quantity		
		1	2	3
Zeolite – 14x40 (g)		87.5	87.5	87.5
Clay	Bentonite (g)	14.1	14	14.2
	EPK (g)	56.1	56	56.2
DDW (g)		38.6+12.6=51.2	38.2+7+5.3=50.5	42+5.8+1.1=48.9
Total DDW (g)		150.6		
Quantity (#)		33	37	33
Total Quantity(#)		103		

TABLE B.7 – PELLET PRE-OPTIMIZATION COMPOSITION AND FORMATION SUMMARY

Pellet Type	Quantity (#)	Appearance	Total Water to Measurable Workability (g)
VE	195	red brown	N/A
1	102	dark grey	175.4
2	101	dark grey	187.8
3	100	light tan	132.1
4	101	light tan	136.7
5	105	light grey	167.5
6	103	light grey	150.6

APPENDIX C – PRE-OPTIMIZATION PELLET DETERMINATION

TABLE C.1 – PRE-OPTIMIZATION - TYPE 7 PELLET TEST

Influent Concentration (mgP/L)	Contact Time (minutes)	Effluent Concentration (mgP/L)
6	7.5	Over-range
	15	
14	7.5	
	15	
18	7.5	
	15	

TABLE C.2 – INFLUENT ANALYSIS

#-50% Dilutions	Dilution Factor (DF)	Influent Concentration (mgP/L)	
		6 mgP/L	20 mgP/L
4	0.0625	6.92	
5	0.03125	8.36	
6	0.015625	12.04	25.80
7	0.007813		30.60
8	0.003906		43.40

TABLE C.3 – PRE-OPTIMIZATION - TYPE 6 PELLET

Influent Concentration (mgP/L)		Contact time (minutes)	Effluent Concentration (mgP/L)
Theoretical	Experimental		
6	DF=0.0625	7.35	Over-range
	DF=0.015625	11.75	
		15	
		30	

TABLE C.4 – PRE-OPTIMIZATION NON-CONDITIONED PELLET ANALYSIS

Pellet Type	Influent Concentration (mgP/L)		DF=0.125 Effluent Concentration (mgP/L)	TP Removal	
	Theoretical	Experimental – DF=0.0625		(mgP/L)	(%)
	5	6	7.89	5.57	2.32
6	6.85		6.17	0.68	9.93
7	7.01		5.85	1.16	16.56

TABLE C.5 – PRE-OPTIMIZATION CONDITIONED PELLET ANALYSIS

Pellet Type	Influent Concentration (mgP/L)		DF=0.125 Effluent Concentration (mgP/L)	TP Removal	
	Theoretical	Experimental – DF=0.0625		(mgP/L)	(%)
	5	6	7.09	6.01	1.08
6	7.25		6.73	0.52	7.18
7	7.65		5.29	2.36	30.87

APPENDIX D – OPTMIZATION PELLET COMPOSITION AND FORMATION

TABLE D.1 – TYPE 6I PELLET PRE-OPTIMIZATION

Material		<i>Batch Quantity</i>				
		<i>1</i>	<i>2</i>	<i>3</i>	<i>4</i>	<i>5</i>
<i>Zeolite – 14x40 (g)</i>		175				135
<i>Clay</i>	<i>Bentonite (g)</i>	28				21.6
	<i>EPK (g)</i>	112				86.4
<i>DDW (g)</i>		86.1+5.5	86.6+5.2	92.3	94.7	63+4.9+1.9
<i>Total DDW (g)</i>		440.2				
<i>Quantity (#)</i>		66	65	67	66	36
<i>Total Quantity(#)</i>		306				

TABLE D.2 – TYPE 6II PELLET PRE-OPTIMIZATION

Material		<i>Batch Quantity</i>				
		<i>1</i>	<i>2</i>	<i>3</i>	<i>4</i>	<i>5</i>
<i>Zeolite – 14x40 (g)</i>		175				60
<i>Clay</i>	<i>Bentonite (g)</i>	28				9.6
	<i>EPK (g)</i>	112				38.4
<i>DDW (g)</i>		89.6+5.6	93.5	94.5	93.2	32.1
<i>Total DDW (g)</i>		440.2				
<i>Quantity (#)</i>		70	71	72	71	22
<i>Total Quantity(#)</i>		306				

APPENDIX E – OPTMIZATION PELLET DETERMINATION

TABLE E.1 – OPTIMIZATION NON-CONDITIONED TYPE 6I PELLET ANALYSIS

	Code*	pH	Total Phosphorus Concentration (mgP/L)	Removal	
				(mgP/L)	(%)
<i>Influent</i>	NC:6	6.01	6.50		
	NC:18	5.68	21.06		
<i>Effluent</i>	NC:6:15	5.55	4.30	2.20	34
	NC:6:45	5.94	2.90	3.60	55
	NC:18:15	6.09	17.22	3.84	18
	NC:18:45	6.33	15.78	5.28	25

*NC (Non-Conditioned):# (Theoretical Influent Concentration):# (Contact Time)

TABLE E.2 – OPTIMIZATION CONDITIONED 1&2 A TYPE 6I PELLET ANALYSIS

	Code*	pH	Total Phosphorus Concentration (mgP/L)	Removal	
				(mgP/L)	(%)
<i>Influent</i>	C:A:6	5.66	6.74		
	C:A:18	5.12	21.06		
<i>Effluent</i>	C:1:A:6:15	7.51	6.06	0.68	10
	C:1:A:6:45	8.83	5.50	1.24	18
	C:1:A:18:15	6.84	17.70	3.36	16
	C:1:A:18:45	7.30	16.10	4.96	24
	C:2:A:6:15	6.23	3.58	3.16	47
	C:2:A:6:45	6.34	3.06	3.68	55
	C:2:A:18:15	6.29	15.14	5.92	28
	C:2:A:18:45	6.36	13.54	7.52	36

*C (Conditioned):# (Brine): Letter (Concentration):# (Influent Concentration):# (Contact Time)
 Brine 1=Hydrated Lime; Brine 2=Salt – A=Minimum Concentration; B=Maximum Concentration

TABLE E.3 – OPTIMIZATION CONDITIONED 1&2 B TYPE 6I PELLET ANALYSIS

	Code*	pH	Total Phosphorus Concentration (mgP/L)	Removal	
				(mgP/L)	(%)
<i>Influent</i>	C:B:6	5.12	6.50		
	C:B:18	5.19	22.02		
<i>Effluent</i>	C:1:B:615	9.9	5.10	1.4	22
	C:1:B:6:45	10.37	3.98	2.52	39
	C:1:B:18:15	8	14.50	7.52	34
	C:1:B:18:45	9.72	8.74	13.28	60
	C:2:B:6:15	6.38	4.54	1.96	30
	C:2:B:6:45	6.4	3.66	2.84	44
	C:2:B:1:8:15	6.24	17.54	4.48	20
	C:2:B:18:45	6.34	13.86	8.16	37

*C (Conditioned):# (Brine): Letter (Concentration):# (Influent Concentration):# (Contact Time)
 Brine 1=Hydrated Lime; Brine 2=Salt – A=Minimum Concentration; B=Maximum Concentration

TABLE E.4 – OPTIMIZATION NON-CONDITIONED TYPE 6II PELLET ANALYSIS

	Code*	pH	Total Phosphorus Concentration (mgP/L)	Removal	
				(mgP/L)	(%)
<i>Influent</i>	NC:6	5.69	7.44		
	NC:18	5.6	22.00		
<i>Effluent</i>	NC:6:15	4.92	4.24	3.20	43
	NC:6:45	5.36	2.88	4.56	61
	NC:18:15	6.05	17.20	4.80	22
	NC:18:45	6.10	14.64	7.36	33

*NC (Non-Conditioned):# (Theoretical Influent Concentration):# (Contact Time)

TABLE E.5 – OPTIMIZATION CONDITIONED 1&2 A TYPE 6II PELLET ANALYSIS

	Code*	pH	Total Phosphorus Concentration (mgP/L)	Removal	
				(mgP/L)	(%)
<i>Influent</i>	C:A:6	5.77	6.96		
	C:A:18	5.27	21.36		
<i>Effluent</i>	C:1:A:6:15	8.54	5.72	1.24	18
	C:1:A:6:45	9.33	5.32	1.64	24
	C:1:A:18:15	7.15	17.04	4.32	20
	C:1:A:18:45	7.59	17.20	4.16	19
	C:2:A:6:15	6.67	4.12	2.84	41
	C:2:A:6:45	6.83	3.32	3.64	52
	C:2:A:18:15	6.58	16.56	4.80	22
	C:2:A:18:45	6.74	14.32	7.04	33

*C (Conditioned):# (Brine): Letter (Concentration):# (Influent Concentration):# (Contact Time)
 Brine 1=Hydrated Lime; Brine 2=Salt – A=Minimum Concentration; B=Maximum Concentration

TABLE E.6 – OPTIMIZATION CONDITIONED 1&2 B TYPE 6II PELLET ANALYSIS

	Code*	pH	Total Phosphorus Concentration (mgP/L)	Removal	
				(mgP/L)	(%)
<i>Influent</i>	C:B:6	5.63	7.04		
	C:B:18	5.27	24.24		
<i>Effluent</i>	C:1:B:6:15	10.04	5.16	1.88	27
	C:1:B:6:45	10.48	4.48	2.56	36
	C:1:B:18:15	8.54	14.00	10.24	42
	C:1:B:18:45	9.79	8.56	15.68	65
	C:2:B:6:15	6.56	4.32	2.72	39
	C:2:B:6:45	6.75	4.00	3.04	43
	C:2:B:18:15	6.55	16.56	7.68	32
	C:2:B:18:45	6.75	14.32	9.92	41

*C (Conditioned):# (Brine): Letter (Concentration):# (Influent Concentration):# (Contact Time)
 Brine 1=Hydrated Lime; Brine 2=Salt – A=Minimum Concentration; B=Maximum Concentration

TABLE E.7 – OPTIMIZATION NON-CONDITIONED TYPE 7I PELLET ANALYSIS

	Code*	pH	Total Phosphorus Concentration (mgP/L)	Removal	
<i>Influent</i>	NC:6	5.44	7.13	(mgP/L)	(%)
	NC:18	5.22	21.69		
<i>Effluent</i>	NC:6:15	9.36	4.29	2.84	40
	NC:6:45	10.00	1.85	5.28	74
	NC:18:15	8.3	12.25	9.44	44
	NC:18:45	9.64	8.57	13.12	60

*NC (Non-Conditioned):# (Theoretical Influent Concentration):# (Contact Time)

TABLE E.8 – OPTIMIZATION CONDITIONED 1&2 A TYPE 7I PELLET ANALYSIS

	Code*	pH	Total Phosphorus Concentration (mgP/L)	Removal	
<i>Influent</i>	C:A:6	6.02	6.89	(mgP/L)	(%)
	C:A:18	5.75	27.77		
<i>Effluent</i>	C:1:A:6:15	9.89	5.01	1.88	27
	C:1:A:6:45	10.47	4.25	2.64	38
	C:1:A:18:15	8.46	13.37	14.40	52
	C:1:A:18:45	9.60	9.85	17.92	65
	C:2:A:6:15	9.49	3.77	3.12	45
	C:2:A:6:45	9.86	2.81	4.08	59
	C:2:A:18:15	8.99	13.85	13.92	50
	C:2:A:18:45	9.40	11.29	16.48	59

*C (Conditioned):# (Brine): Letter (Concentration):# (Influent Concentration):# (Contact Time)
 Brine 1=Hydrated Lime; Brine 2=Salt – A=Minimum Concentration; B=Maximum Concentration

TABLE E.9 – OPTIMIZATION CONDITIONED 1&2 B TYPE 7I PELLET ANALYSIS

	Code*	pH	Total Phosphorus Concentration (mgP/L)	Removal	
<i>Influent</i>	C:B:6	5.65	7.13	(mgP/L)	(%)
	C:B:18	5.50	21.69		
<i>Effluent</i>	C:1:B:6:15	10.83	6.29	0.84	12
	C:1:B:6:45	11.1	5.37	1.76	25
	C:1:B:18:15	9.63	15.77	5.92	27
	C:1:B:18:45	10.7	13.37	8.32	38
	C:2:B:6:15	9.32	4.65	2.48	35
	C:2:B:6:45	9.78	3.97	3.16	44
	C:2:B:18:15	8.86	15.29	6.40	30
	C:2:B:18:45	9.45	14.65	7.04	32

*C (Conditioned):# (Brine): Letter (Concentration):# (Influent Concentration):# (Contact Time)
 Brine 1=Hydrated Lime; Brine 2=Salt – A=Minimum Concentration; B=Maximum Concentration

TABLE E.10 – OPTIMIZATION NON-CONDITIONED TYPE 7II PELLET ANALYSIS

	Code*	pH	Total Phosphorus Concentration (mgP/L)	Removal	
<i>Influent</i>	NC:6	5.41	7.22	(mgP/L)	(%)
	NC:18	5.21	22.98		
<i>Effluent</i>	NC:6:15	10.33	4.94	2.28	32
	NC:6:45	10.86	4.02	3.20	44
	NC:18:15	9.12	13.86	9.12	40
	NC:18:45	10.50	12.74	10.24	45

*NC (Non-Conditioned):# (Theoretical Influent Concentration):# (Contact Time)

TABLE E.11 – OPTIMIZATION CONDITIONED 1&2 A TYPE 7II PELLET ANALYSIS

	Code*	pH	Total Phosphorus Concentration (mgP/L)	Removal	
<i>Influent</i>	C:A:6	5.40	7.30	(mgP/L)	(%)
	C:A:18	5.50	22.02		
<i>Effluent</i>	C:1:A:6:15	10.38	6.14	1.16	16
	C:1:A:6:45	10.70	5.18	2.12	29
	C:1:A:18:15	9.11	14.98	7.04	32
	C:1:A:18:45	10.36	10.98	11.04	50
	C:2:A:6:15	10.31	3.38	3.92	54
	C:2:A:6:45	10.57	2.18	5.12	70
	C:2:A:18:15	9.53	12.10	9.92	45
	C:2:A:18:45	10.17	6.66	15.36	70

*C (Conditioned):# (Brine): Letter (Concentration):# (Influent Concentration):# (Contact Time)
 Brine 1=Hydrated Lime; Brine 2=Salt – A=Minimum Concentration; B=Maximum Concentration

TABLE E.12 – OPTIMIZATION CONDITIONED 1&2 B TYPE 7II PELLET ANALYSIS

	Code*	pH	Total Phosphorus Concentration (mgP/L)	Removal	
				(mgP/L)	(%)
Influent	C:B:6	5.10	7.30		
	C:B:18	5.49	24.26		
Effluent	C:1:B:6:15	10.95	6.58	0.72	10
	C:1:B:6:45	11.20	5.54	1.76	24
	C:1:B:18:15	9.90	18.18	6.08	25
	C:1:B:18:45	10.92	15.30	8.96	37
	C:2:B:6:15	10.16	4.10	3.20	44
	C:2:B:6:45	10.49	3.30	4.00	55
	C:2:B:18:15	9.46	14.66	9.60	40
	C:2:B:18:45	9.96	10.98	13.28	55

*C (Conditioned):# (Brine): Letter (Concentration):# (Influent Concentration):# (Contact Time)
 Brine 1=Hydrated Lime; Brine 2=Salt – A=Minimum Concentration; B=Maximum Concentration

TABLE E.13 – NON-CONDITIONED TYPE 7II – SURFACE AREA ANALYSIS

	Code*	pH	Total Phosphorus Concentration (mgP/L)	Removal	
				(mgP/L)	(%)
Influent	NC:6	5.29	6.72		
	NC:18	5.21	19.12		
Effluent	NC:6:15	10.49	4.92	1.8	27
	NC:6:45	10.8	4.12	2.6	39
	NC:18:15	9.24	14.48	4.64	24
	NC:18:45	10.32	11.44	7.68	40

*NC (Non-Conditioned):# (Theoretical Influent Concentration):# (Contact Time)

TABLE E.14 – NON-CONDITIONED BR1&2 TYPE 7II – SURFACE AREA ANALYSIS

	Code*	pH	Total Phosphorus Concentration (mgP/L)	Removal	
				(mgP/L)	(%)
Influent	BR:6	5.69	6.96		
	BR:18	5.41	23.92		
Effluent	BR:1:6:15	10.84	5.40	1.56	22
	BR:1:6:45	11	4.44	2.52	36
	BR:1:18:15	10.22	15.28	8.64	36
	BR:1:18:45	10.74	12.72	11.2	47
	BR:2:6:15	10.66	4.16	2.8	40
	BR:2:6:45	10.93	3.88	3.08	44
	BR:2:18:15	9.98	12.56	11.36	47
	BR:2:18:45	10.73	10.00	13.92	58

*BR (Brown):# (% Broken):# (Theoretical Influent Concentration):# (Contact Time)
 BR1=10%; BR2=40%

TABLE E.15 – FINAL APPARATUS TEST

	Code*	pH	Total Phosphorus Concentration (mgP/L)		Removal	
					(mgP/L)	(%)
<i>Influent</i>	INF:BOT	5.70	13.05	13.21		
	INF:TOP	5.97	13.44			
<i>Effluent</i>	A:15	9.21	7.29		5.92	45
	B:15	8.90	7.53		5.68	43
	C:15	8.58	7.85		5.36	41
	D:15	8.64	8.17		5.04	38
	E:15	7.86	9.29		3.92	30
	A:45	9.50	5.77		7.44	56
	B:45	9.47	5.77		7.44	56
	C:45	9.32	6.01		7.20	55
	D:45	9.34	6.65		6.56	50
	E:45	8.89	7.53		5.68	43
	A:60	9.83	5.21		8.00	61
	B:60	9.76	5.29		7.92	60
	C:60	9.66	5.77		7.44	56
	D:60	9.65	5.69		7.52	57
	E:60	9.12	7.53		5.68	43
	A:90	10.00	4.73		8.48	64
	B:90	9.95	4.73		8.48	64
	C:90	9.83	4.73		8.48	64
	D:90	9.83	5.29		7.92	60
	E:90	9.40	5.53		7.68	58
	A:180	10.16	3.93		9.28	70
B:180	10.17	3.93		9.28	70	
C:180	10.15	3.61		9.60	73	

*Letter (Layer) :# (Contact Time)

APPENDIX F – ORBECO MC500 COLORIMETER PROCEDURE

For each sample drawn, two (2) trials were analyzed and averaged. It is to be noted that with reference to the Orbeco manual steps indicated in the insertion that follows, the steps employed are as below:

1. As per Step 1, for each sample, the two (2) vials were filled.
2. As per Step 2, the first vial filled with sample was filled with the Potassium Persulfate F10 Powder Packs. As per Step 3, it was slowly inverted five (5) times. Steps 2 and 3 were repeated for the second sample vial. This was followed by slowly inverting the two vials five (5) additional times.
3. Prior to Step 4, all prepared vials were slowly inverted three (3) times to ensure thorough reagent distribution.
4. The vials were allowed to cool, coming to room temperature at 1.5 hours after being removed from the reactor (Orbeco TR125).
5. As per Step 7, the vials were slowly inverted ten (10) times.
6. As per Step 12, the vials were slowly inverted fifteen (15) times to ensure the reagent was thoroughly distributed.

1.1 Methods

3
2
6

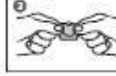
Phosphate, total with Tube Test

0.02 – 1.1 mg/l P (±0.06 – 3.5 mg/l PO₄)



∅ 16 mm






Insert the adapter for 16 mm ∅ vials.

1. Open the white cap of one **digestion tube PO4-P Acid reagent** and add **5 ml of the water sample**.
2. Add the contents of one **Potassium Persulfate F10 Powder Pack** straight from the foil to the vial (Note 2).
3. Close the vial tightly with the cap and invert several times to mix the contents.
4. Heat the vials for **30 minutes** in the preheated reactor at a temperature of **100°C**.
5. After 30 minutes remove the vial from the reactor. **(CAUTION: The vials are hot!)** Allow the vials to cool to room temperature.
6. Open the cooled digestion vial and add **2 ml 1.54 N Sodium Hydroxide Solution** to the vial.
7. Close the vial with the cap and invert gently several times to mix the contents.
8. Place the vial in the sample chamber making sure that the marks are aligned.
9. Press **ZERO** key.
10. Remove the vial from the sample chamber.
11. Add the contents of one **Phosphate Rgt. F10 Powder Pack** straight from the foil to the vial (Note 2).
12. Close the vial tightly with the cap and swirl several times to mix the contents (approx. 10-15 sec., Note 3).
13. Place the vial in the sample chamber making sure that the marks are aligned.
14. Press **TEST** key.
Wait for a **reaction period of 2 minutes**.

After the reaction period is finished the measurement starts automatically.

The result is shown in the display in mg/l total Phosphate.

Notes:

1. Use appropriate safety precautions and good lab technique during the procedure for most accurate results.
2. Use a funnel to add the reagent.
3. The reagent will not dissolve completely.
4. see also page 145
5. Conversions:
mg/l PO₄ = mg/l P x 3.07
mg/l P₂O₅ = mg/l P x 2.29
6. ▲ P
 PO₄
 ▼ P₂O₅

prepare Zero
press ZERO

Zero accepted
prepare Test
press TEST

Countdown
2:00

REFERENCES

1. Amethyst Galleries. (2011). *The Mineral Clinoptilolite*. Retrieved 01/01/11 from: <http://www.galleries.com/minerals/silicate/clinopti/clinopti.htm>
2. Bear River Zeolite. (2011). *Surface Modified Zeolite*. Retrieved 01/01/11 from: http://www.bearriverzeolite.com/brz_particle_sizes.htm
3. Bekkkum H. van et al. (1991). *Introduction to Zeolite Science and Practice*. Elsevier Science Publishers B.V.
4. Bowker, R.P.G. et al. (1990). *Phosphorus Removal from Wastewater*. Pollution Technology Review No. 189. Noyes Data Corporation.
5. Callister, W. D. (2007). *Materials Science and Engineering-An Introduction*. 7th Edition. Wiley & Sons, Inc.
6. Carlson, R.E. and J. Simpson. 1996. *A Coordinator's Guide to Volunteer Lake Monitoring Methods*. North American Lake Management Society. 96 pp. Retrieved 04/10/2011 from <http://www.secchidipin.org/Phosphorus.htm>
7. Cheney Lime & Cement Company. (2012). Lime Facts. Allgood, Al. Retrieved 26/01/2012 from: <http://www.cheneylime.com/limefact.htm>.
8. Cloern, J. E. et al. (2010). *Eutrophication*. Encyclopedia of Earth. Eds. Cutler J. Cleveland. Environmental Information Coalition, National Council for Science and the Environment. Retrieved 03/05/11 from: <http://www.eoearth.org/article/Eutrophication>
9. Echlin, P. (2009). *Handbook of Sample Preparation for Scanning Electron Microscopy and X-Ray Microanalysis*. Springer.
10. Encyclopædia Britannica. (2011). *Eutrophication*. Retrieved 06/05/11 from: <http://www.britannica.com/EBchecked/topic/196751/eutrophication>
11. EPA. (2012). *Onsite Wastewater Treatment Systems Technology Fact Sheet 8 – Enhanced Nutrient Removal – Phosphorus*. EPA 625/R-00/008. Retrieved 01/04/2011 from <http://www.epa.gov/nrmrl/pubs/625r00008/html/tfs8.htm>
12. Greenberg, A. E. et al. (1992). *Standard Methods for the Examination of Water and Wastewater*. 18th Edition. Acid Persulfate Digestion (4500-P.B.5) -Ascorbic Acid Method (4500-P.E).
13. Imbrium Systems Inc. (2012). *A Breakthrough in Total Phosphorus Removal: The Science behind Sorbtive™ MEDIA*. Retrieved 12/04/2012 from: <http://www.imbriumsystems.com/pdf/SorbitiveMEDIATechBrief.pdf>
14. Jasra, R. V. et al. (2003). *Effect of Clay Binder on Sorption and Catalytic Properties of Zeolite Pellets*. Central Salt and Marine Chemical Research Institute. Indian Petrochemical Corp. Ltd. American Chemical Society. Indian Engineering Chemical Research. 42. 3263-3272.
15. Johansson Westholm, L. (2006). *Substrates for phosphorus removal—Potential benefits for on-site wastewater treatment?*. Water Research 40. 23-36.
16. Keattch, C. J. (1975). *An Introduction to Thermogravimetry*. Heyden & Son Ltd. Second Edition.
17. Kesraoul-Oukl, S. (1993). Effects of Conditioning and Treatment of Chabazite and Clinoptilolite Prior to Lead and Cadmium Removal. *Environmental Science Technology*. Vol 27. No 6. 1108-1116.
18. Li, M. et al. (2011). *Application of Modified Zeolite for Ammonium Removal from Drinking Water*. *Desalination* 271. 295-300.
19. Masel, R. I. (1996). *Principles of Adsorption and Reaction on Solid Surfaces*. John Wiley & Sons, Inc. 235-248.
20. Ministry of the Environment (MOE) (2010). *Lake Simcoe – Phosphorus Reduction Strategy*. Queen's Printer for Ontario.

21. Morse, G.K. et al. (1998). *Review: Phosphorus removal and recovery technologies*. The Science of the Total Environment 212. 69-81.
22. Mumpton, F.A. et al. (1977). *Mineralogy and Geology of Natural Zeolites*.
23. PHOSLOCK. (2010). *Phoslock – Water Solutions Ltd*. Retrieved 12/04/2012 from: <http://www.phoslock.com.au/index-main.php>
24. Phosphate Standard Operating Procedure (Spec-20).
25. Regents of the University of Minnesota. (2010). *On-Site Sewage Treatment Program – Parameters to Monitor Septic System Performance*. Retrieved 01/04/2011 from: <http://septic.umn.edu/factsheets/systemperformancemonitoring/index.htm>
26. Seidel, R. et al. (1993). *The Influence of clay binder materials on the physical properties of the molecular sieve used in a hydrocarbon separation process*. Chemie-AG Bitterfeld-Wolfen, Germany. ZEOLITES. Vol. 13.
27. Skei, J. et al. (2000). *Eutrophication and Contaminants in Aquatic Ecosystems*. Royal Swedish Academy of Sciences. *Ambio*, Vol. 29, No. 4/5. Springer. 184-194. Retrieved 03/05/11 from: <http://www.jstor.org/stable/4315028>
28. Song, C. et al. (2008). *A phase diagram for jammed matter*. Vol 453. Nature Publishing Group.
29. Vohla, C. et al. (2011). *Filter materials for phosphorus removal from wastewater in treatment wetlands-A review*. *Ecological Engineering* 37. 70-89.
30. Wanchun, T. et al. (2011). *Adsorption of nitrogen and phosphorus on natural zeolite and its influencing factors*. 2011 Third Internal Conference on Measuring Technology and Mechatronics Automation. doi: 10.1109/ICMTMA.2011.88.
31. Wang, S. et al. (2010). *Natural zeolites as effective adsorbents in water and wastewater treatment*. *Chemical Engineering Journal* 156. 11-24.
32. Waseda, Y. et al. (2011). *X-Ray Diffraction Crystallography: Introduction, Examples and Solved Problems*. Springer.
33. Wright, P.A. (2008). *Microporous Framework Solids*. The Royal Society of Chemistry.
34. Sun, X. et al. (2010). *The phosphorus-adsorption capacity and influencing factors of Zeolite*. *Advanced Materials Research Vols. 113-114 pp. 766-769*.

BIBLIOGRAPHY

1. Veith, J. A et al. (1977). *On the Use of the Langmuir Equation in the Interpretation of "Adsorption" Phenomena*. *Soil SCI. SOC. AM. J.* 41. 697-702.